FINAL REPORT

(Sept. '82 - Aug. '83)

'Investigation of the effects of mechanical stress on the magnetic properties of pipelines steels for pipeline stress monitoring.'

Research supported by Dept. of Energy Mines & Resources (CANMET, Physical Metallurgy Research Labs.) and National Research Council (Industrial Materials Research Institute) under DSS Contract No. 1 SU81-00265.

Crown Copyright of this report is reserved.

APR 5 1984
MICROMEDIA

157 AP

D. L. Atherton
and D.C. Jiles
Dept. of Physics
Queen's University

REQ. NO. 1-9074

CONTRACT REPORT NO. 1SU81-00265

FINAL REPORT

(Sept. '82 - Aug. '83)

'Investigation of the effects of mechanical stress on the magnetic properties of pipelines steels for pipeline stress monitoring.'

Research supported by Dept. of Energy Mines & Resources (CANMET, Physical Metallurgy Research Labs.) and National Research Council (Industrial Materials Research Institute) under DSS Contract No. 1 SU81-00265

Crown copyright of this report is reserved.

D. L. Atherton
and D. C. Jiles
Dept. of Physics
Queen's University
Kingston, Ontario
K7L 3N6

157 pp

ABSTRACT

Anomlous stresses or changes in stresses in pipelines may be defected by magnetometer survey although the interpretation of the survey logs is difficult partly because of the lack of previous data or understanding of the effects of mechanical stress on the magnetic properties of pipeline steels. The present work provides basic data and understanding. The major achievements are firstly the development of a unified theory of ferromagnetic hysteresis and secondly an explanation of the apparently conflicting magnetisation changes when steel is stressed. Our theory states that the result of a mechanical stress cycle is to shift the magnetisation towards the anhysteretic magnetisation (which is also stress dependent). Experimental data is presented for three samples of pipeline steels. This is obtained in a special apparatus designed to stress small samples in an external magnetic field. Special instrumentation includes very low drift voltmeter/fluxmeter and strain gauge bridge and complete computer control and data logging of all experimental parameters such as stress and magnetic field. Special computer routines are used for sample demagnetisation and for measuring the anhysteretic magnetisation curve. Associated work on the effects of stress on magnetic inspection techniques for pipelines is reported.

Résumé

Il est possible prévoir les contraintes anormales ou les variations des contraintes dans un pipe-line par l'exécution au préalable de levés au magnétomètre, bien que l'interprétation des résultats soit difficile en partie à cause du manque de données antérieures et de connaissances sur les effets des contraintes mécaniques sur les propriétés magnétiques des aciers de pipe-line. Le présent rapport fournit des données fondamentales sur le sujet. Les réalisations principales sont l'élaboration d'une théorie unifiée de l'hystérésis ferromagnétique et l'explication des variations en apparence incompatibles de la magnétisation qui se produisent lorsque l'acier est soumis à une contrainte. Selon cette explication, un cycle de contrainte mécanique a pour résultat de déplacer la magnétisation vers la magnétisation anhystérétique (également fonction de la contrainte). Le rapport présente des données pour trois échantillons d'acier de pipe-line. Les essais on été effectués au moyen d'un appareil spécial permettent de faire subir à de petits échantillons les contraintes d'un champ magnétique externe. Au nombre des instruments spéciaux utilises, on compte un voltmètre/fluxmètre à dérive très lente et un point de jauge. Le contrôle et l'enregistrement de tous les paramètres expérimentaux comme la contrainte et les caractéristiques du champ magnétique on été complètement informatisés. Des sous-programmes spéciaux ont été utilisés pour démagnétiser les échantillons et mesurer la courbe de magnétisation anhystérétique. Des travaux connexes sur les effets des contraintes sur les méthodes d'inspection magnétique des pipe-line sont aussi présentés.

ACKNOWLEDGEMENTS

The members of the group contributing to this work were:

D.L. Atherton (project leader)

D.C. Jiles (research associate)

H.E. Lassen (electronics engineer)

L.G. Dobranski, W. Mizera (graduate students)

B. Ziomkiewicz (technologist)

T. Astle (undergraduate student)

J. De Vette, P. Harvey, S.Y. Kong and

R. Stoner (summer research assistants)

We would like to thank R.W. Revie, M. Godden and D. Mak Department of Energy Mines and Resources (CANMET, Physical Metallurgy Research Labs.) and J. Bussiére of National Research Council (Industrial Materials Research Institute) for their continuing encouragement and guidance and also H.A. French, R.M. Jamieson and A. Teitsma of TransCanada Pipelines Ltd. for numerous enthusiastic discussions and mutually supportive investigations. Any data presented, opinions, results and conclusions expressed in this report are those of the authors and do not necessarily reflect the views of the sponsors.

CONTENTS

		Page
1.	Introduction	1
2.	Experimental Apparatus	4
2.1	Stress Mechanisms	4
2.2	The Turnbuckle	5
2.3	The Scissors	5
2.4	Integrating Voltmeter/Fluxmeter	6
2.5	Strain Measurement	7
2.6	The Electromagnet	9
2.7	Microprocessor Based Control and Data Logging	
3.	Hysteresis Theory	11
3.1	Theory of the Magnetisation Process in Ferromagnets	11
3.2	Domain Wall Motion	12
3.3	Effects of Domain Wall Pinning on the Magnetisation	14
3.4	Variation of the Parameter k with Magnetisation	18
4.	The Magnetomechanical Effect	19
4.1	Effects of Stress on Magnetisation	19
4.2	Effects of Stress on Pinning of Domain Walls	20
4.3	Dependence of the Changes in Magnetisation on the Initial Conditions	22
5.	Experimental Results	24
6.	Related Work	25
7.	Conclusions	27

Appendices

I. "Detection of Anomalous Stresses in Gas Pipelines by Magnetometer Survey"
II. "The Development of an Above Ground Stress Measurement Method"
III. "Stress Shadow Magnetic Inspection Technique for Stress Anomalies in Steel Pipes"
IV. "Ferromagnetic Hysteresis"
V. "Effects of Stress on the Magnetisation of Steel (1)"
VI. "Theory of Ferromagnetic Hysteresis"
VII. "Effects of Stress on the Magnetisation of Steel (2)"
VIII. "Stress Induced Magnetisation Changes of Steel Pipes - Laboratory Tests"
IX. "Algorithm for Obtaining the Anhysteretic Curve"

Figure Captions

Fig. 1 Magnetostriction of Iron as a function of field H for various constant stresses after Kuruzar & Cillity [2].

Fig. 2 The 'turnbuckle' stressing mechanism.

Fig. 3 Cross Sectional Diagram of the sample holder in the 'turnbuckle' stressing mechanism.

Fig. 4 Diagram of the 'turnbuckle' stressing mechanism.

Fig. 5 Diagram of sample cross sections for both the 'turnbuckle' and 'scissors' mechanisms.

Fig. 6 The 'scissors' stressing mechanism.

Fig. 7 Cross sectional diagram of the 'scissors' stressing mechanism.

Fig. 8 Themally insulated rack for mounting of the high stability integrating voltmeters/fluxmeters and strain gauge bridge.

Fig. 9 Diagram of high stability self calibrating strain gauge bridge.

Fig. 10 Schematic diagram of the control and data logging system.

Fig. 11a Theoretical anhysteretic curves obtained from equation (4) with $M_s = 1.6 \times 10^6$ A/m and $\alpha = 0.0033$. —— a = 5000 A/m; --- a = 4000 A/m; -·-·- a = 3000 A/m; -·-·-·- a = 2000 A/m.

Fig. 11b Theoretical anhysteretic curves obtained from equation (4) with $M_s = 1.6 \times 10^6$ A/m and a = 4000 A/m. —— $\alpha = 0.000$; --- $\alpha = 0.002$; -·-·- $\alpha = 0.004$; -·-·-·- $\alpha = 0.006$.

Fig. 11c Theoretical initial magnetisation curves with constant k, obtained from solutions of equation (19) with $M_s = 1.6 \times 10^6$ A/m, a = 3000 A/m and $\alpha = 0.0033$. —— k = 0; --- $k/\mu_o = 3000$; -·-·- $k/\mu_o = 4500$.

Fig. 12a Comparison of experimental and theoretical anhysteretic curves. O experimental anhysteretic at zero stress, ● experimental anhysteretic at 200 MPa compression. ···· theoretical curve with $M_s = 1.6 \times 10^6$ A/m, a = 3750 A/m, $\alpha = 0.0033$. --- theoretical curve with $M_s = 1.6 \times 10^6$ A/m, a = 4750 A/m, $\alpha = 0.00379$.

Fig. 12b Comparison of experimental and theoretical initial magnetisation curves obtained from solutions of equation (19) with constant k. O experimental curve at zero stress, ● experimental curve at 200 MPa compression. ···· theoretical curve with $M_s = 1.6 \times 10^6$ A/m, a = 3750 A/m, $\alpha = 0.0033$, $k/\mu_o = 3.5 \times 10^3$, --- theoretical curve with $M_s = 1.6 \times 10^6$ A/m, a = 4750 A/m, $\alpha = 0.00379$, $k/\mu_o = 3.5 \times 10^3$.

Figure Captions (cont'd)

Fig. 13 Theoretical hysteresis loops obtained from the solution of equation (19) using the k dependence of equation (24) with $M_s = 1.6 \times 10^6$ A/m, a = 3750 A/m, $\alpha = 0.0033$, $k_o = 3250$ and $k_1 = 2000$. This should be compared with the corresponding experimental loops of figure 15 for which the values of the parameters were chosen.

Fig. 14 Experimental anhysteretic curves at different levels of stress. —— 200 MPa compression; -·-·- 100 MPa compression; -·-·-·- zero stress; --- 100 MPa tension; ···· 200 MPa tension.

Fig. 15 Experimental hysteresis loops for the steel sample under zero stress.

Fig. 16 Experimental hysteresis loops for the steel sample under 200 MPa tension.

Fig. 17 Experimental hysteresis loops for steel sample under 200 MPa compression.

Fig. 18 Changes in flux density with tension and compression up to 150 MPa at the same point on the initial magnetisation curve. The result shows that the direction of the change is independent of the sign of the stress.

Fig. 19 Changes in flux density B caused by a single stress cycle of 100 MPa tension at various different points along the initial magnetisation curve and around a hysteresis loop. ·-·-· changes in B with direction at constant H.

Fig. 20 Changes in flux density B caused by a single stress cycle of 100 MPa compression at various different points along the initial magnetisation curve and around a hysteresis loop. ·-·-· changes in B with direction at constant H.

Fig. 21 Changes in flux density B with stress at different points along the initial magnetisation curve. —— 0.32 kA/m; --- 0.96 kA/m; -·-·- 1.6 kA/m; ···· 3.2 kA/m.

Fig. 22 O Changes in flux density for a stress cycle of 140 MPa tension starting on the initial magentisation curve at various values of H.

● Changes in flux density for a stress cycle of 140 MPa tension starting from the anhysteretic curve at various values of H. It can be seen that in this case the net changes in B are almost negligible compared to the changes from the initial magnetisation curve.

—— The curve is the difference between initial and anhysteretic values of B as a function of H.

Fig. 23 Iso stress hysteresis loops for sample S5 under -200 MPa compression.

Figure Captions (cont'd)

Fig. 24 Iso stress hysteresis loops for sample S5 under -100 MPa compression.

Fig. 25 Iso stress hysteresis loops for sample S5 under 0 MPa.

Fig. 26 Iso stress hysteresis loops for sample S5 under +100 MPa tension.

Fig. 27 Iso stress hysteresis loops for sample S5 under +200 MPa tension.

Fig. 28 Iso stress anhysteretic curves for sample S5.

Fig. 29 Iso stress initial magnetisation curves for sample S5.

Fig. 30 Iso stress hysteresis loops for sample S2 under 36 MPa tension.

Fig. 31 Iso stress hysteresis loops for sample S2 under zero stress.

Fig. 32 Iso stress hysteresis loops for sample S2 under -200 MPa compression.

Fig. 33 Iso stress anhysteretic curves for sample S2.

Fig. 34 Iso stress initial magnetisation curves for sample S2.

Fig. 35 Changes in flux density B caused by a single stress of +140 MPa tension at different points along the initial magnetisation curve and around a hysteresis loop. The dashed line is the anhysteretic curve.

Fig. 36 Iso stress anhysteretic curves for sample S1.

Fig. 37 Iso stress initial magnetisation curves for sample S1.

1. INTRODUCTION

Magnetometer surveys above gas pipelines have shown large magnetic anomalies associated with known regions of high stress produced by cold bending (see Appendices I and II). It has been suggested that the method could be developed for non invasive monitoring of pipelines for changes in stress or localised regions of high stress. The method could be used to particular advantage for the diagnosis of problems in pipelines constructed on unstable terrain such as permafrost, river crossings or in submarine lines. The technique would also be of potential use in other applications such as monitoring the stress in the supports or risers of offshore platforms. The changes in fringing fields are typically several kilogamma (1 gamma = 10^{-9} tesla = 10^{-5} gauss) measured on the ground above buried pipelines (at typical depths of 1.2 m = 4 ft) and are therefore large and readily detectable. Consequently the technique could be utilized even for lines constructed without the launchers and traps needed for inspection pigs.

Magnetometer survey logs are however complex and difficult to interpret precisely without both experience, fundamental data and understanding of the effects of stress on the magnetisation of pipeline steels. Unfortunately the needed fundamental knowledge available previously was inadequate and even misleading. The objective of this project has been to obtain this fundamental knowledge. Despite the shortage of published data on the magnetomechanical effect on any material, the inverse effect, magnetostriction (the measurement of strain due to changes in magnetisation) is very well documented and understood. The magnetostrictive behaviour of iron has been measured (fig. 1) previously (1) and is known to be rather

complicated, particularly since a change in sign of the magnetostriction coefficient occurs at sufficiently high fields (see Appendix I). Fortunately in the case of pipeline steel, it now appears that this reversal may occur at much higher field strengths than we are interested in and that in any case, the magnetostrictive effect is not directly significant.

We have developed apparatus to measure experimentally the effects of stress on the magnetic properties of samples of pipeline steels. There have been three major problems to overcome in this experimental work.

The first difficulty was to devise a mechanism for applying controlled variable stresses to a sample in a controlled magnetic field since the space available in a typical electromagnet is very restrictive. We designed and constructed two mechanisms one of which, a compressed turnbuckle concept, has been used extensively.

The second problem was instrumental drift, particularly of the integrating voltmeter needed for flux density determinations, during the relatively long experimental cycles. This has been solved mainly by taking extreme precautions to prevent thermal fluctuations in the device and partly by computer control which allows a shorter time interval for measurements.

The third experimental challenge was to minimize drift by rapid cycling of the field H, and to ensure use of the same magnetisation and demagnetisation routines in all cases. Computer control was needed for the magnetic field and the stepper motor driven stress mechanism. Computer data logging has also been included.

The experimental apparatus and techniques developed are described in Section 2 of this report.

A major potential problem at the start of this project was of course that since magnetisation curves and hysteresis loops are relatively complex

the addition of a further parameter, namely stress, might make data interpretation and presentation very complex. Descriptions of ferromagnetic hysteresis behaviour (eg. Rayleigh loops) tended to be restricted to special regions such as the low field region or the approach to saturation. A major accomplishment during this project has been the development of a unified theory of ferromagnetic hysteresis describing all the possible magnetisation and hysteresis curves. This is described in Section 3 and in Appendices IV and VI. A result of the theory which is of special importance is that the parameters describing all the possible major and minor hysteresis loops are nearly defined by the unique initial and anhysteretic magnetisation curves. (The anhysteretic magnetisation curve is the reversible magnetisation curve which would be obtained if hysteresis effects were suppressed. Points on it may be obtained, rather similarly to demagnetising, by supplying ac of steadily diminishing amplitude but superimposed on dc bias).

Our experimental work described in Section 5 therefore is concerned partly with the effects of stress on the initial and anhysteretic magnetisation curves which should define the isostress magnetic behaviour and partly with the effect on the magnetisation of changing the stress at constant field H.

The few reported results of previous work on the effects of stress on magnetisation were apparently conflicting. Our work on varying stresses covered in Section 4 and in Appendices V and VII shows that the effect of stress cycling is to decrease the magnetic hysteresis, i.e. to shift the magnetisation towards the anhysteretic curve which may result in either increase or decrease in magnetisation depending on the initial conditions. The anhysteretic curve is also stress dependent and cycles during the stress cycle. This explanation resolves the previous apparent conflicts.

In order to help correlate the basic studies of uniform stress on a small sample of steel in a uniform magnetic field with magnetometer surveys of pipelines, we have made laboratory scale tests, under a separate NSERC Strategic grant, conducting magnetometer surveys near small pipes with controlled bending stresses. These and other work on the effects of stress on magnetic inspection techniques are briefly reported in Section 6 and Appendices III and VIII.

The conclusions are presented in Section 7. In short, the aims of the project have been met with great success. The major achievements have been the development of a unified theory of ferromagnetic hysteresis, the achievement of a sound fundamental understanding of the effects of stress on pipeline steels and the development of sophisticated experimental techniques.

2. EXPERIMENTAL APPARATUS

2.1 Stress Mechanisms

Two mechanisms have been designed and constructed which can apply both compressive and tensile uniaxial stress. The stresses applied by these mechanism can be varied continuously. The dimensions of the apparatus were chosen to allow them to fit within the 62 mm (2.5") pole gap of an electromagnet. Subsequently, they have been used in a 70 mm (2.75") gap magnet. Calibration and testing of these mechanisms revealed serious problems with bending of the sample om the case of the "scissors", however, the other device, the "turnbuckle" has been used extensively in our investigations of the magnetomechanical effect in steel. The mechanisms have been built mainly of aluminum and stainless steel to minimize stray induced flux.

2.2 The Turnbuckle

The turnbuckle mechanism is shown in figs. 2, 3, 4 and 5. It is designed to stress a 9.5 mm x 9.5 mm cross section sample to 3.2×10^8 Pa (45,000 p.s.i.), that is to apply a nominal maximum load of 29 kN (6,3000 lbs. f.) using a high ratio, step-down gear.

Some initial problems were encountered due to overstressing of the bearings and plastic chains which were used in the gear drive. These were overcome by the introduction of improved bearings and the use of steel chains instead of plastic. Further problems arose due to bending deflection of the pivot pins, and accumulated tolerances, which resulted in excess slack in the mechanism. Investigations of these various problems were necessary in order to improve the design and also to modify the dimensional specifications for the samples slightly to ensure compressive loading to the required limit.

The mechanism is driven through the step down gear train by a Superior Electric stepper motor system interfaced to the Commodore microcomputer controller.

2.3 The Scissors

The scissors mechanism is shown in figs. 6 and 7. It was designed to subject a 9.5 mm x 9.5 mm cross section sample to a stress of 4.3×10^8 Pa (60,000 p.s.i.), that is to apply a nominal maximum load of 38 kN (8,400 lb. f) using a high ratio screw driven lever. The mechanism had the advantage that a similar device might be used to allow rotation of the stress axis within the magnetic field to any desired angle. Considerations of the effect of line pressure, which manifests itself as circumferential stress in the pipe wall, and would consequently be predominantly perpendicular to

axial bending stress or magnetisation direction, indicates that such measurements would be worthwhile. However problems arose in the preliminary calibration and testing which have led to preference being given to the turnbuckle.

Initial measurements made with strain gauges mounted on the back and front surfaces of both aluminum and steel samples indicated that the strain on the front surface was much larger than on the back, the ratio of strains being between three and six to one depending on the sample used. It appeared therefore that significant bending of the specimen was occurring. Lubrication of the moving parts of the sample holder did not result in any reduction of this bending. This was a serious problem and further attempts to overcome it have not been successful.

2.4 Integrating Voltmeter/Fluxmeter

Two commercial integrating voltmeter/fluxmeters have been obtained in order to determine flux density B. These were an LDJ Electronics Inc., model 702 fluxmeter and an O.S. Walker Co. Inc. fluxmeter model MF-IR. Some problems were encountered with drift on the output of these instruments in their condition as supplied by the manufacturer, particularly in the case of the LDJ instrument. It was found that a drift of 3×10^{-4} Webers per minute occurred under normal laboratory conditions, corresponding to field drift of 3×10^{-2} Tesla with a 100 turn coil on the samples used in the present work.

The problems with drift were overcome by enclosing both meters in a thermally insulated environment as shown in fig. 8. An additional zero offset potentiometer was included in the LDJ instrument at this stage also, to improve the sensitivity of the drift control, and the device was powered from four twelve volt acid batteries connected in series, instead of from

the mains, to ensure that the supply voltage was smooth. It was found that under these conditions the instruments were sensitive enough and stable enough to detect the presence of someone standing near by thermal radiation, which would result in the onset of drift after stability had been achieved. The LDJ meter which was to be used for subsequent readings was then shielded against heat radiation using aluminised plastic sheeting.

The drift on the instruments under these conditions could be controlled easily to within 3.0×10^{-7} Webers per minute, and in principle down to zero if sufficient care were taken with the adjustment of the offset potentiometer. The resolution of the digital display of the LDJ instrument was 1.5×10^{-5} Webers on the range used, although this could be greatly improved, down to less than 0.5×10^{-6} Webers by displaying the output on a chart recorder. The flux limit of this instrument was 3×10^{-2} Webers, 3×10^{6} Maxwell turns. The Walker fluxmeter was somewhat less sensitive, although in general rather more stable. Its resolution on the range used was 3×10^{-5} Webers on its own display, although once again this could be improved to down to 0.5×10^{-6} Webers if the output was displayed on a chart recorder. The maximum field that the instrument was capable of measuring on the range used was also 3×10^{-2} Webers or 3×10^{6} Maxwell turns.

It is considered that with the development of such high stability instruments their performance is now well in excess of our present requirements and no further improvement is likely to be necessary.

2.5 Strain Measurements

The sample strains are measured by strain gauges, type EA-06-090DH-350 as supplied by Micromeasurements Inc. The resistance of the sample gauge (or active gauge as it is known) is determined by including it as one arm

of a Wheatstone bridge network. Temperature compensation is achieved by having another unstrained gauge, the dummy gauge, placed close to the active gauge and bonded onto similar material. The dummy gauge is then used as another arm of the bridge as shown in fig. 9, so that temperature variations of the sample cause no change in the output of the bridge. However without further precautions this circuit would require zero offset adjustment every few minutes as the out of balance voltage drifts. The need for such frequent adjustment has been eliminated by enclosing the whole bridge network, with the exception of the active and dummy gauges in a thermally isolated environment. The leads to the active and dummy gauges are provided by a length of three core cable so that any thermal variations in resistance of the leads would occur identically in both arms of the bridge. In this way the drift of the out of balance voltage has been reduced to typically less than 1 mV per hour after amplification (amplifier gain approx. 220) corresponding to an equivalent strain of 5μ strain. As this drift is much smaller than the strain levels which we wish to measure, by typically a factor of a hundred, the zero offset can be adjusted once a day.

An improved circuit for the strain gauge bridge has been designed and built incorporating digital potentiometers, as shown in fig. 9. This allows calibration of the output voltage directly in terms of change in resistance of one arm of the bridge, and hence in terms of strain given the gauge factor of the strain gauges used. Consequently the bridge is self calibrating and it is not necessary to know the amplifier gain or supply voltage. In particular the latter may vary over long periods as the lead acid batteries become discharged.

The instrument developed for the present work is capable of measuring

the sample strain to an accuracy of 5μ strain (0.0005%) with a precision of 0.5μ strain (0.00005%). The performance of the instrument is now well in excess of our immediate requirements and could even be used for magnetostriction measurements if required.

Both the integrating voltmeter/fluxmeter and the strain gauge bridge have achieved sufficient stability for the drift to be almost negligible for our requirements during a set of experiments lasting one day. This allows the present experimental arrangement to detect reptation in the BH loop, which might otherwise be simply attributed to drift and also to ascertain whether any creep occurs in the strain gauge bond which could cause inaccuracies in quoted results and might also be attributed to thermal shift in less stable conventional measuring arrangements.

2.6 The Electromagnet

A conventional twelve inch Varian V-4012-38 electromagnet has been obtained and is dedicated to the system. This electromagnet is capable of producing fields of up to 2.0 Tesla in air (1.6×10^6 A/m) although at present a bipolar KEPCO BOP-36-5M power supply which produces fields up to 10^5 A/m has been found sufficient for our field requirements. The electromagnet has a fixed pole gap of 7 cm and the output of the power supply, and hence the magnetic field produced, is controlled remotely from the micro computer. The magnetic field produced is monitored using a Hall probe.

2.7 Microprocessor Based Control and Data Logging

A microprocessor based control and data logging system has been completed which allows on-line control of magnetic field and applied stress. The system is based on a Commodore PET 4032 microcomputer which controls the electromagnet coil current and the position of the stepper motor applying

the stress.

Data logging is achieved via a fast sampling digital voltmeter (Hewlett Packard model HP3437A) which is interfaced to the computer using the standard IEEE-488 bus. It is connected to one of up to eight separate 2 wire channels for voltage measurement, using a pair of analog multiplexers (MC14051) with eight channels each. This allows the one voltmeter to sample the magnetic field H (Hall probe emf.), the mechanical strain (strain gauge bridge voltage), magnetic flux density B (fluxmeter voltage) and other additional parameters as desired such as magnet coil current, Hall probe current and thermocouple emf. for temperature measurement.

A schematic of the control and data logging system is shown in fig. 10. The range select on the DVM and the channel select on the multiplexers are controlled via a non-standard composite IEEE/J2 bus. The power supply current control and the stepper motor position selector are also controlled from the same bus. The magnet power supply is connected to the IEEE/J2 bus via an 8-bit digital to analog converter (D/A).

For permanent storage of data the results are dumped periodically onto mini-floppy magnetic discs run on a Commodore model 4040 dual disc drive unit.

The Superior Electric stepper motor control unit consists essentially of an IDD008 index-card circuit board, and a DRD003 driver card. The stepper motor itself was a model M092-FD09. The indexer card was programmable from the IEEE/J2 bus and provided the driver card with the necessary phase signals for any required stepping sequence. The driver card was basically a power supply for the stepper motor.

Additional features not shown in fig.10 were also included, for example pen- and servo-control of a Hewlett Packard 7044B X-Y chart recorder which was used to provide hard copy graphical results of B v. H or B v. strain.

3. HYSTERESIS THEORY

3.1 Theory of the Magnetisation Process in Ferromagnets

The interpretation of the magnetising process in ferromagnetic materials has generally required the consideration of two related mechanisms. The first of these is that the domain wall move under the influence of an applied field in such a way that favourably aligned domains grow at the expense of unfavourably aligned domains. The second mechanism is that the unfavourably aligned magnetic moments, within an unfavourably aligned domain, can rotate into the field direction. This has the effect of causing domain rotation.

Consider the energy per unit volume E of a typical domain with magnetic moment m per unit volume in a magnetic field H. If there is coupling between the magnetisation in different domains then

$$E = -\mu_o \, \underline{m} \cdot (\underline{H} + \alpha \underline{M}) \qquad (1)$$

where α is a mean field parameter representing the interdomain coupling and is to be determined experimentally, and M is the bulk magnetisation. The equation may then be expressed as

$$E = - \underline{m} \cdot \underline{B}_e \qquad (2)$$

where the effective field $\underline{B}_e$ is

$$\underline{B}_e = \mu_o (\underline{H} + \alpha \underline{M}) \qquad (3)$$

Such an effective field has been used by Callen, Liu and Cullen (2). It will be seen that the effective field is analogous to the Weiss (3) field, although the mean field parameter α is different in the two cases.

Applying Maxwell-Boltzmann statistics and integrating over 4π solid angle leads, in the case of $\alpha = 0$ to the Langevin (4) equation, and in the case of $\alpha \neq 0$ to a modified Langevin equation for the bulk magnetisation (5).

$$M = M_s \left[\coth\left(\frac{\mu_o m(H+\alpha M)}{k_B T}\right) - \frac{k_B T}{\mu_o m(H+\alpha M)} \right] \qquad (4)$$

$$= f\left(\frac{B_e}{\mu_o a}\right)$$

where $a = k_B T/\mu_o m$

Although the Langevin equation works well for paramagnets the modified Langevin equation above does not give such a good description of the behaviour of a ferromagnet because the model ignores the possibility of the change of magnetisation being impeded such as when the motion of domain walls is inhibited by pinning sites. Instead it applies only to the case of an ideal or perfect crystal in which the domain walls move until they reach thermodynamic equilibrium. This situation can be created artificially in a sample by the application of a decaying A.C. field superimposed on the D.C. field as described by Cullity (6). This yields the ideal magnetisation curve, also known as the anhysteretic curve, which is described by the modified Langevin equation. In this case the pinning sites have been overcome and the final value of magnetisation is that which would have been achieved by the D.C. field in the absence of pinning.

The initial magnetisation curve of a ferromagnet always lies below the anhysteretic curve however it approaches the anhysteretic assymptotically at higher fields. In the high field regions therefore the magnetisation is described fairly well by equation (4).

3.2 Domain Wall Motion

The motion of domain walls under the influence of an applied magnetic field is impeded by the presence of pinning sites in the lattice. This leads to smaller initial permeability and larger coercive forces. A perfect single crystal would therefore be expected to exhibit a large initial permeability and small coercive force, while polycrystalline specimens would, according to

Morrish (7) have smaller permeability and larger coercive force since the grain boundaries introduce additional imperfections and hence pinning sites.

There have been a number of theories regarding the nature of the pinning sites. Becker and Döring (8) suggested that inhomogeneous internal stresses which affect the wall energy were responsible. Kersten (9, 10) considered that imperfections such as non magnetic inclusions or voids in the material were responsible. Later Néel (11) modified both theories and included the concept of flexible domain walls such that, when stationary, a wall would always be located on pinning sites. Correlation between domain wall motion and net or macroscopic magnetisation has been observed experimentally by Williams and Shockley (12).

These concepts have been utilised in the present work in conjunction with the idea of Kersten (13) that the changes in wall energy are balanced by the changes in mutual energy of the field H and the magnetisation M. However there has been no consideration of the different types of pinning site. All types of pinning site have been considered equivalent and a mean pinning energy associated with each site used. From this an energy equation for the magnetisation process has been obtained and an equation of state derived.

If a domain wall is displaced in a completely uniform (i.e. constant) potential then no change in wall energy would occur (Chikazumi (14) p. 264) and therefore when the field was removed the wall would remain in its final position. Therefore in order to have reversible wall displacement, as would occur in an ideal (or unpinned) specimen, it is necessary to invoke a potential which increases with the magnetisation. The domain boundary will then come to rest when the work done by the field is balanced by the magnetisation energy of the sample as indicated by Hoselitz (15) and when the field is removed the domain wall will return to its original position.

Consider the total work done per unit volume by a magnetic field

$$E = \int H.dB = \frac{1}{\mu_o} \int B.dB - \int M.dB \qquad (5)$$

where the second term on the right hand side is the work done in changing the magnetisation of the material.

In the case of a paramagnet the magnetisation is reversible and consequently the work done per unit volume by the magnetic field on the sample is

$$\int MdB = \int f\left(\frac{B}{\mu_o a}\right) dB \qquad (6)$$

In the absence of pinning the domain walls of a ferromagnet are acted upon by what may be envisaged as a pressure which tends to move them in such a way that the magnetisation reaches equilibrium at the corresponding anhysteretic value. Using the effective field B_e for the ferromagnet,

$$\int MdB_e = \int f\left(\frac{B_e}{\mu_o a}\right) dB_e \qquad (7)$$

If for some reason M does not reach this value then the material will have a net potential energy E_{mag} such that

$$E_{mag} = \int \left\{ f\left(\frac{B_e}{\mu_o a}\right) - M \right\} dB_e \qquad (8)$$

and for an ideal or unpinned ferromagnet all of the potential is converted into magnetisation energy and $E_{mag} = 0$.

3.3 Effects of Domain Wall Pinning on the Magnetisation

When considering a real ferromagnet the consequences of domain wall pinning must be included in the energy equation. This leads to irreversible changes in the magnetisation with field and hence to hysteresis in the

magnetisation, which is generally attributed to impedance of domain wall motion according to Carey and Isaac (16) p. 32 .

Consider a pinning site on a domain wall between domains with magnetisation $\underline{m}$ and $\underline{m}'$ where $\underline{m}$ is aligned parallel to the field and is the growing domain while $\underline{m}'$ is aligned at some arbitrary angle θ to the field and hence to $\underline{m}$. The energy required to overcome the pinning site will depend on two factors, the nature of the pinning site itself and the relative orientations of the magnetisations in the domains on either side of the wall. Suppose the energy required to overcome the pinning site is proportional to the change in energy per unit volume of the $\underline{m}'$ domain caused by rotating its moments into the field direction and hence parallel to $\underline{m}$.

$$\Delta E = \underline{m} \cdot \underline{B} - \underline{m}' \cdot B \qquad (9)$$

and consequently if ε_{pin} the pinning energy of the one pinning site is proportional to ΔE

$$\varepsilon_{pin} \propto mB(1 - \cos\theta) \quad . \qquad (10)$$

If the pinning energy of the site for 180° walls is ε_π then $\varepsilon_\pi \propto 2mB$. Therefore the pinning energy of the typical site may be expressed as

$$\varepsilon_{pin} = \frac{\varepsilon_\pi}{2} (1 - \cos\theta) \quad . \qquad (11)$$

and taking $\langle \varepsilon_\pi \rangle$ as the average pinning energy of all the sites for 180° walls, and assuming a uniform density of pinning sites of n per unit volume throughout the solid,

$$\langle \varepsilon_{pin} \rangle = \frac{\langle \varepsilon_\pi \rangle}{2} (1 - \cos\theta) \qquad (12)$$

$$E_{pin}(x) = \int_0^x n \frac{\langle \varepsilon_\pi \rangle}{2} (1 - \cos\theta) \, A \, dx \qquad (13)$$

where E_{pin} is the total energy lost through pinning when a domain wall of area A is moved through a distance x, between domains whose magnetisations lie at and angle θ.

The net change in magnetisation of the ferromagnet (remembering that by symmetry there will be a number of domains at an angle θ to the field direction such that the component of magnetisation perpendicular to the field due to these domains will sum to zero) will be,

$$dM = m(1 - \cos\theta)\, A.dx \tag{14}$$

and substituting for A.dx in the equation for energy leaves,

$$E_{pin} = \int \frac{n\langle\varepsilon_\pi\rangle}{2m}\, dM \tag{15}$$

which is independent of the relative orientations of the domains. That is although the energy required to move a domain wall through a more unfavourably oriented domain is greater, the change in magnetisation achieved by doing so is also proportionally greater.

Replacing the terms on the right hand side by the constant k

$$k = \frac{n\langle\varepsilon_\pi\rangle}{2m} \tag{16}$$

$$E_{pin} = k\int dM \tag{17}$$

Hence under the assumptions of a uniform distribution of pinning sites, and treating each one as having the average pinning energy, the total work done against pinning is proportional to the change in magnetisation.

The magnetisation energy $\int M.dB_e$ is therefore the difference between the energy which would be attained in the ideal or unpinned case $\int f\left(\frac{B_e}{\mu_o a}\right) dB_e$ minus the loss due to hysteresis.

$$\int M dB_e = \int f\left(\frac{B_e}{\mu_o a}\right) dB_e - \int k\left(\frac{dM}{dB_e}\right) dB_e \qquad (18)$$

and consequently, differentiating with respect to B_e.

$$M = f\left(\frac{B_e}{\mu_o a}\right) - \delta.k\left(\frac{dM}{dB_e}\right) \qquad (19)$$

This is the equation of state of a ferromagnet under the given conditions as indicated previously Jiles and Atherton (5). It is felt that the coefficient k probably varies with M. The directional parameter δ takes the values ± 1 and is introduced as the effect of pinning is always to oppose the rate of change of M.

Solutions of equation (19) for various values of the parameters are shown in fig.11. Fig. 11(a) shows a set of anhysteretic or ideal magnetisation curves, which are obtained by setting k = 0, for different values of the parameter a with Ms and α held constant. Fig.11(b) shows a set of anhysteretic curves for different values of the parameter α with Ms and a held constant. Fig.11(c) shows how the initial magnetisation curve varies with different constant values of the parameter k.

In fig. 12(a) experimentally determined anhysteretic curves for two different stress levels are shown compared with theoretical curves obtained from equation (19) by setting k = 0 with the values of the other parameters as given. Fig. 12(b) shows the experimental initial magnetisation curves for the same two stress levels which are again compared with theoretical initial magnetisation curves for the values of the parameters given in the figure.

3.4 Variation of the Parameter k with Magnetisation

In practice the parameter k of equation (19) varies with M and H since equation (14) is an approximation which is only valid when the change in magnetisation is due to uniformly impeded domain wall motion. In fact,

$$dM = dM_r + dM_{wm} \tag{20}$$

where dM_r is the change in M due to rotation and dM_{wm} is the change due to wall motion. Taking the loss due to domain rotation equal to γ times the loss due to pinning gives,

$$dE_{loss} = \frac{n<\varepsilon_\pi>}{2m}\left(dM_{wm} + \gamma dM_r \right) \tag{21}$$

where γ will be determined later.

$$k = \frac{dE_{loss}}{dM} = \frac{n<\varepsilon_\pi>}{2m}\left[1 - (1-\gamma)\frac{dM_r}{dM} \right] \tag{22}$$

and since at the origin of coordinates (H=0,M=0) in the demagnetised state any changes in magnetisation will be due exclusively to domain wall motion the value of k at this point is $k = k_o = \frac{n<\varepsilon_\pi>}{2m}$ and $\frac{dM_r}{dM} = 0$.

$$k = k_o\left[1 - (1-\gamma)\frac{dM_r}{dM} \right] \tag{23}$$

Therefore for $0 < \gamma < 1$, k decreases with field. The exact form of the k dependence must be determined empirically in each case. In the present sample it was found that,

$$k = k_o\left[1 + \frac{k_1}{k_o}\exp\left(-\frac{H_{max}}{1500}\right)\right]\left[1 - \left(\frac{M_{max}}{M_s}\right)^2\left[1 - \left(\frac{H}{H_{max}}\right)^2\right]\right] \tag{24}$$

where $k_o = 3250$ and $k_1 = 2000$. With this k dependence the hysteresis curve of fig.13 was obtained. The values of the other parameters, as given in the caption, were chosen to correlate with those obtained under zero stress conditions.

4. THE MAGNETOMECHANICAL EFFECT

4.1 Effects of Stress on Magnetisation

The influence of stress on magnetisation may be understood in terms of the dependence of the coefficient "a" and "α" upon stress and the effect of stress on domain wall pinning Jiles and Atherton (17). Measurements in the present work have indicated that the anhysteretic curve, and hence a and α, is stress dependent as shown in Fig.14. The dependence of the anhysteretic on stress is also partly the cause of the different shapes of the major hysteresis loops under iso stress conditions as shown in Figs. 15,16 and 17, where the stress has been held constant at the indicated values while the field was cycled.

The isostress anhysteretic curves are reversible with respect to both field and stress. If the stress is cycled when the magnetisation is at the anhysteretic value then the magnetisation returns to its original anhysteretic value on completion of the stress cycle. It is clear however that the actual value of the magnetisation changes during the stressing since the anhysteretic curve itself changes with stress.

When the initial, zero stress, conditions are on the anhysteretic, or alternatively when the applied field is sufficiently high that the magnetisation must of necessity lie very close to the anhysteretic then the sign of $\frac{dM}{d\sigma}$ depends upon the magnetostriction coefficient. However when considering the effects of stress on magnetisation at low fields, that is when the initial conditions may lie far from the anhysteretic then in general the sign of $\frac{dM}{d\sigma}$ does not depend upon the magnetostriction coefficient. The results of Fig.18. taken with the same zero stress conditions at 1.6 kA/m along the initial magnetisation curve show that the direction of change of magnetisation is here independent of the sign of the applied stress.

The crucial factor in these cases is whether the dominant mechanism behind the change in magnetisation is domain wall motion or not. The effect of an applied stress is to cause some of the domain walls to break away from their pinning sites and consequently they will move in such a way as to cause the magnetisation to approach the anhysteretic. In the low field region domain wall motion is the dominant mechanism and under these conditions experimental results, such as those of Fig. 18, have indicated that the change of magnetisation has the same direction independent of the sign of stress. These results are in accordance with the theory which predicts that when the initial magnetisation condition lies above the anhysteretic the application of a stress cycle of either sign causes a decrease in magnetisation. Conversely when the zero stress magnetisation lies below the anhysteretic the application of a stress cycle of either sign causes an increase in magnetisation.

4.2 The Effects of Stress on Pinning of Domain Walls

If a solid is subjected to uniaxial stress then this will cause the dislocations in the lattice to move and change the energy associated with point defects. The superimposing of an applied stress on the existing internal residual stresses will cause changes in the total stress. The effect of stress on various inclusions is not entirely clear, however the applied stress will certainly cause changes in the stress fields associated with any voids in the solid.

Therefore the external stress will cause changes in the energy of the various imperfections and impurities, including inhomogeneous residual stresses, all of which have been considered to be responsible for pinning domain walls by earlier theories of the magnetisation process. Becker and Döring (8). Kersten (9, 10) and Neel (11).. The diversity of different types of pinning site makes it difficult to make a precise statement about the effect of stress. However it is reasonable to assume that the pinning energy of

some sites will be decreased while the pinning energy of other sites is increased.

Consider the effect of applying a varying stress σ, of either sign, under conditions of constant field strength H. If the pinning sites which the domain walls are located on under the initial conditions are considered then some of these will have their pinning energy increased and hence the wall will simply remain pinned at these sites causing no overall change in the magnetisation. However among the group of pinning sites for which the pinning energy is reduced will be some for which the reduction of energy causes the domain walls to break away and begin moving. It is then necessary to consider how these walls which succeed in breaking away from their pinning sites are likely to move.

Returning to the original equation for the potential energy of a ferromagnet in the absence of pinning sites, it is clear that the domain walls will move towards the anhysteretic curve in the absence of pinning. Therefore, once a domain wall has succeeded in breaking away from the pinning site it will be subject locally to this potential and hence this will cause changes in magnetisation towards the anhysteretic value until it becomes pinned again. If this behaviour is summed over the whole of the solid then, on the basis of the model presented, the application of a stress would cause the bulk magnetisation M to move towards its anhysteretic value M_{an}, simply because this is the thermodynamic equilibrium point in the absence of pinning.

Experimental results which have been taken to test this hypothesis have all tended to confirm it. The results in Fig.19 and 20 show the changes in flux density B, caused by application of a cyclic stress of 100MPa tension and compression at different points around the hysteresis loop. These show that the changes in magnetisation are towards the anhysteretic. This emphasises the need to specify the exact location of the initial conditions on the (B,H) plane in order to obtain meaningful results. Other measurements showing the change in flux density ΔB with stress σ at various points on the initial magnetisation

It seems that the guiding principle in these cases is that the application of stress, of either sign, causes the magnetisation (or the flux density B, since for ferromagnets in this region $B \approx \mu_o M$) to approach the anhysteretic (Jiles and Atherton (17)) since this represents the global thermodynamic equilibrium state.

It is necessary to emphasise that the anhysteretic curve itself changes with stress, so for example, if a ferromagnet with $\lambda > 0$ is subjected to a compressive stress when the initial conditions of (M,H) are on the normal magnetisation curve, below the anhysteretic, then the change in M will be positive at first since M will approach the anhysteretic. If the magnitude of stress is sufficiently large however, the anhysteretic level of magnetisation, which decreases with compression, will eventually reach the level of the sample magnetisation causing M to decrease with further stress since it will, according to the above principle, move towards the anhysteretic.

4.3 Dependence of the Changes in Magnetisation on the Initial Conditions

Measurements were taken of the change in magnetisation caused by a stress cycle from 0MPa to a tension of σ_{max} = 140MPa and back to zero at different points along the initial magnetisation curve. The locus of the anhysteretic curve was also measured and it was found that the change in flux density $\Delta B(\sigma_{max}, H)$ was proportional to the difference between the anhysteretic value of flux density $B_{an}(H)$ and the initial value $B_i(H)$ at a given field strength H. The results are shown in fig. 22, where the plot of $\Delta B(\sigma_{max}, H)$ is given against the curve $B_{an}(H) - B_i(H)$. These results seem to indicate the following relationship

$$\Delta B(\sigma_{max}, H) \propto B_{an}(H) - B_i(H) \qquad (25)$$

It can also be seen from the earlier graphs of ΔB against σ in Fig.21 that to a first approximation also,

$$\Delta B(\sigma, H) \propto \sigma \qquad (26)$$

although the general behaviour under compression and tension is slightly different.

Furthermore from Fig. 22 it can be seen that the net change in flux density with stress cycling is negligible when the initial conditions lie on the anhysteretic.

5. EXPERIMENTAL RESULTS

In addition to the results presented in sections 3 and 4, which have been used to elucidate our theories of hysteresis and of the magneto mechanical effect, a large amount of basic data on the three samples of pipeline steel has been compiled. The results fall into three categories:

i) hysteresis loops under isostress,

ii) initial magnetisation curves under isostress, and

iii) anhysteretic curves under isostress.

In figs. 23 to 27 families of hysteresis loops under different stresses are shown for sample S5 (EMR Pipelines sample see Table 1). Comparison of these shows that definite changes in the shapes of the major hysteresis loops of a sample occur when that sample is subjected to stress. The parameters were fitted to the data for this sample in section 3. The anhysteretic curves under the same isostress conditions are shown in fig.28 and the initial magnetisation curves in fig. 29.

A set of hysteresis loops over a somewhat smaller range of H field for sample S2 (TransCanada Pipelines Ltd., see Table 1) are shown in Figs. 30 to 32. From these it may be seen even more clearly how the loops change under isostress conditions at different stress levels. The anhysteretic data for this sample are shown in fig. 33 and the initial magnetisation data under stresses of up to 200 MPa are shown in fig. 34. Furthermore in fig. 35 is shown the effects of a single stress cycle at various points around the hysteresis loop, showing once again that the change in magnetisation is towards the anhysteretic curve. There is appreciable drift in B on this experimental set of data which was taken before complete automation of the control and data logging system and hence the whole set took two hours.

More recent results on sample S5 with complete automation now take approximately fifteen minutes.

The results for sample S1 (TransCanada Pipelines Ltd., see Table 1) consist of a set of anhysteretic curves under constant pressure of up to 200 MPa as shown in fig. 36 and a set of initial magnetisation curves for the same stress levels in fig. 37. At present we are completing parameter fittings to the data from samples S1 and S2. It is clear that most of the information on the various parameters is contained in the initial and anhysteretic curves. For example M_s, a, α, k_o and k_1 can be easily determined from these two curves alone. It is however not entirely clear yet whether the variation of k around a complete loop can be determined solely from the initial and anhysteretic curves. Nevertheless we can say that characteristics of ferromagnetic samples can be achieved using only the initial and anhysteretic curves, and that in this respect complete sets of hysteresis loops to arbitrarily large values of H are unnecessary.

6. RELATED WORK

The project has obtained basic data on the changes in magnetisation of pipeline steels under varying mechanical stress in order to help interpret the bending stresses evident in pipeline magnetometer surveys. Whilst this basic data is essential and helpful, interpretation of the complex survey logs is still not easy. In order to help this correlation we have undertaken some demonstrations and tests of intermediate complexity under NSERC funding. We have conducted laboratory scale tests on the changes in magnetic fringing fields of 110 mm diameter pipes due to bending stresses within the elastic range and also due to hydraulically simulated line pressure and have investigated the effects of the orientation of the pipes in the earth's magnetic field, the effects of stress cycling etc. This work is

reported in Appendix VIII. These laboratory scale tests and the basic investigations carried out under this contract have been mutually supportive as the work progressed in parallel and the results from each investigation helped to elucidated the results from the other in particular both programs show the importance of hysteresis effects.

We have also considered how stress effects are relevant to our program for the development of magnetic inspection techniques for gas pipelines funded under an NSERC strategic grant. We believe the local stress anomalies can have a significant effect of the results obtained by some magnetic inspection pigs and we have devised a special technique of detecting far side (exterior) metal loss by detecting the anomalous stress shadow patterns produced on the near side (inside) of the pipewall by line pressure. This work is described in Appendix III and is a good example of how our improved basic understanding of the effects of stress on magnetisation can be used to improve the interpretation of practical non-destructive magnetic inspection techniques.

7. CONCLUSIONS

The achievements of this work have been the development of a complete theory of ferromagnetic hysteresis, including the differential equation describing the process, and an explanation of the magnetomechanical effect and consequently of certain apparently contradictory earlier results. Construction of apparatus for the investigation of the magnetic properties of materials under varying conditions of stress and applied field has been completed and the whole system has been interfaced to a Commodore PET 4032 for microprocessor control and data logging. A vast amount of data has been compiled on the properties of representative pipeline samples, and the results interpreted in terms of the theory that has been developed.

The understanding of the magnetomechanical effect provided by the theory has contributed greatly to the interpretation of laboratory scale tests of the change in magnetisation caused by bending pipelines. The changes in magnetisation have been measured by magnetometer surveys simulating above-ground stress-monitoring surveys.

The development of high stability integrating voltmeter/fluxmeter and strain gauge bridge has far exceeded their original performances. The stability of the integrating voltmeter/fluxmeter of 0.5×10^{-5} Webers per minute was required particularly for results of change in flux against strain, where the changes in flux were typically 10^{-2} Tesla for a stress cycle of 150 MPa, which corresponds to a change of typically 10^{-4} Webers in our measurements, with a sampling time of typically one minute.

The computer control of experiments and data logging of results has provided a rapid and efficient method of determining the properties of the pipeline samples. Furthermore, it has enabled precise algorithims to be developed for the demagnetisation process and for attaining anhysteretic magnetisation.

It has originally been expected that the effect of stress on magnetisation would be dominated by magnetostriction however it has been found that the major influence is in fact hysteresis. The discovery of the significance of the anhysteretic curve indicates the need to measure the magnetostriction along the anhysteretic. Furthermore, although this effect is secondary in determining the behaviour of the materials under stress, it is necessary to measure the magnetostriction coefficient of these materials under differing conditions.

The natural extension of this work, to further improve understanding and interpretation of pipeline surveys, should therefore include the following:

i) The inclusion of stress due to line pressure in laboratory or other testing facilities. Consequently, the existing open line tests must be supplemented with results under pressure.

ii) An examination of the magnetostriction coefficient of these materials with particular emphasis on the magnetostriction along the anhysteretic curve.

iii) The extension of our investigations to include other commercially important materials such as grain oriented silicon steel which is used for the laminations in transformer cores. The application of theories evolved in the present work is likely to provide an exact description of the magnetic behaviour of these materials.

References

1. Kuruzar, M.E. and Cullity, B.D., Inter. J. Magnetism 1 323 (1971).

2. Callen, E., Liu, Y.J., and Cullen, J.R., Phys. Rev. B16 263 (1977).

3. Weiss, P. J. de Phys. Radium 6 661 (1907).

4. Langevin, P. Ann. de Chem. et. Phys. 5 70 (1905).

5. Jiles, D.C. and Atherton, D.L., International Magnetics Conference, 1983, and IEEE Transactions on Magnetics MAG 19 Sept. 1983 (I).

6. Cullity, B.D., "Introduction to Magnetic Materials" (1972).

7. Morrish, A.H., "The Physical Principles of Magnetism" Wiley (1965).

8. Becker, R. and Doring, W., "Ferromagnetismus", Springer (1939).

9. Kersten, M., "Problem der Technischer Magnetisierungskurve" Springer (1938).

10. Kersten, M., "Grundlagen einer Theorie der Ferromagnetischen Hysterese und Koerzitivkraft" Hirzel (1943).

11. Neel, L., Ann. Univ. Grenoble 22 299 (1947).

12. Williams, H.J. and Shockley, W. Phys. Rev. 75 155 (1949).

13. Kersten, M. Z. Physik 124 714 (1948).

14. Chikazumi, S., "Physics of Magnetism" Wiley (1964).

15. Hoselitz, K., "Ferromagnetic Properties of Metals and Alloys" Oxford (O.U.P.) (1952).

16. Carey, R. and Isaac, E.D., "Magnetic Domains and Techniques for their Observation" Academic Press (1963).

17. Jiles, D.C. and Atherton, D.L., International Magnetics Conference, 1983, and IEEE Transactions on Magnetics MAG 19 Sept. 1983 (II).

Figure Captions

Fig. 1 Magnetostriction of Iron as a function of field H for various constant stresses after Kuruzar & Cillity [2].

Fig. 2 The 'turnbuckle' stressing mechanism.

Fig. 3 Cross Sectional Diagram of the sample holder in the 'turnbuckle' stressing mechanism.

Fig. 4 Diagram of the 'turnbuckle' stressing mechanism.

Fig. 5 Diagram of sample cross sections for both the 'turnbuckle' and 'scissors' mechanisms.

Fig. 6 The 'scissors' stressing mechanism.

Fig. 7 Cross sectional diagram of the 'scissors' stressing mechanism.

Fig. 8 Themally insulated rack for mounting of the high stability integrating voltmeters/fluxmeters and strain gauge bridge.

Fig. 9 Diagram of high stability self calibrating strain gauge bridge.

Fig. 10 Schematic diagram of the control and data logging system.

Fig. 11a Theoretical anhysteretic curves obtained from equation (4) with $M_s = 1.6 \times 10^6$ A/m and $\alpha = 0.0033$. —— a = 5000 A/m; --- a = 4000 A/m; -·-·- a = 3000 A/m; -·-·-·- a = 2000 A/m.

Fig. 11b Theoretical anhysteretic curves obtained from equation (4) with $M_s = 1.6 \times 10^6$ A/m and a = 4000 A/m. —— $\alpha = 0.000$; --- $\alpha = 0.002$; -·-·- $\alpha = 0.004$; -·-·-·- $\alpha = 0.006$.

Fig. 11c Theoretical initial magnetisation curves with constant k, obtained from solutions of equation (19) with $M_s = 1.6 \times 10^6$ A/m, a = 3000 A/m and $\alpha = 0.0033$. —— k = 0; --- $k/\mu_o = 3000$; -·-· $k/\mu_o = 4500$.

Fig. 12a Comparison of experimental and theoretical anhysteretic curves. O experimental anhysteretic at zero stress, ● experimental anhysteretic at 200 MPa compression. ···· theoretical curve with $M_s = 1.6 \times 10^6$ A/m, a = 3750 A/m, $\alpha = 0.0033$. --- theoretical curve with $M_s = 1.6 \times 10^6$ A/m, a = 4750 A/m, $\alpha = 0.00379$.

Fig. 12b Comparison of experimental and theoretical initial magnetisation curves obtained from solutions of equation (19) with constant k. O experimental curve at zero stress, ● experimental curve at 200 MPa compression. ···· theoretical curve with $M_s = 1.6 \times 10^6$ A/m, a = 3750 A/m, $\alpha = 0.0033$, $k/\mu_o = 3.5 \times 10^3$, --- theoretical curve with $M_s = 1.6 \times 10^6$ A/m, a = 4750 A/m, $\alpha = 0.00379$, $k/\mu_o = 3.5 \times 10^3$.

Figure Captions (cont'd)

Fig. 13 Theoretical hysteresis loops obtained from the solution of equation (19) using the k dependence of equation (24) with $M_s = 1.6 \times 10^6$ A/m, a = 3750 A/m, $\alpha = 0.0033$, $k_o = 3250$ and $k_1 = 2000$. This should be compared with the corresponding experimental loops of figure 15 for which the values of the parameters were chosen.

Fig. 14 Experimental anhysteretic curves at different levels of stress. —— 200 MPa compression; -·-·- 100 MPa compression; -·-·-·- zero stress; --- 100 MPa tension; ···· 200 MPa tension.

Fig. 15 Experimental hysteresis loops for the steel sample under zero stress.

Fig. 16 Experimental hysteresis loops for the steel sample under 200 MPa tension.

Fig. 17 Experimental hysteresis loops for steel sample under 200 MPa compression.

Fig. 18 Changes in flux density with tension and compression up to 150 MPa at the same point on the initial magnetisation curve. The result shows that the direction of the change is independent of the sign of the stress.

Fig. 19 Changes in flux density B caused by a single stress cycle of 100 MPa tension at various different points along the initial magnetisation curve and around a hysteresis loop. ··>·· changes in B with direction at constant H.

Fig. 20 Changes in flux density B caused by a single stress cycle of 100 MPa compression at various different points along the initial magnetisation curve and around a hysteresis loop. ··>·· changes in B with direction at constant H.

Fig. 21 Changes in flux density B with stress at different points along the initial magnetisation curve. —— 0.32 kA/m; --- 0.96 kA/m; -·-·- 1.6 kA/m; ···· 3.2 kA/m.

Fig. 22 O Changes in flux density for a stress cycle of 140 MPa tension starting on the initial magentisation curve at various values of H.

● Changes in flux density for a stress cycle of 140 MPa tension starting from the anhysteretic curve at various values of H. It can be seen that in this case the net changes in B are almost negligible compared to the changes from the initial magnetisation curve.

—— The curve is the difference between initial and anhysteretic values of B as a function of H.

Fig. 23 Iso stress hysteresis loops for sample S5 under -200 MPa compression.

Figure Captions (cont'd)

Fig. 24 Iso stress hysteresis loops for sample S5 under -100 MPa compression.

Fig. 25 Iso stress hysteresis loops for sample S5 under 0 MPa.

Fig. 26 Iso stress hysteresis loops for sample S5 under +100 MPa tension.

Fig. 27 Iso stress hysteresis loops for sample S5 under +200 MPa tension.

Fig. 28 Iso stress anhysteretic curves for sample S5.

Fig. 29 Iso stress initial magnetisation curves for sample S5.

Fig. 30 Iso stress hysteresis loops for sample S2 under 36 MPa tension.

Fig. 31 Iso stress hysteresis loops for sample S2 under zero stress.

Fig. 32 Iso stress hysteresis loops for sample S2 under -200 MPa compression.

Fig. 33 Iso stress anhysteretic curves for sample S2.

Fig. 34 Iso stress initial magnetisation curves for sample S2.

Fig. 35 Changes in flux density B caused by a single stress of +140 MPa tension at different points along the initial magnetisation curve and around a hysteresis loop. The dashed line is the anhysteretic curve.

Fig. 36 Iso stress anhysteretic curves for sample S1.

Fig. 37 Iso stress initial magnetisation curves for sample S1.

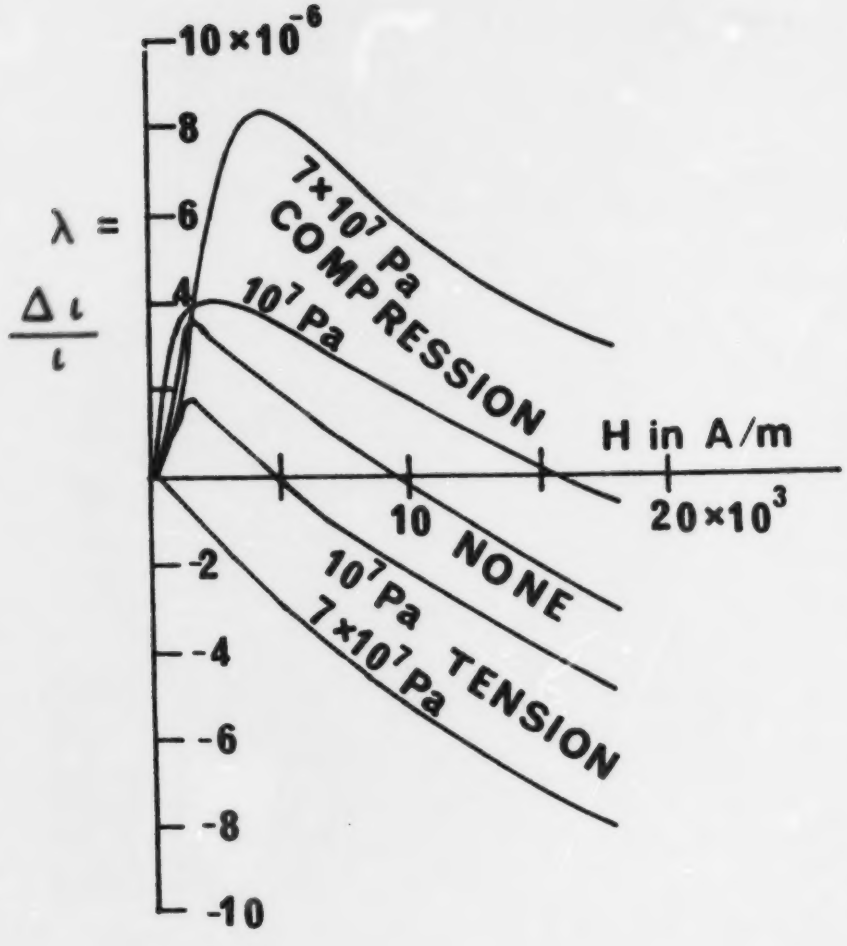
10×10^{-6}
8
6
4
-2
-4
-6
-8
-10
$\lambda = \frac{\Delta l}{l}$
7×10^7 Pa
COMPRESSION
10^7 Pa
H in A/m
10
20×10^3
NONE
10^7 Pa
TENSION
7×10^7 Pa

fig 1

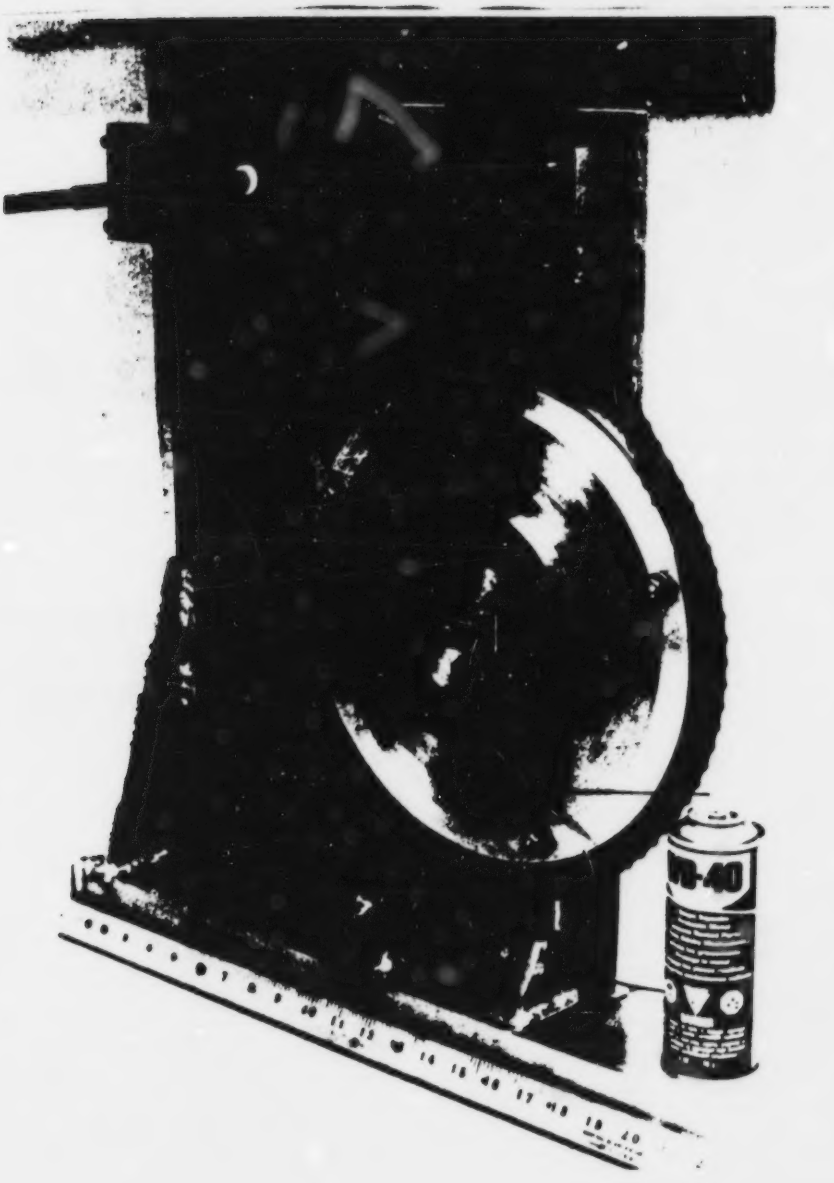

fig. 2

curve are shown in fig. 21

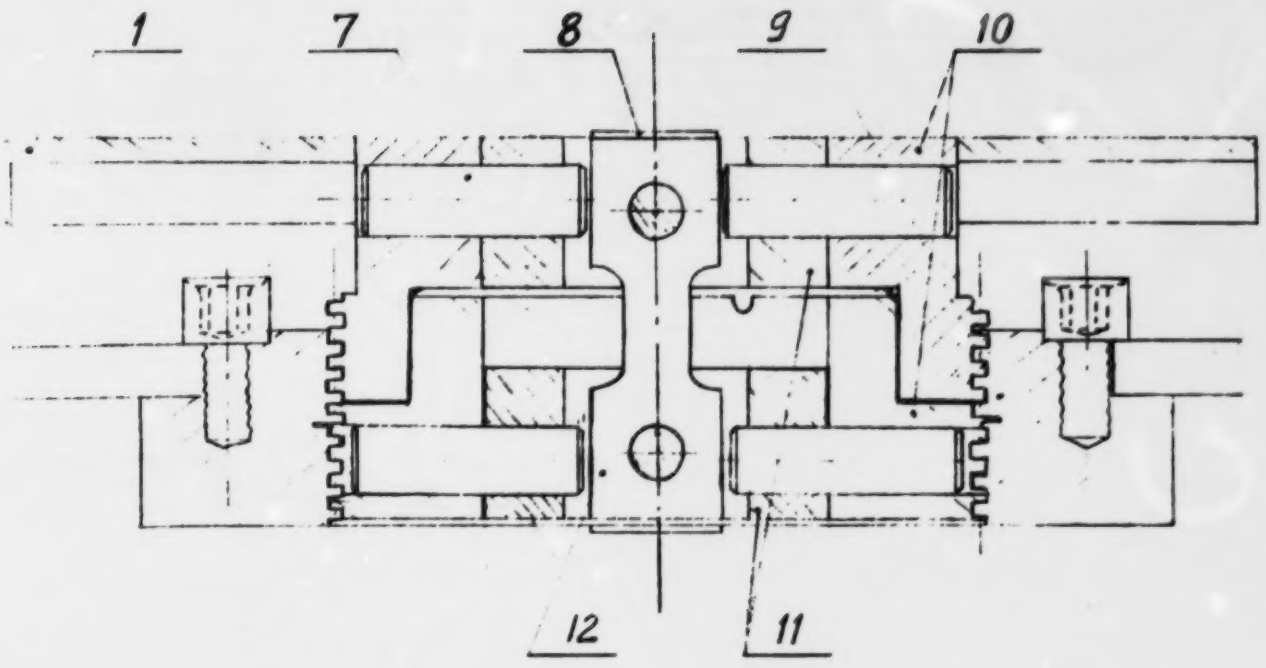

1 Supporting Plate
2 Stepping Motor Shaft
3 Gear Assembly
4 Hand Crank
5 Roller Chain
6 Chain Sprocket
7 Pivot
8 Guiding pins
9 Turnbuckle
10 Threaded End Piece
11 Sample Holder
12 Sample
13 Magnet Pole
14 Magnet Yoke

fig. 3

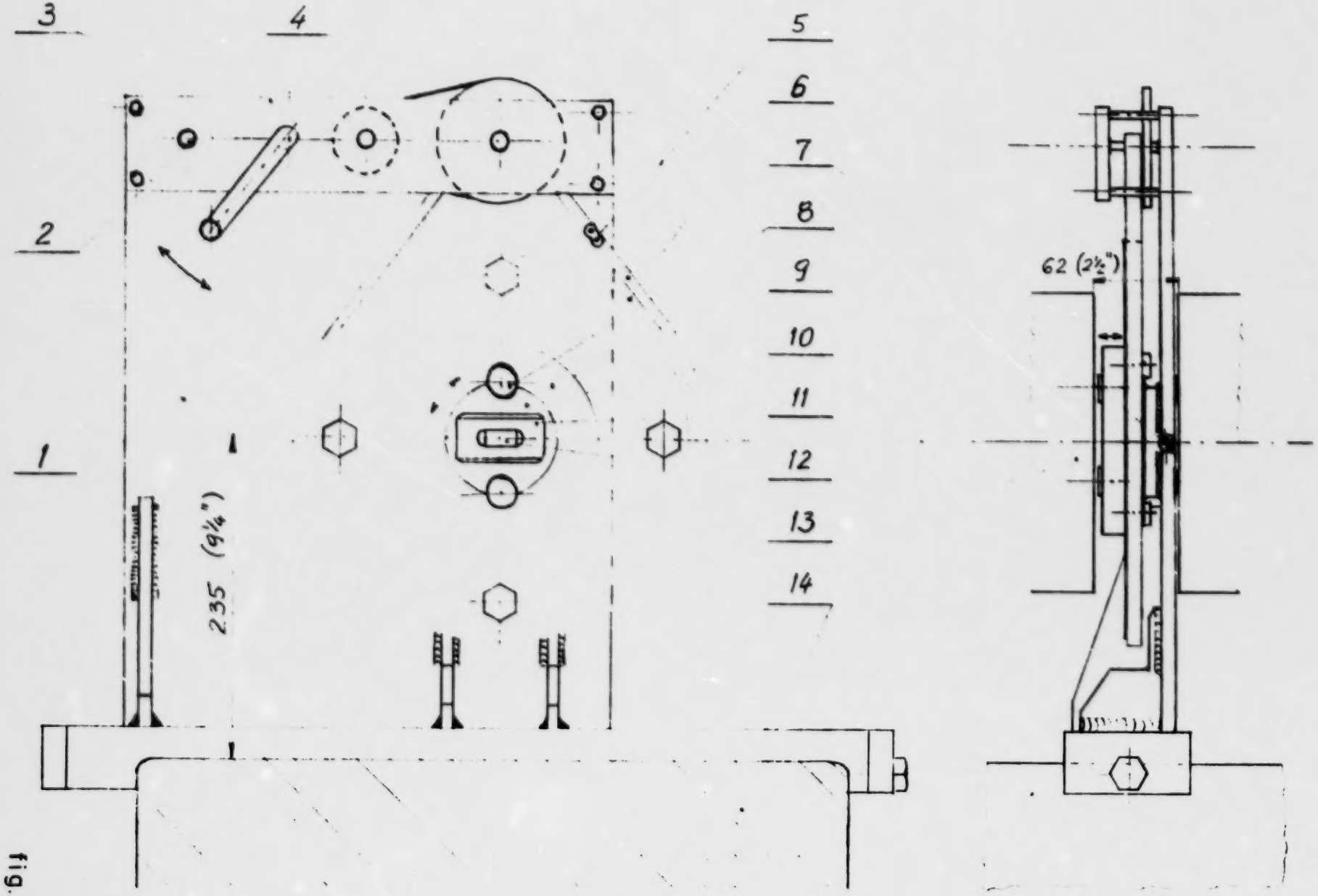

fig.4

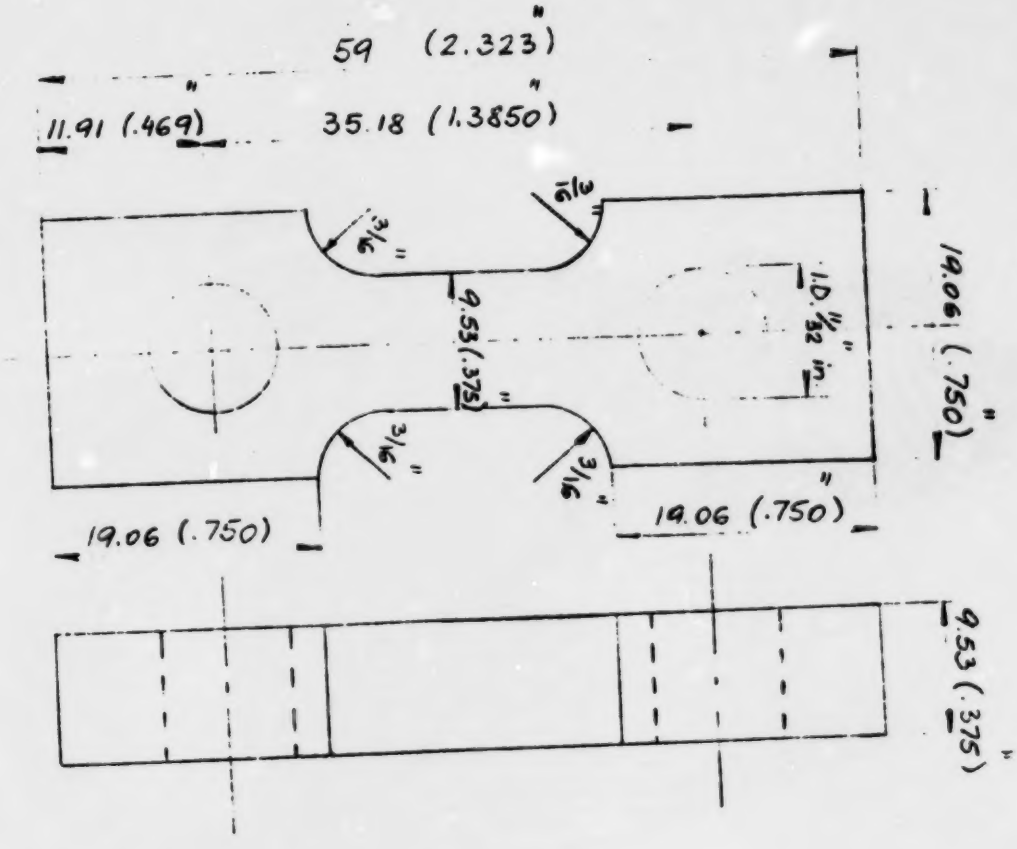
59 (2.323)"
11.91 (.469)"
35.18 (1.3850)"
3/16"
1/16"
9.53 (.375)"
I.D. 11/32"
19.06 (.750)"
3/16"
3/16"
19.06 (.750)"
19.06 (.750)"
9.53 (.375)"

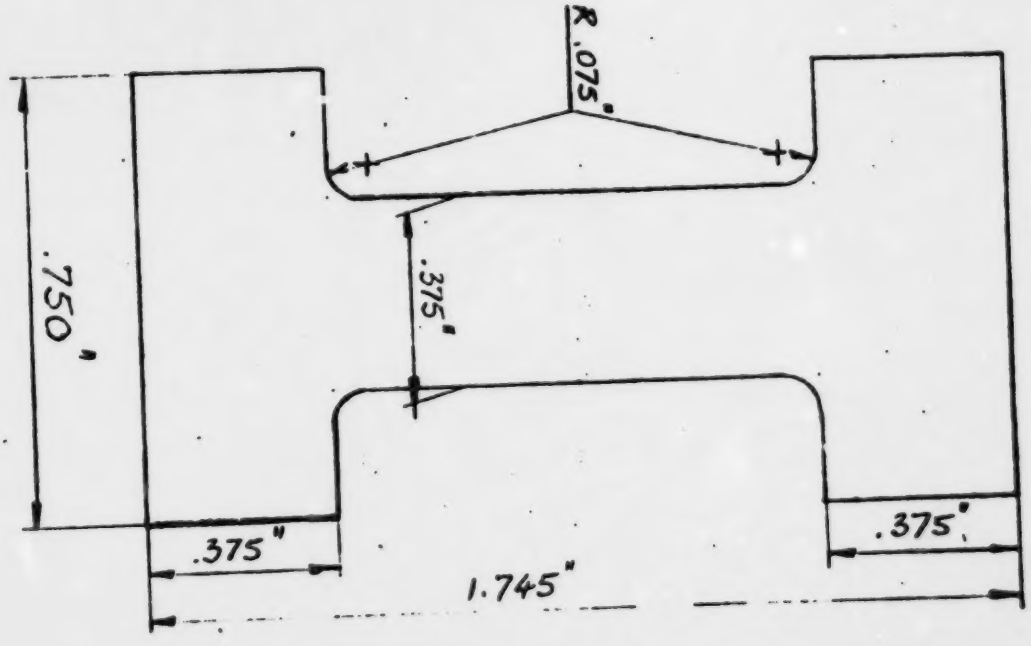
R .075"
.750"
.375"
.375"
.375"
1.745"

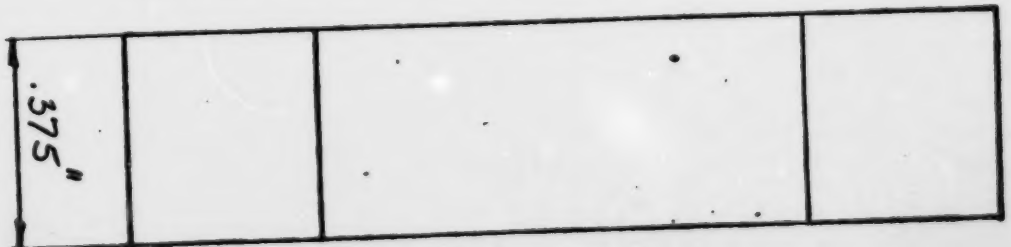
.375"

fig 5

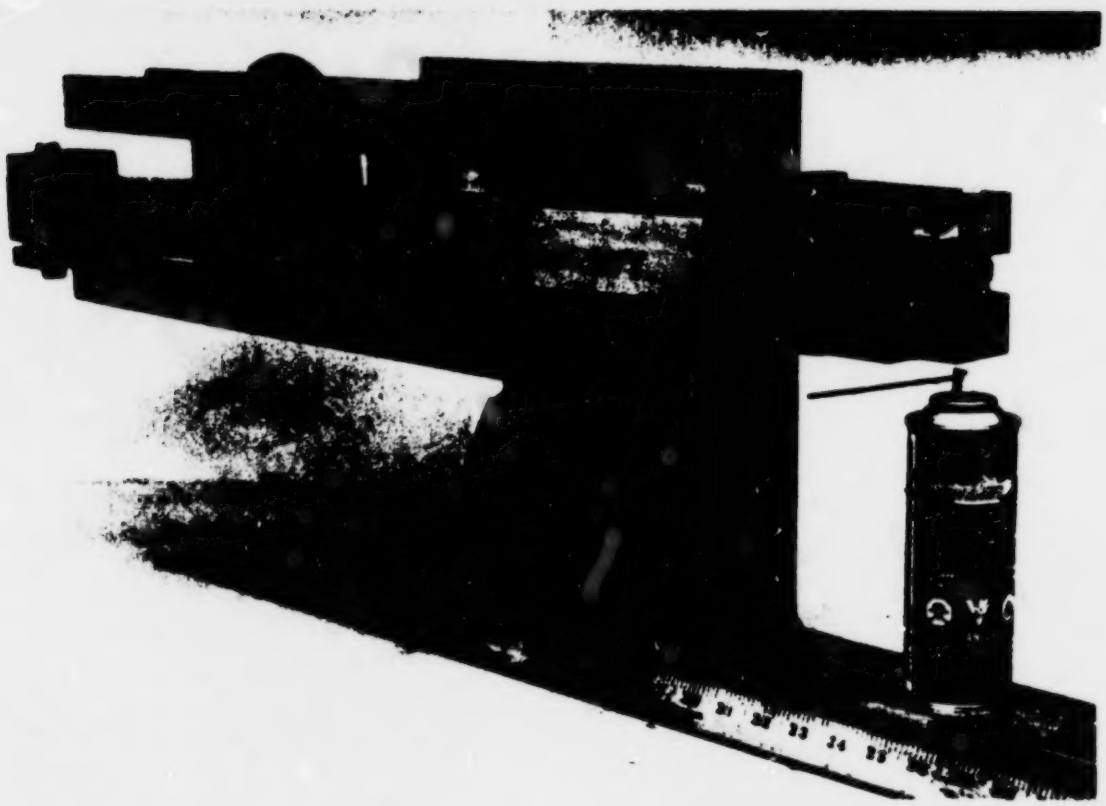

fig. 6

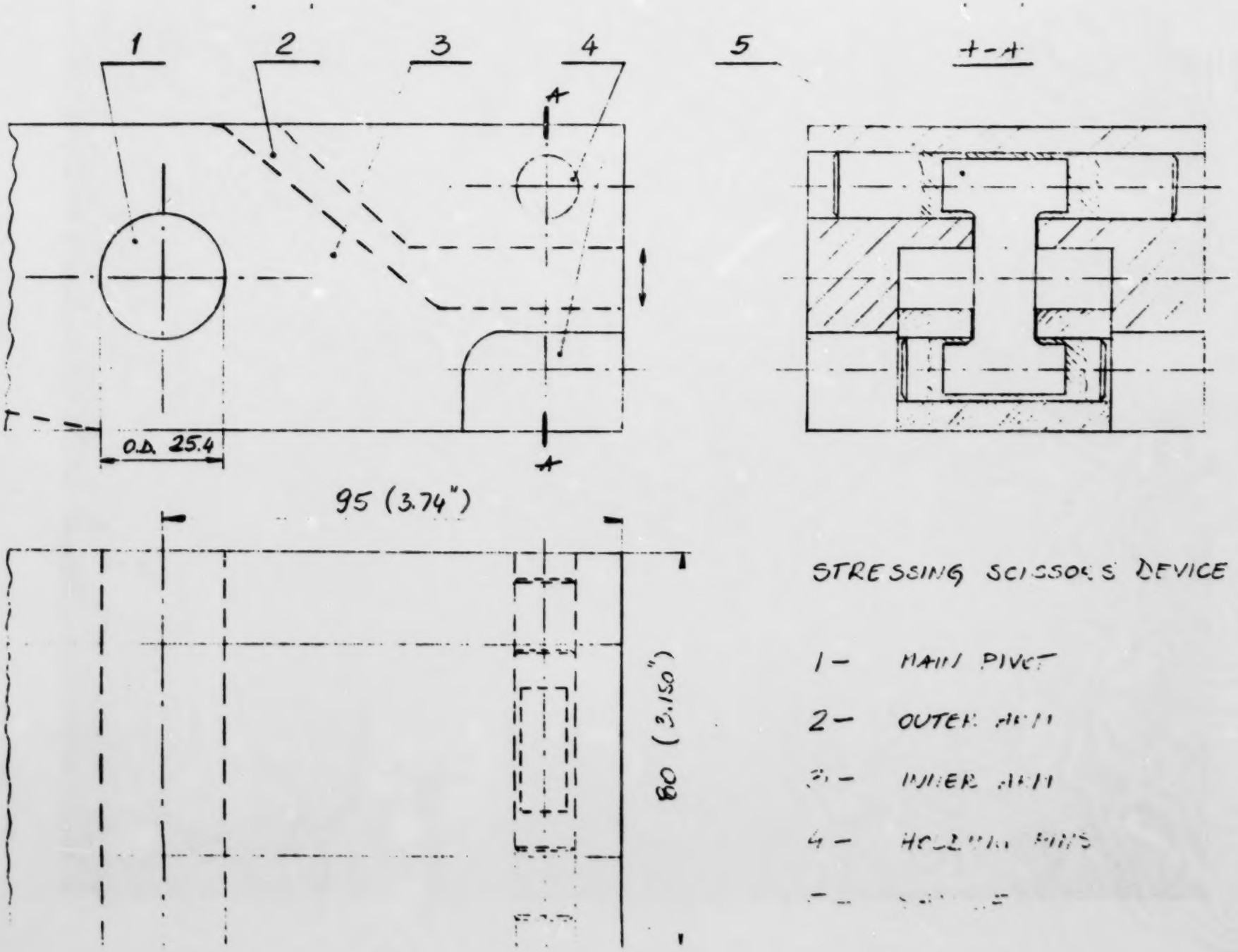

Fig. 7

STRESSING SCISSORS DEVICE

1 – MAIN PIVOT

2 – OUTER ARM

3 – INNER ARM

4 – HOLDING PINS

5 – [illegible]

fig. 8

CIRCUIT DIAGRAM FOR THE STRAIN GAUGE BRIDGE

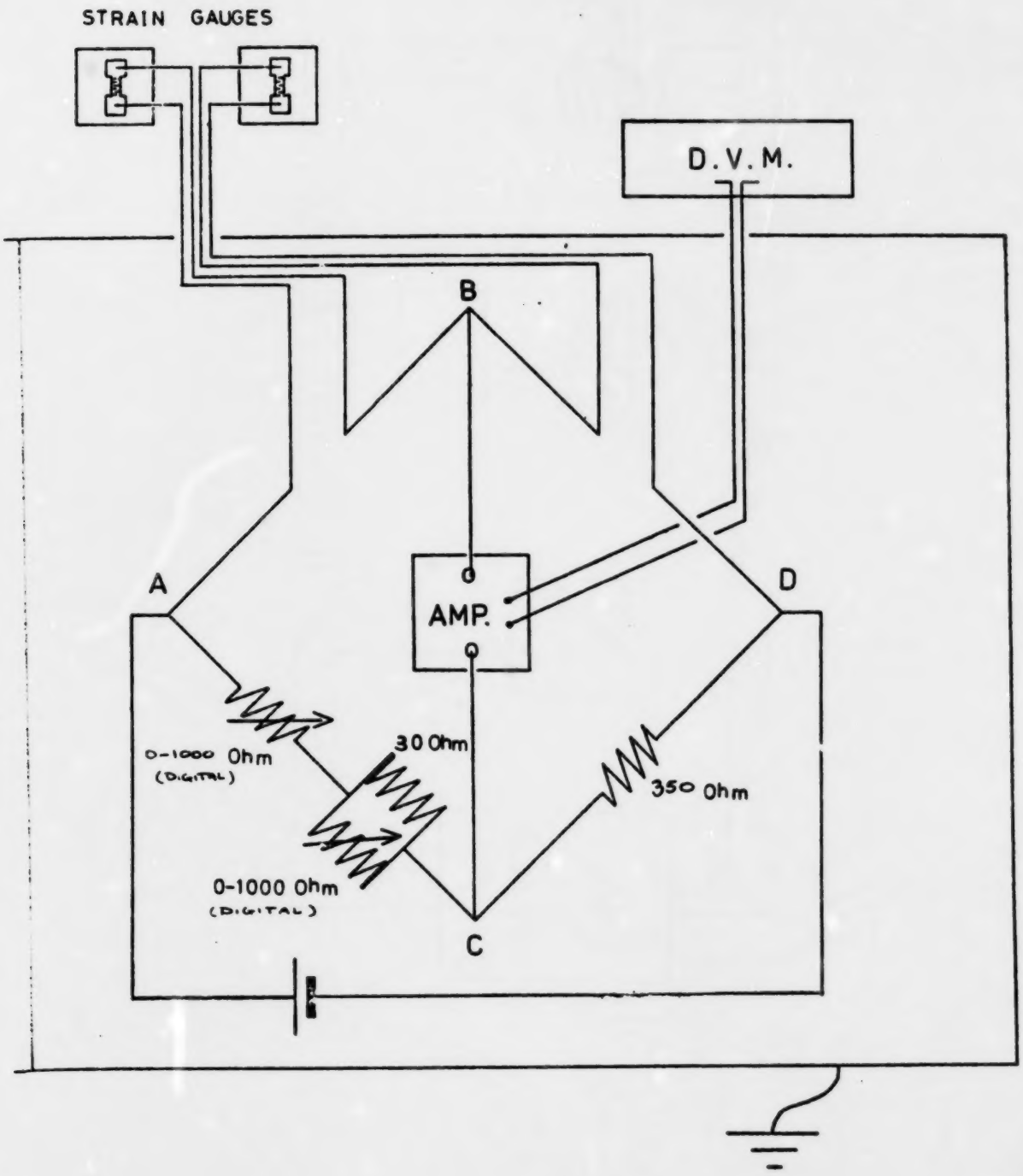

fig. 9

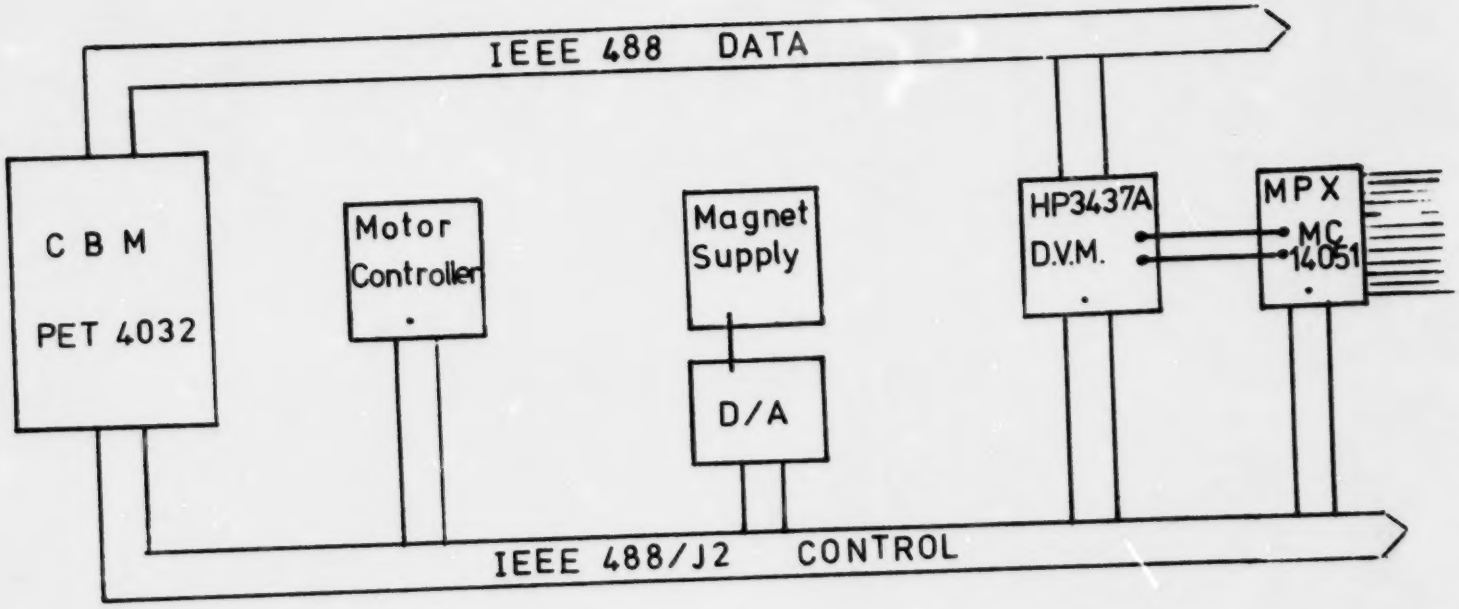
IEEE 488 DATA
C B M
PET 4032
Motor
Controller
Magnet
Supply
D/A
HP3437A
D.V.M.
MPX
MC
14051
IEEE 488/J2 CONTROL

fig. 10

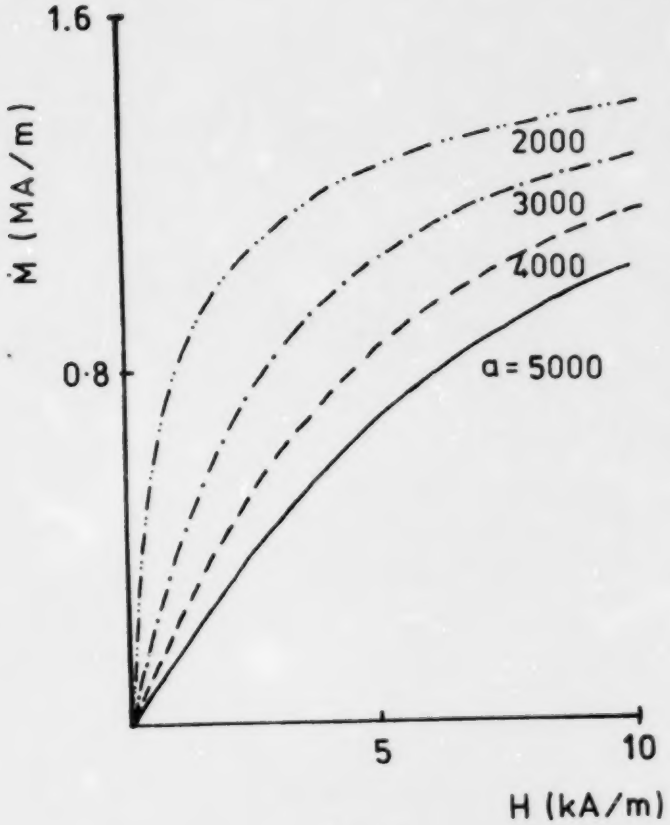

fig.11a

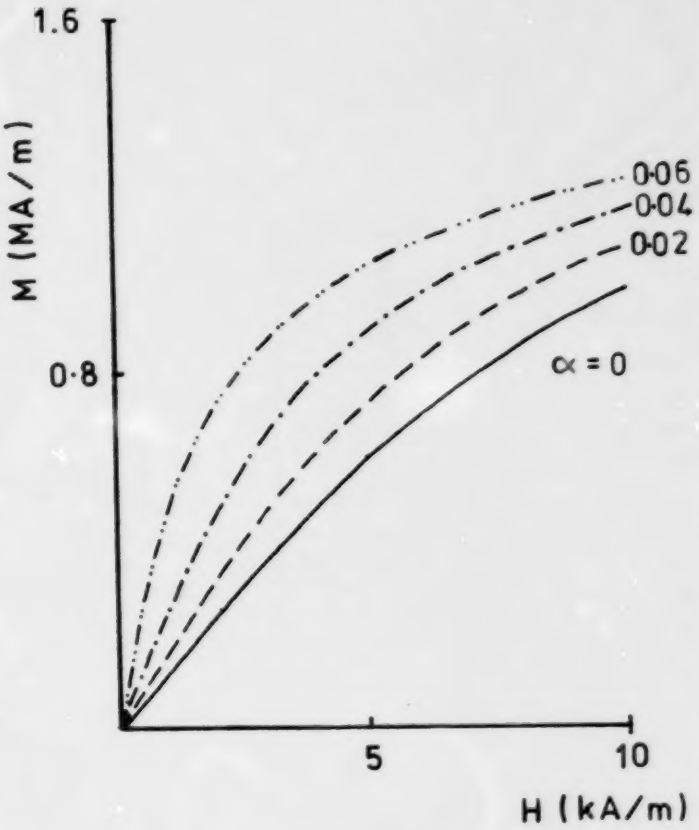

fig.11b

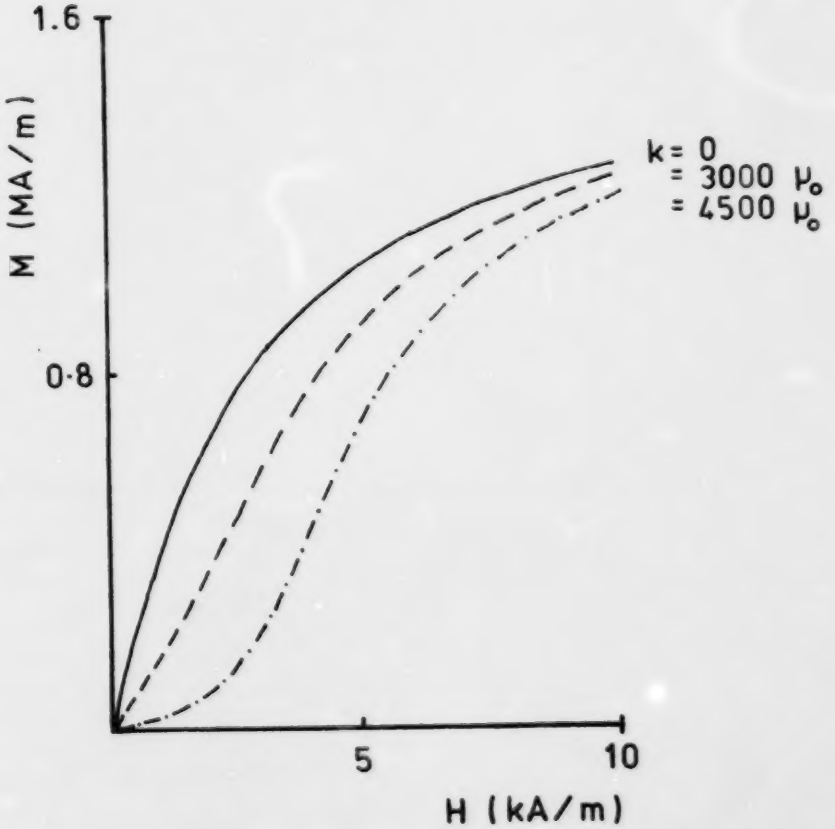

fig.11c

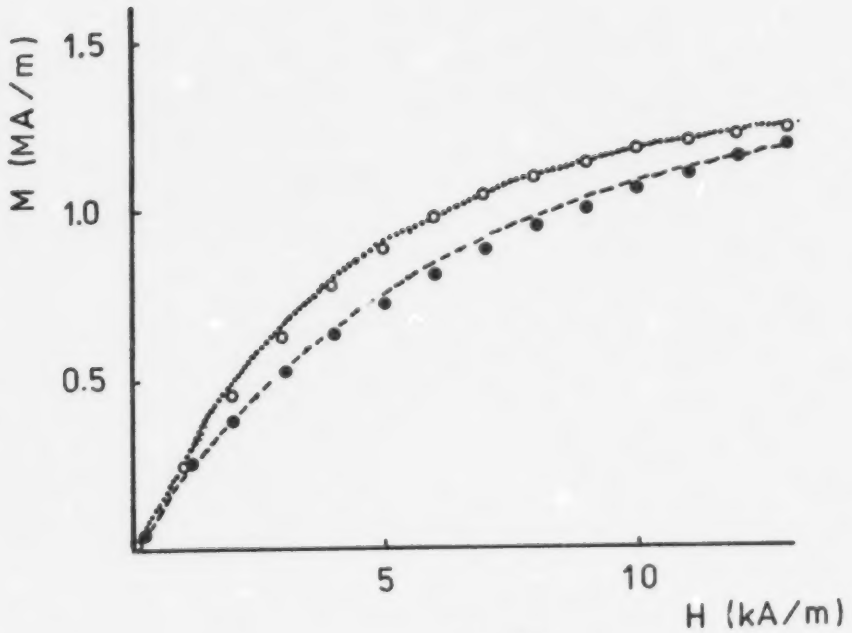

fig.12a

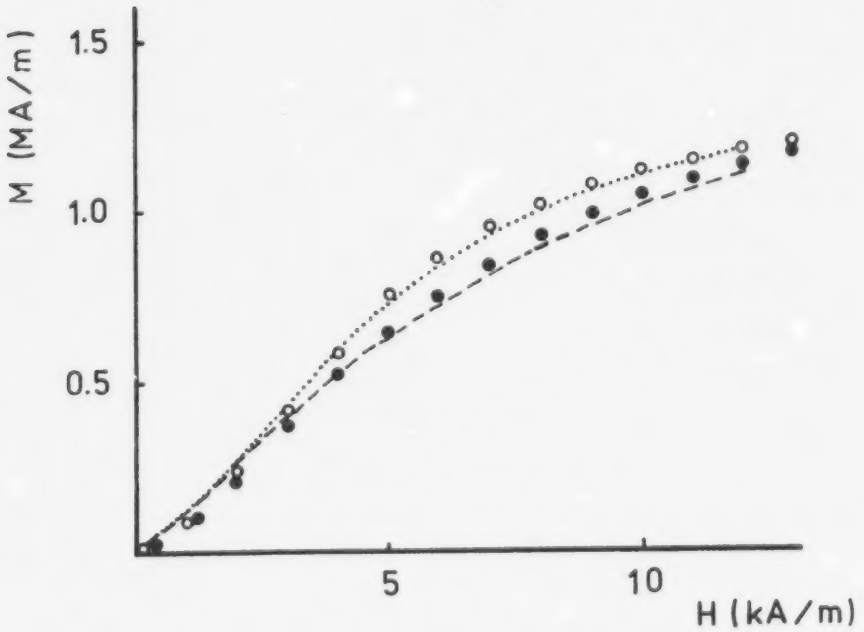

fig.12b

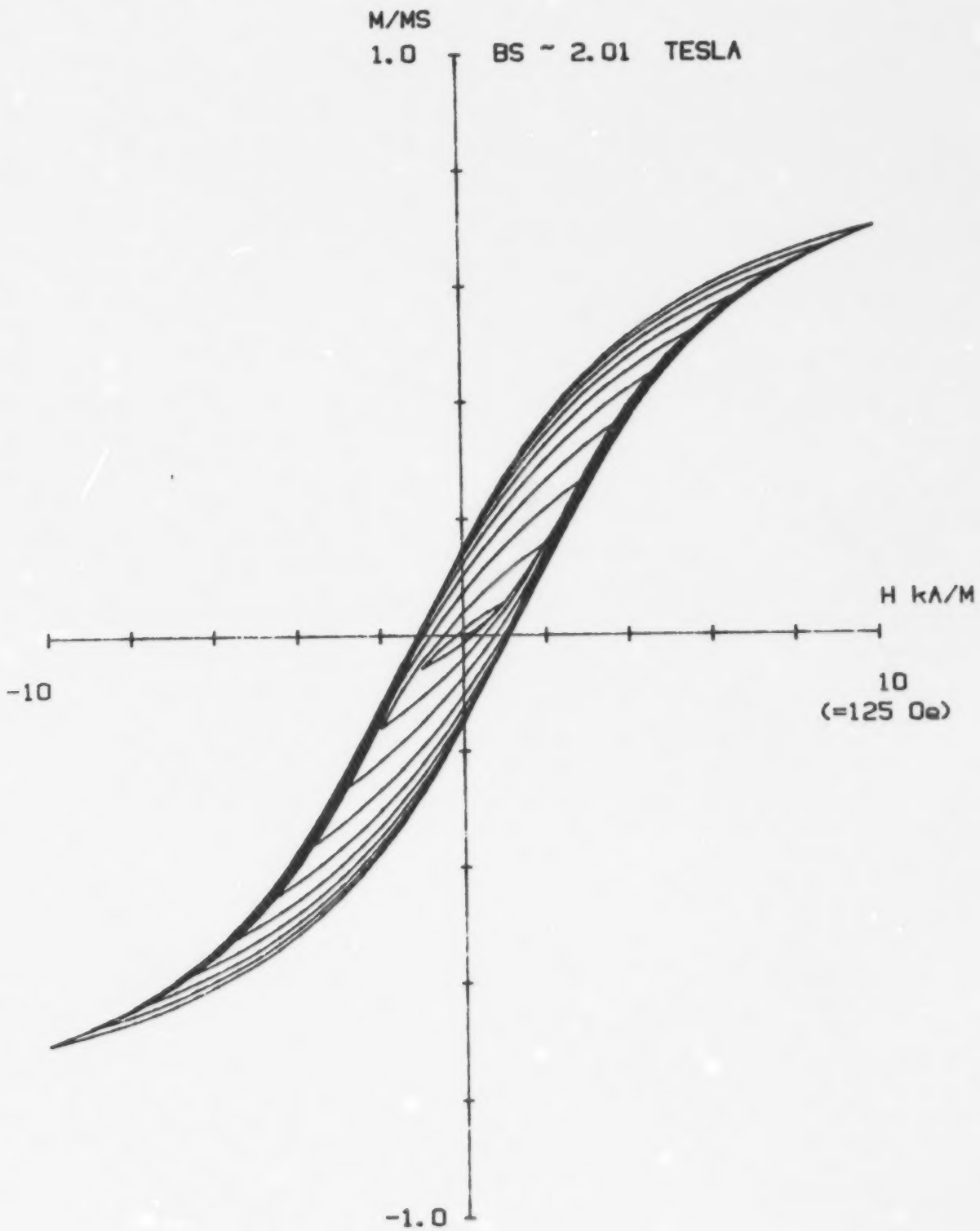

fig.13

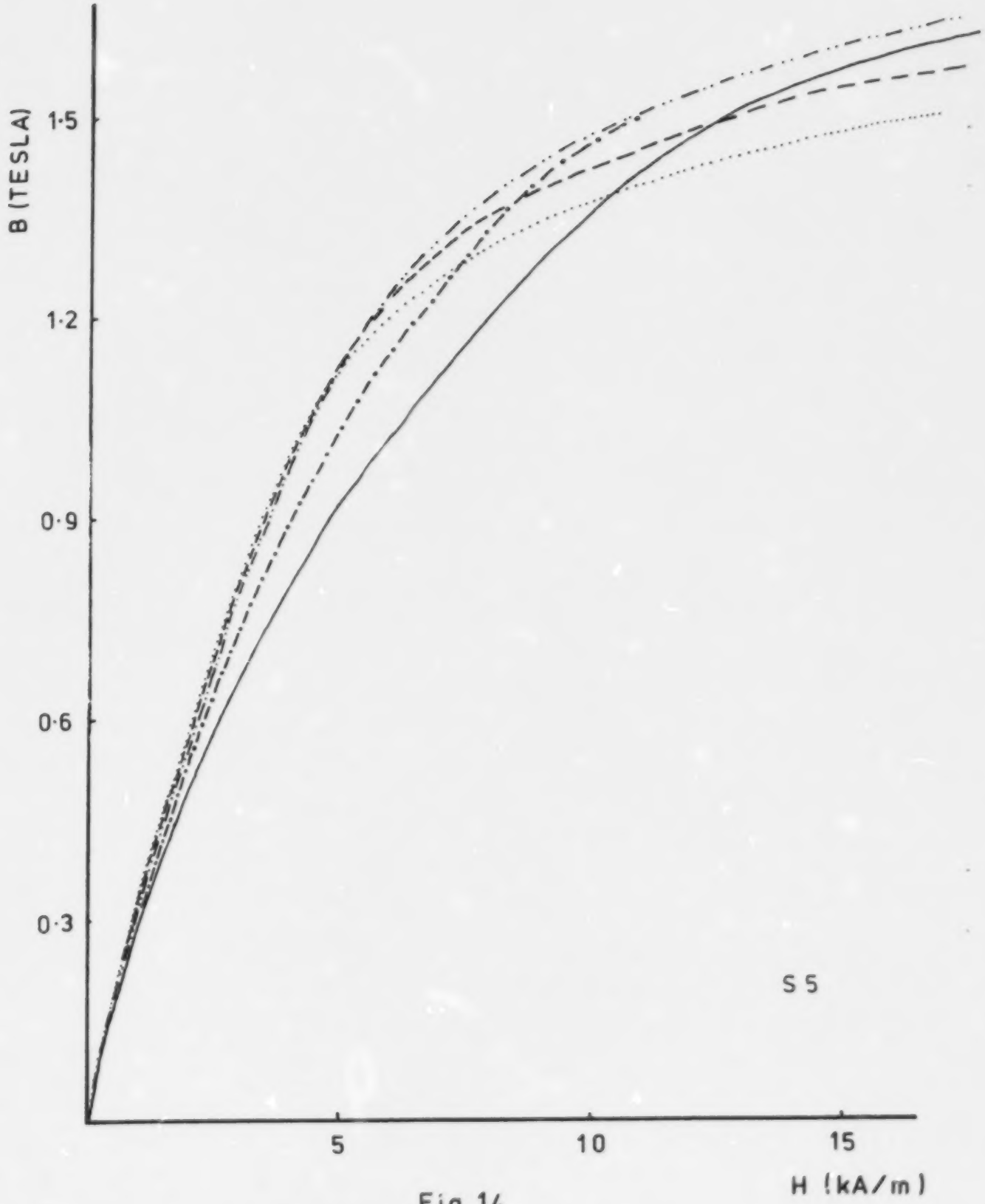

Fig. 14

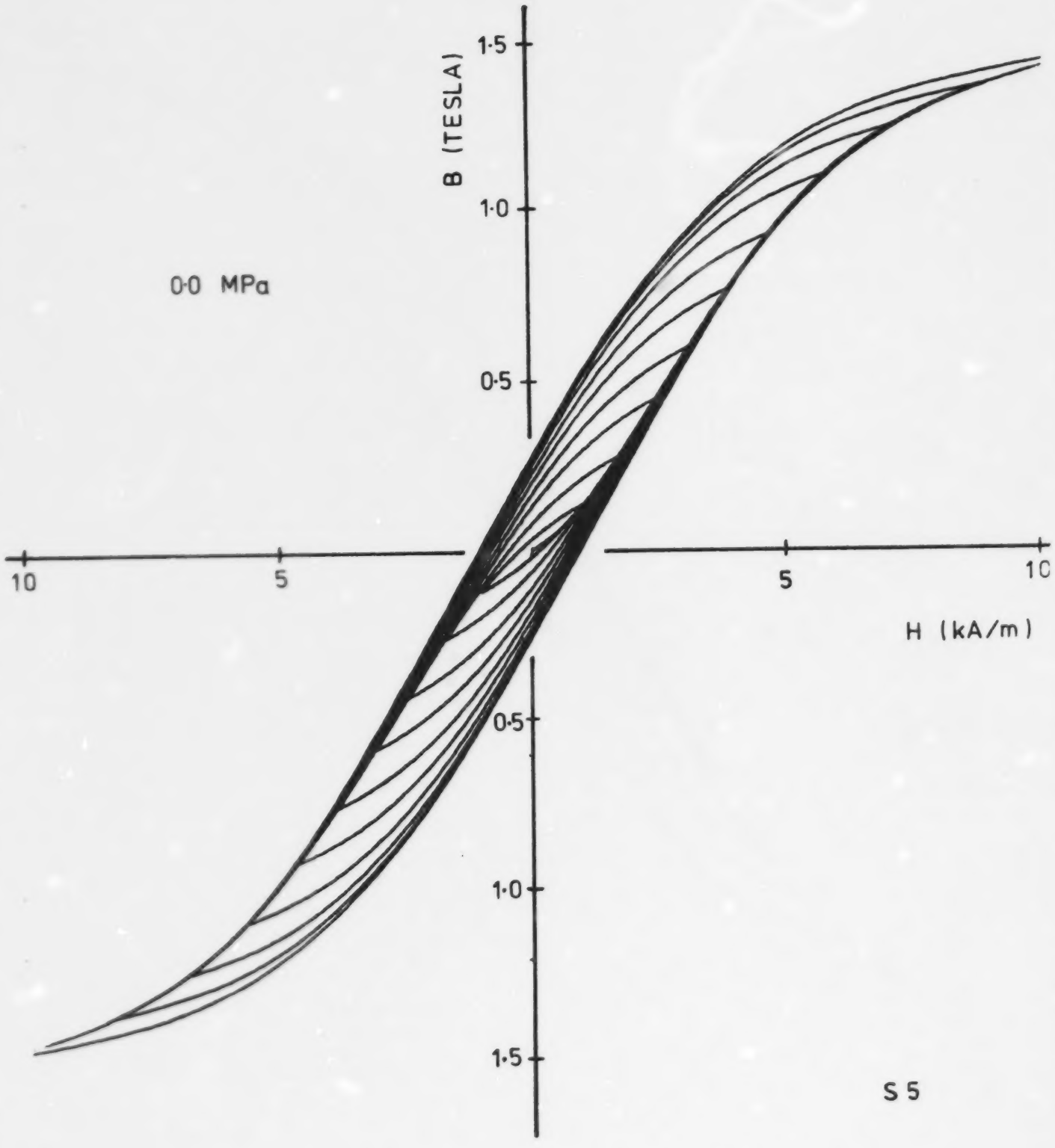

fig. 15

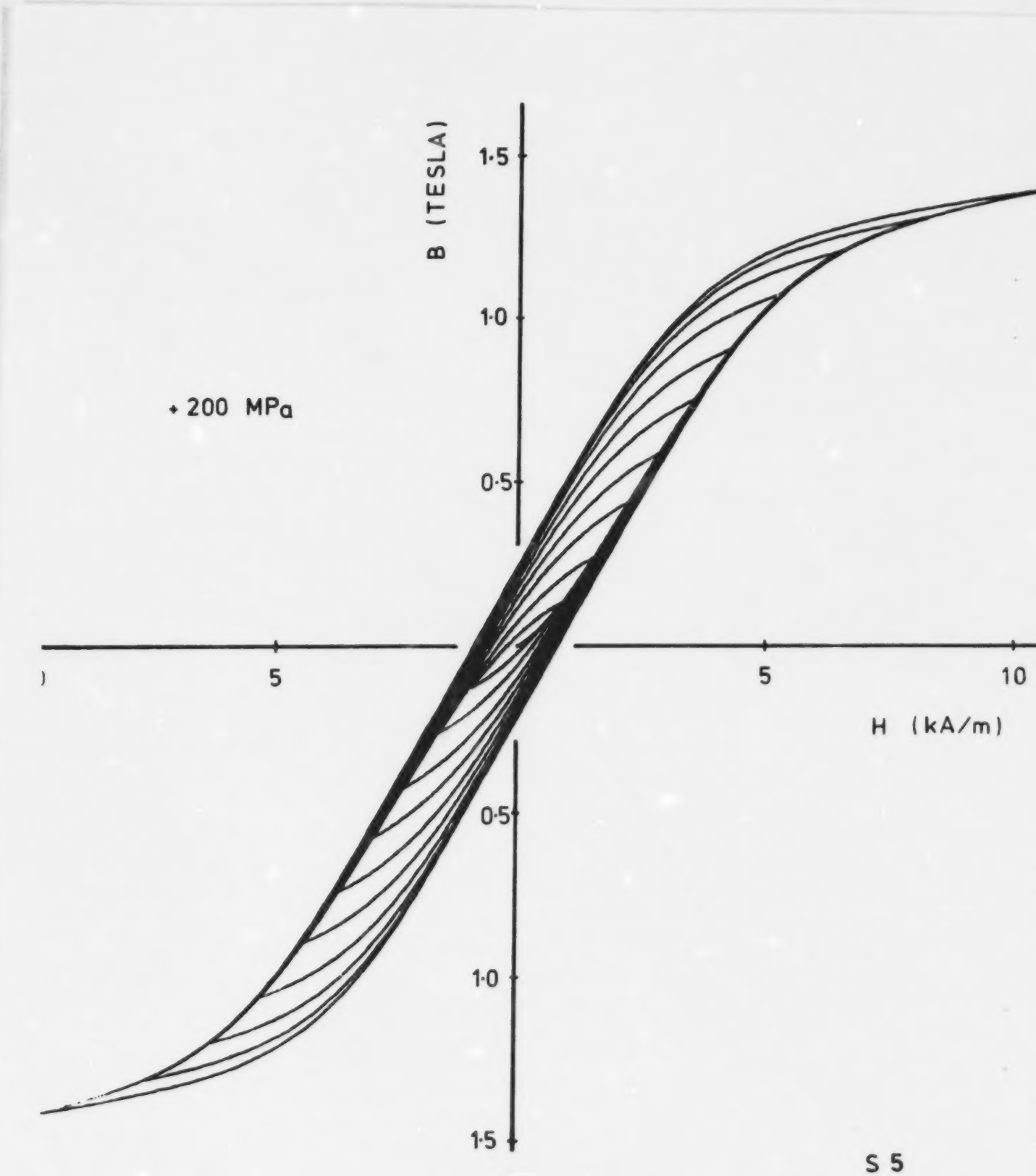

fig. 16

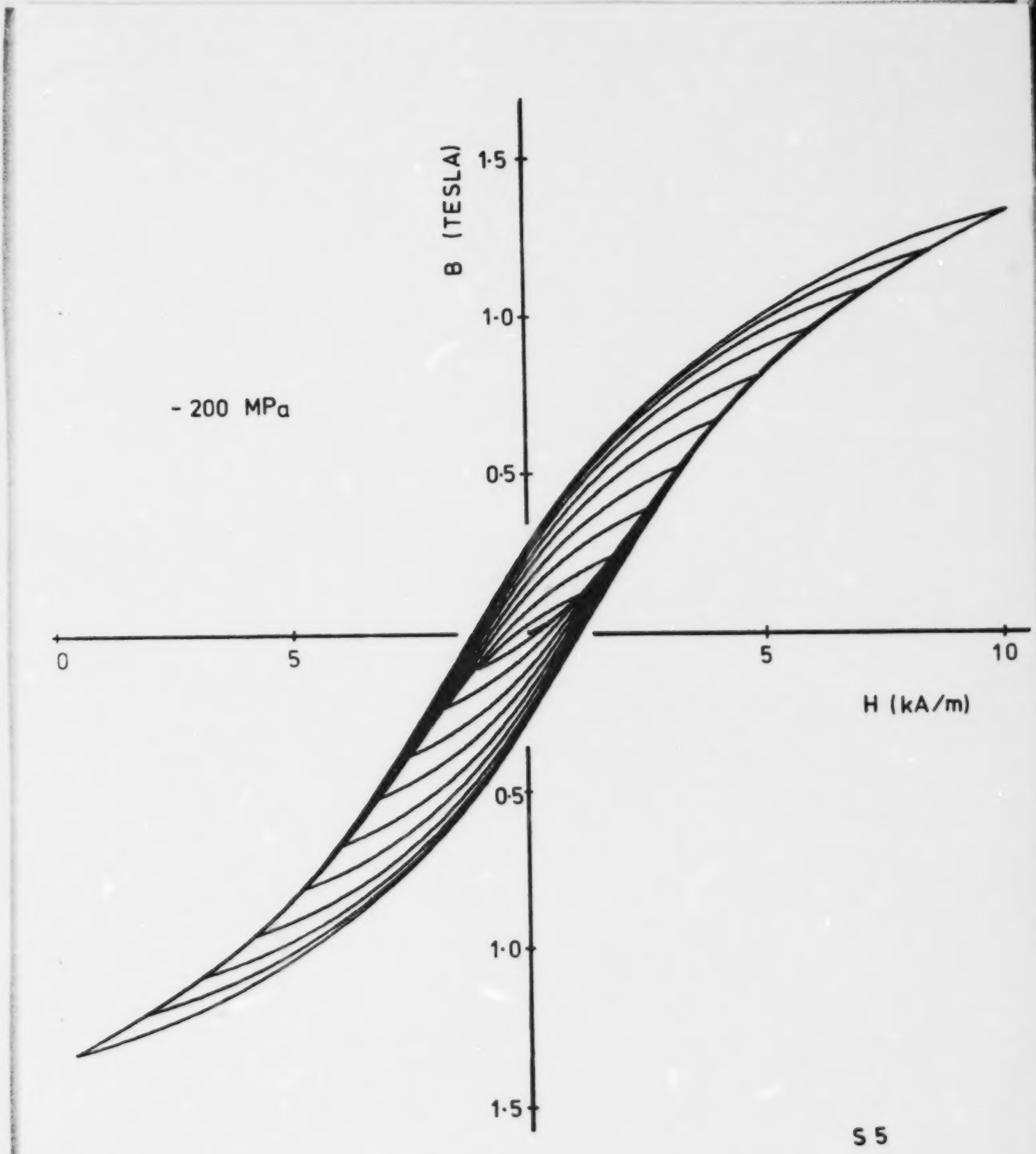

fig.17

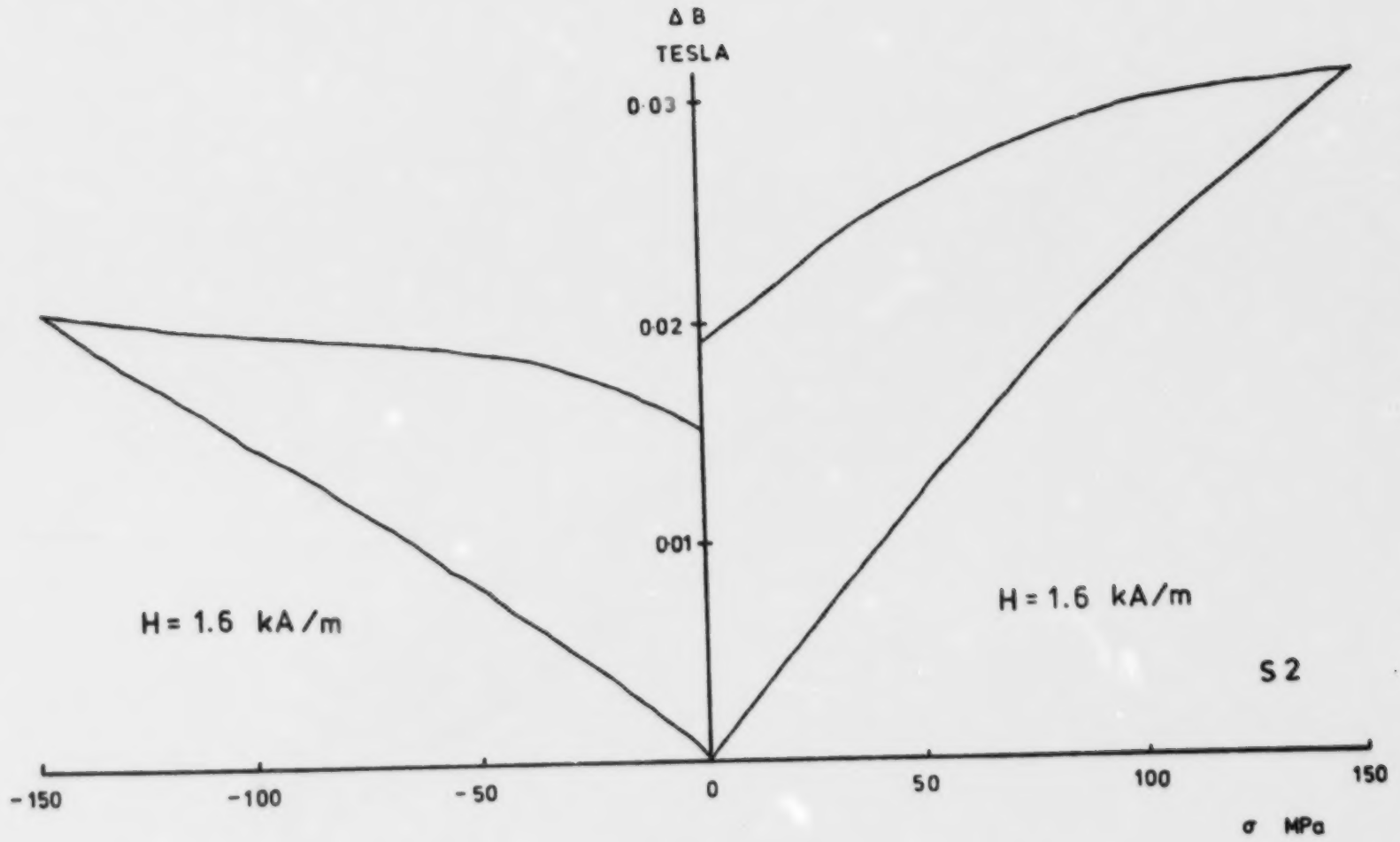
ΔB
TESLA
0·03
0·02
0·01
H = 1.6 kA/m
H = 1.6 kA/m
S 2
-150
-100
-50
0
50
100
150
σ MPa

fig. 18

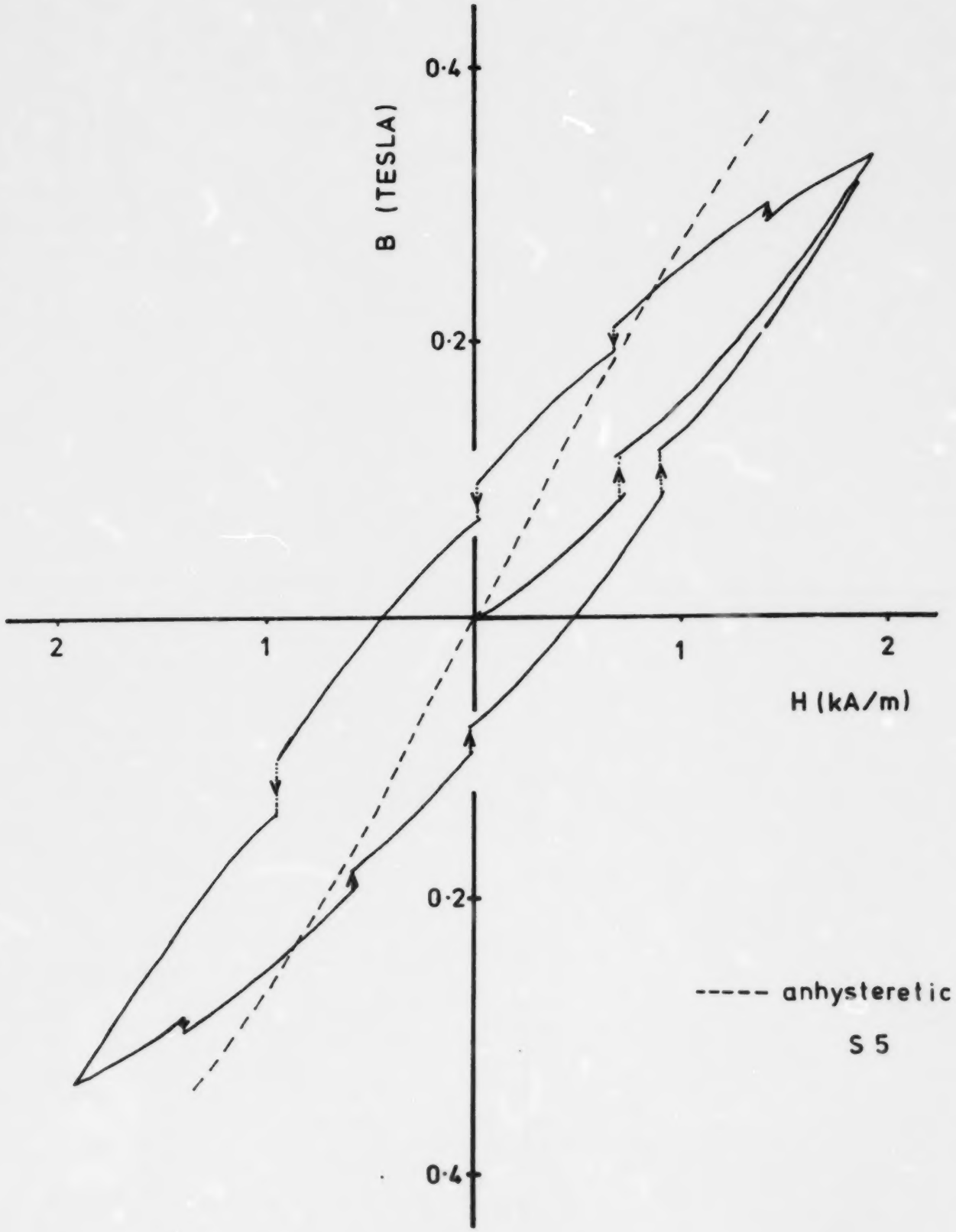

fig. 19

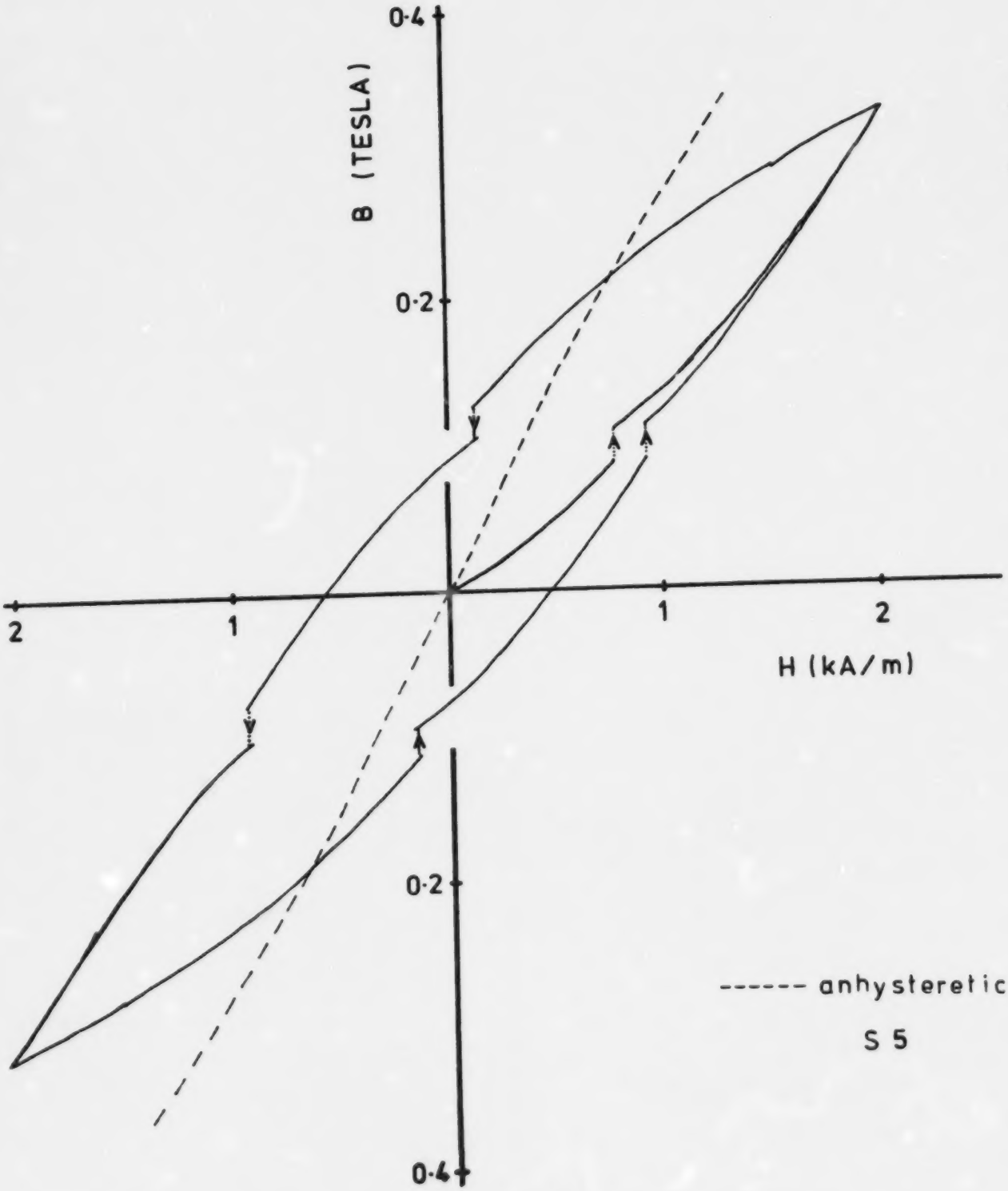

fig.20

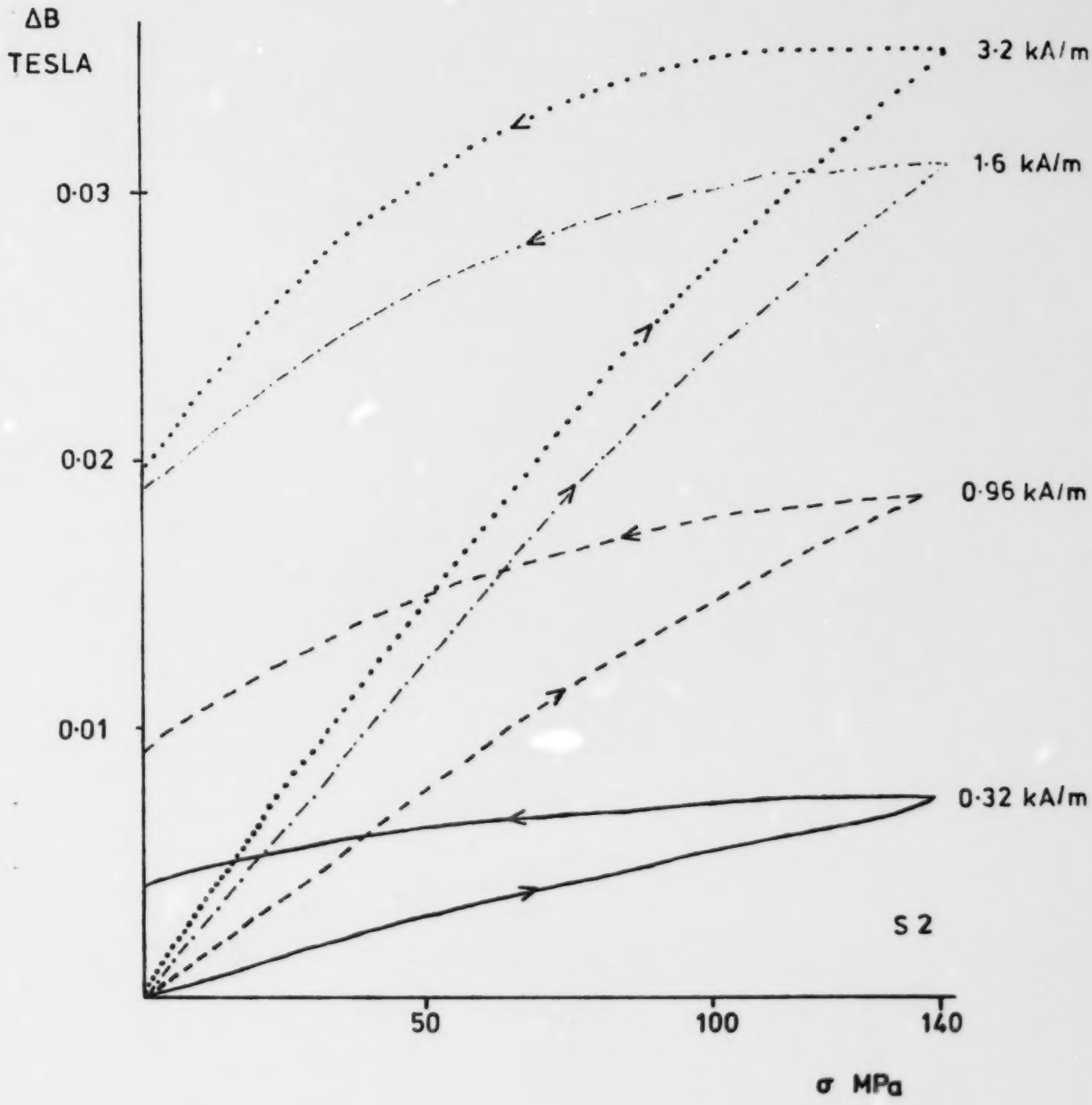
ΔB
TESLA
0·03
0·02
0·01
3·2 kA/m
1·6 kA/m
0·96 kA/m
0·32 kA/m
S 2
50
100
140
σ MPa

fig. 21

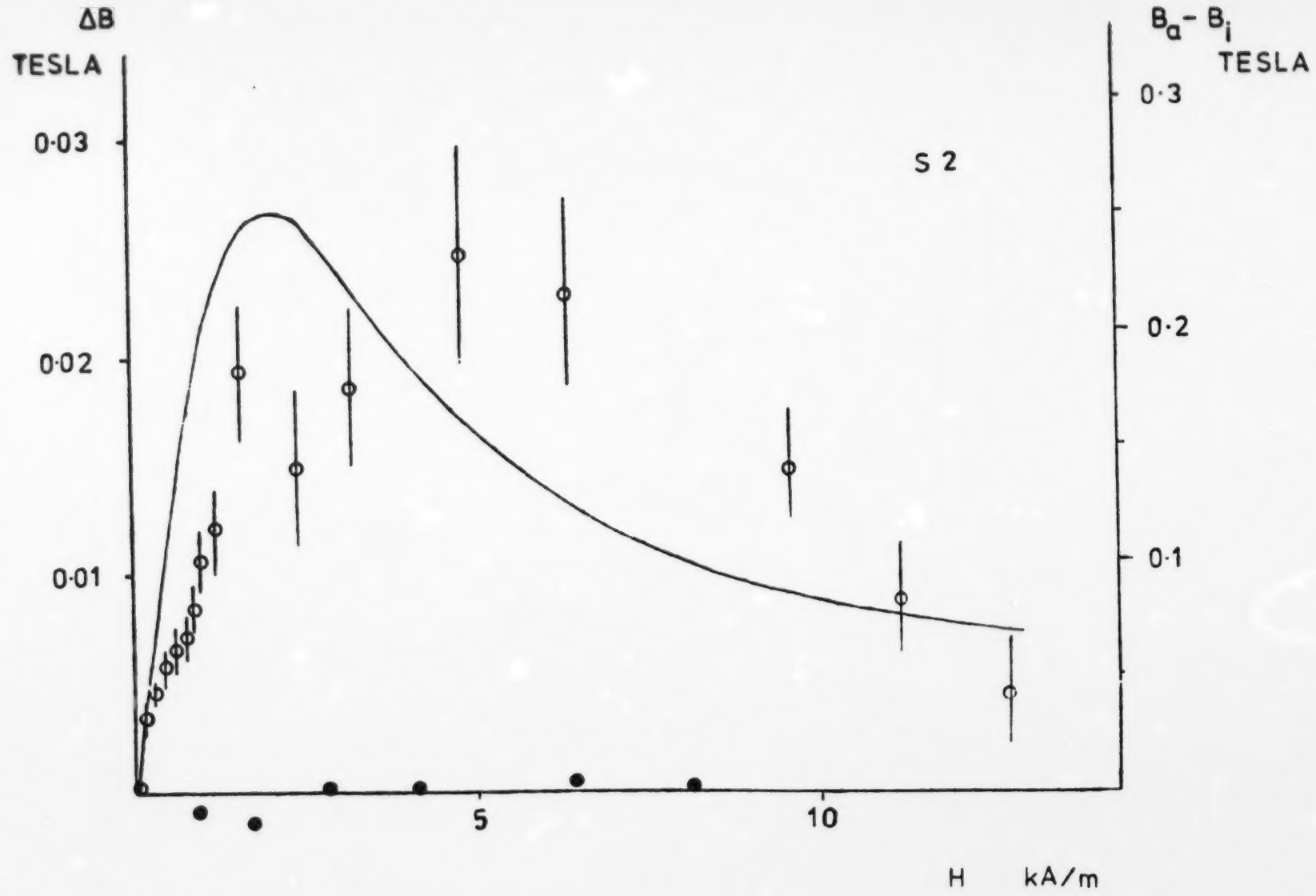

fig. 22

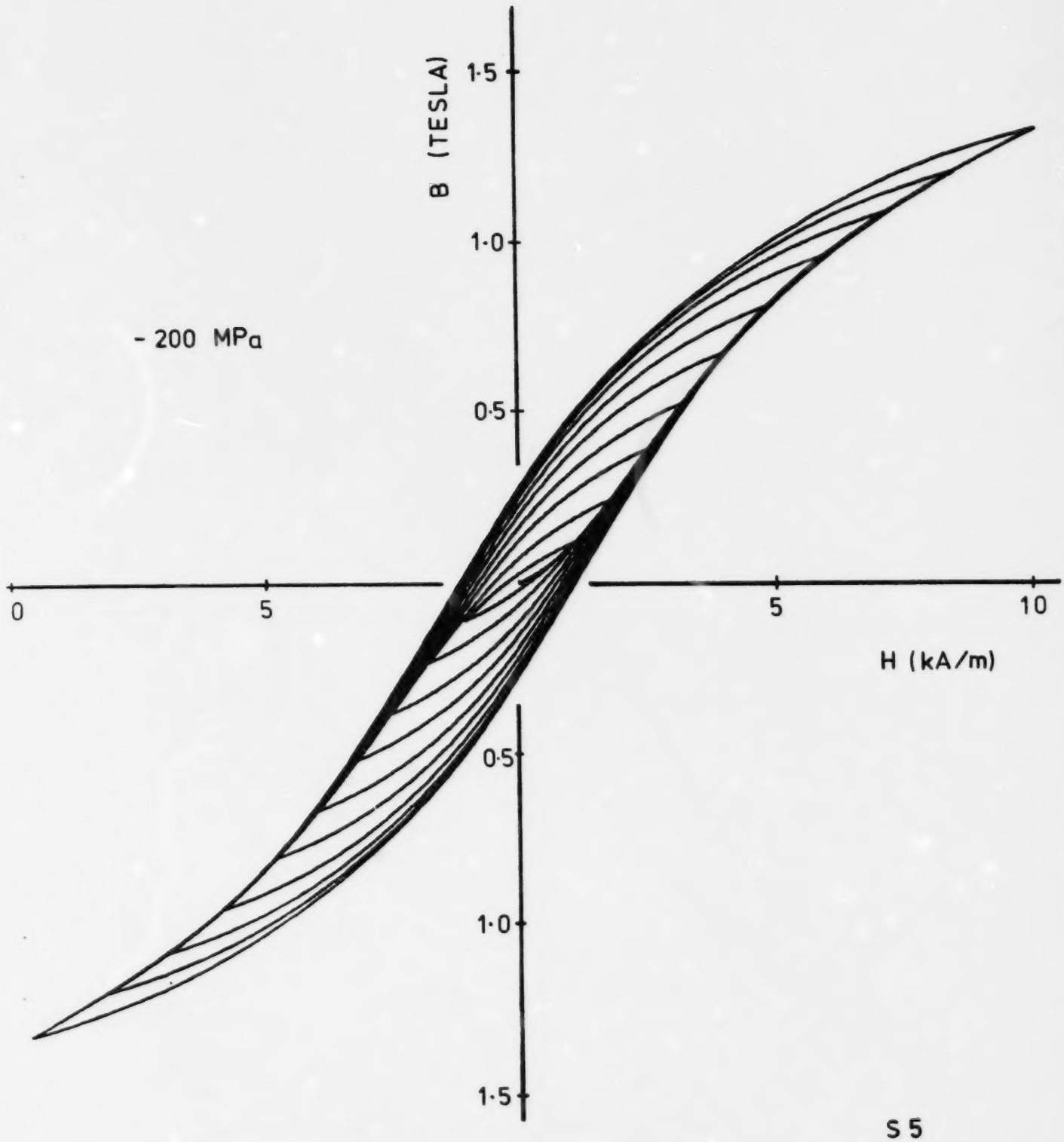

fig. 23

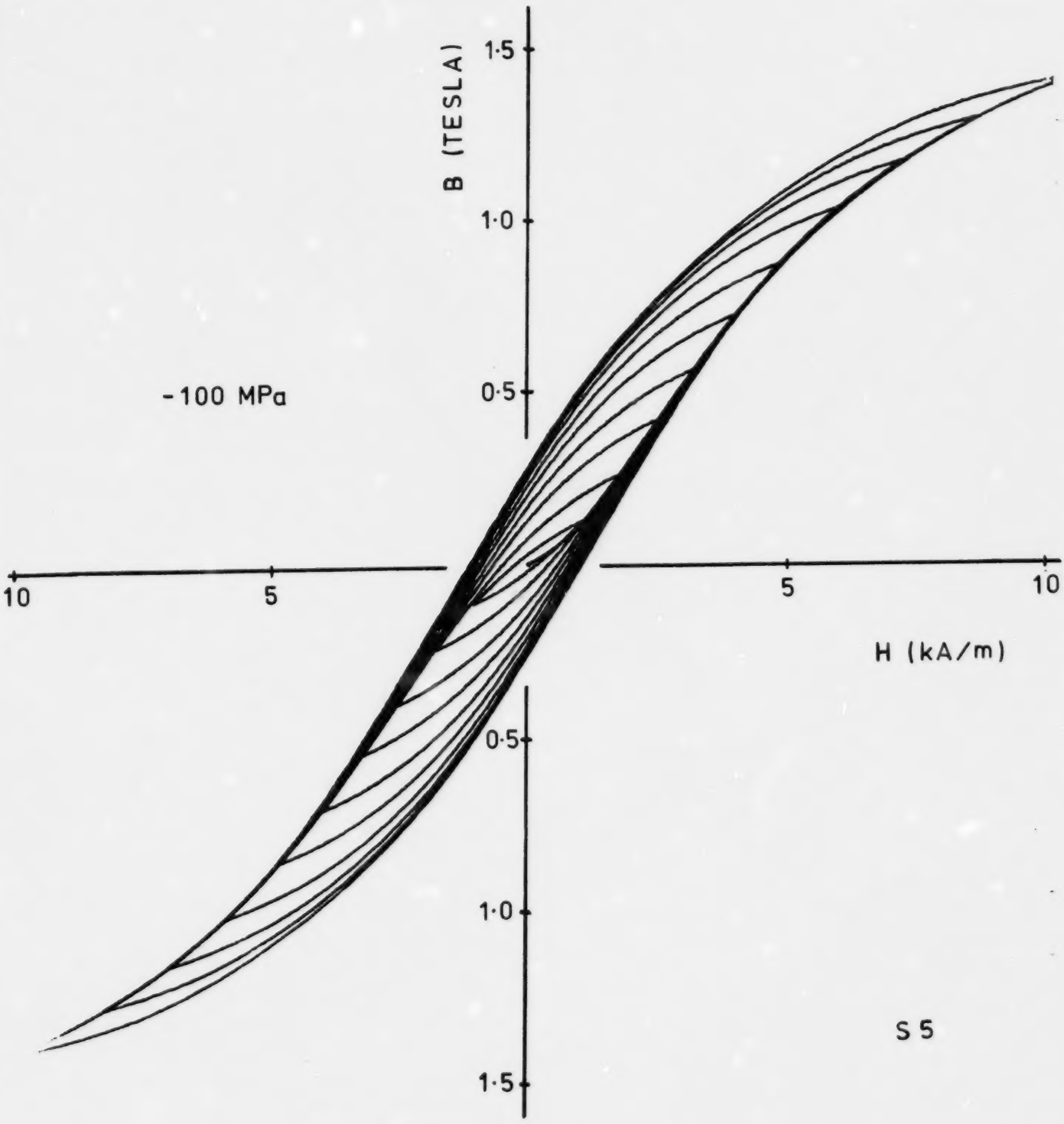

fig. 24

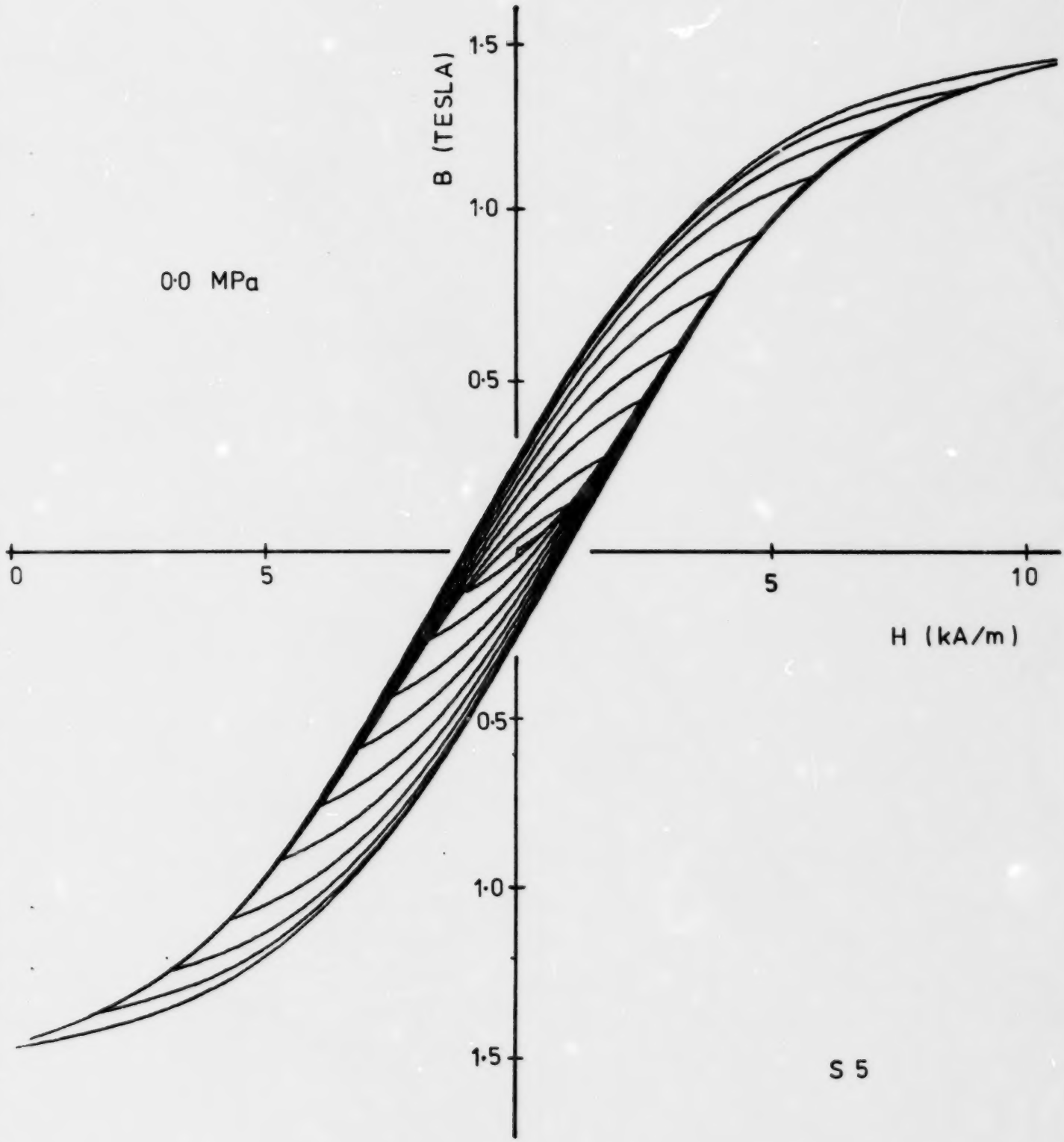

fig. 25

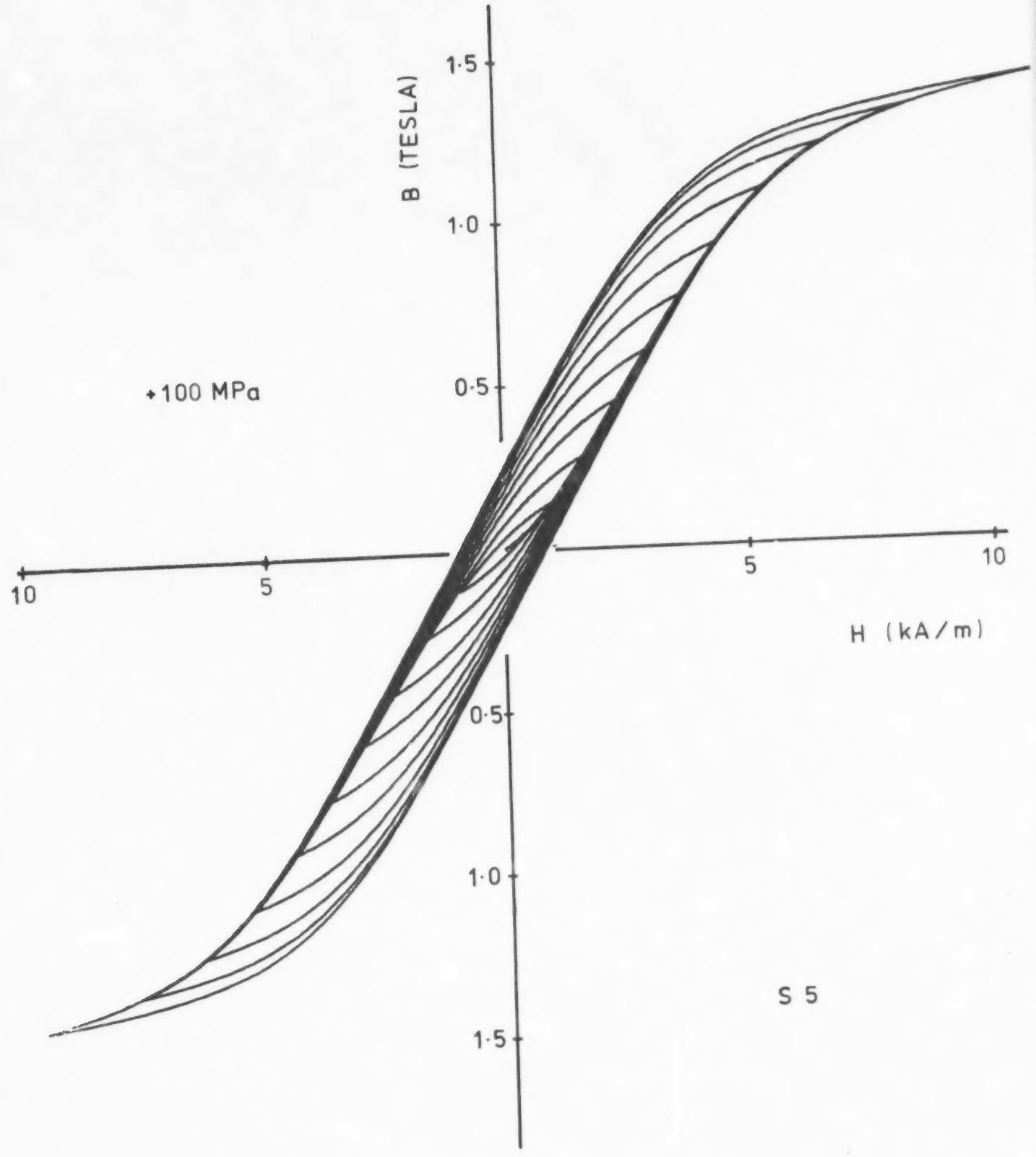

fig. 26

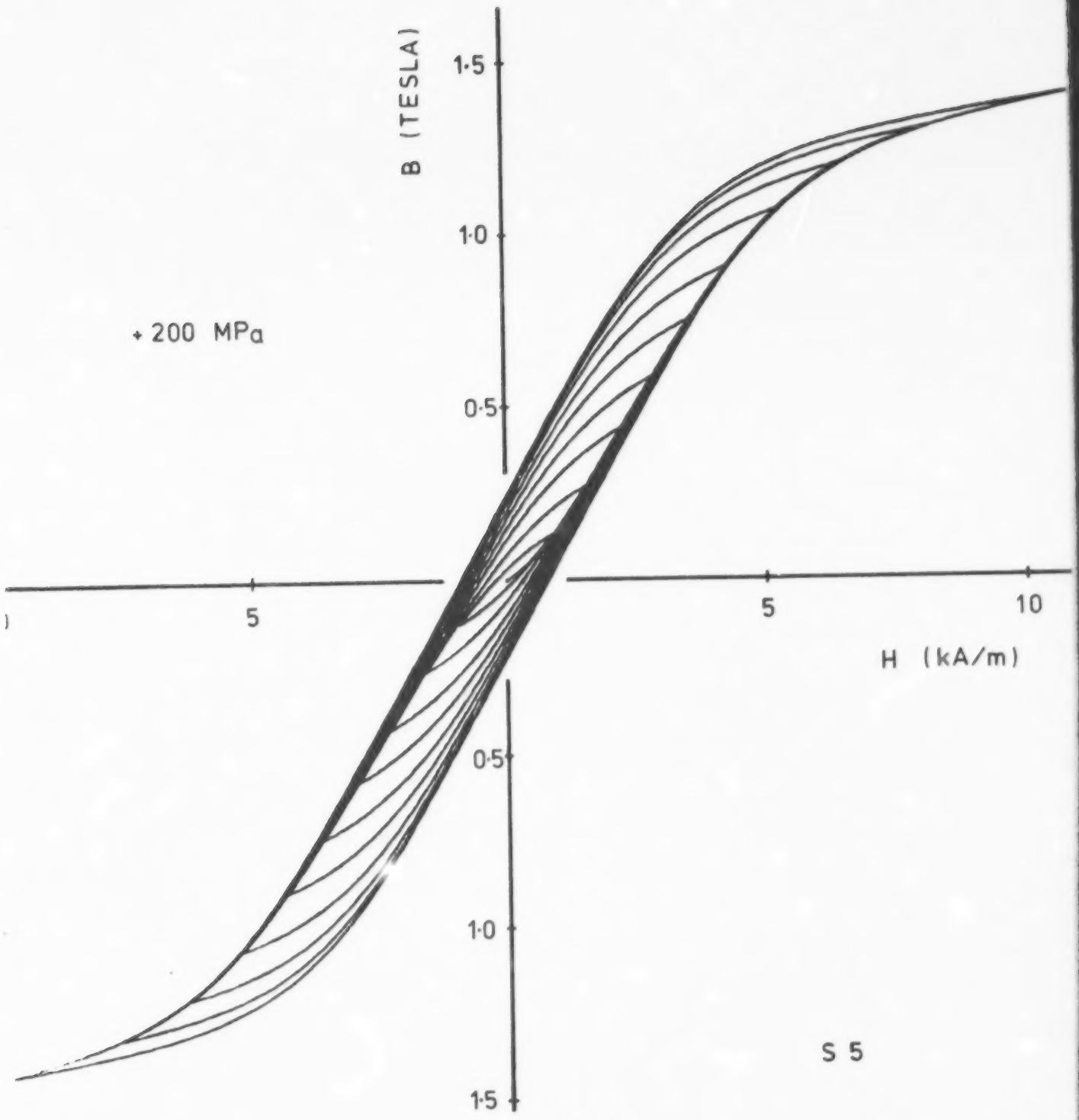

fig. 27

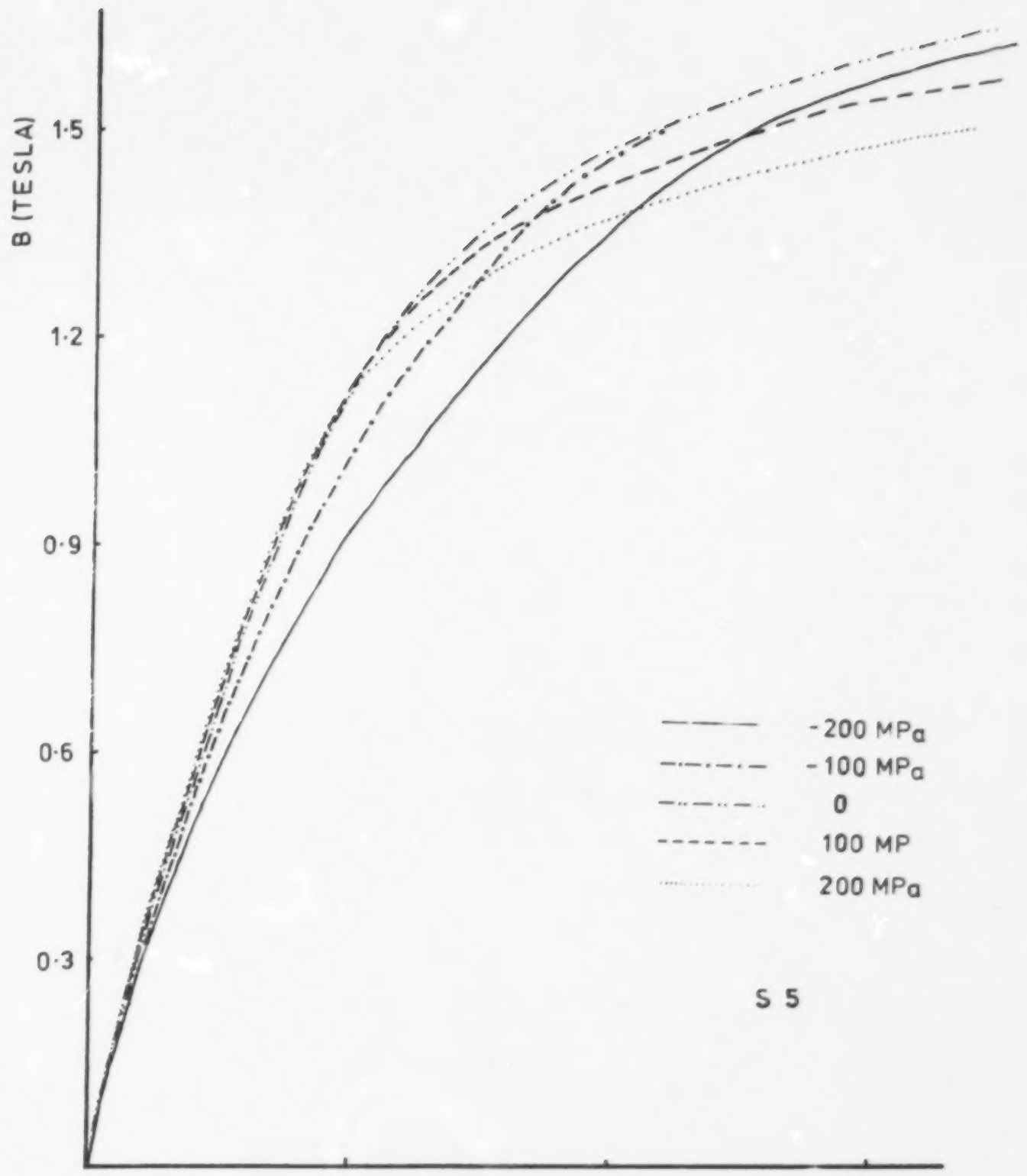
B (TESLA)
1·5
1·2
0·9
0·6
0·3
5
10
15
H (kA/m)
-200 MPa
-100 MPa
0
100 MP
200 MPa
S 5

fig 28

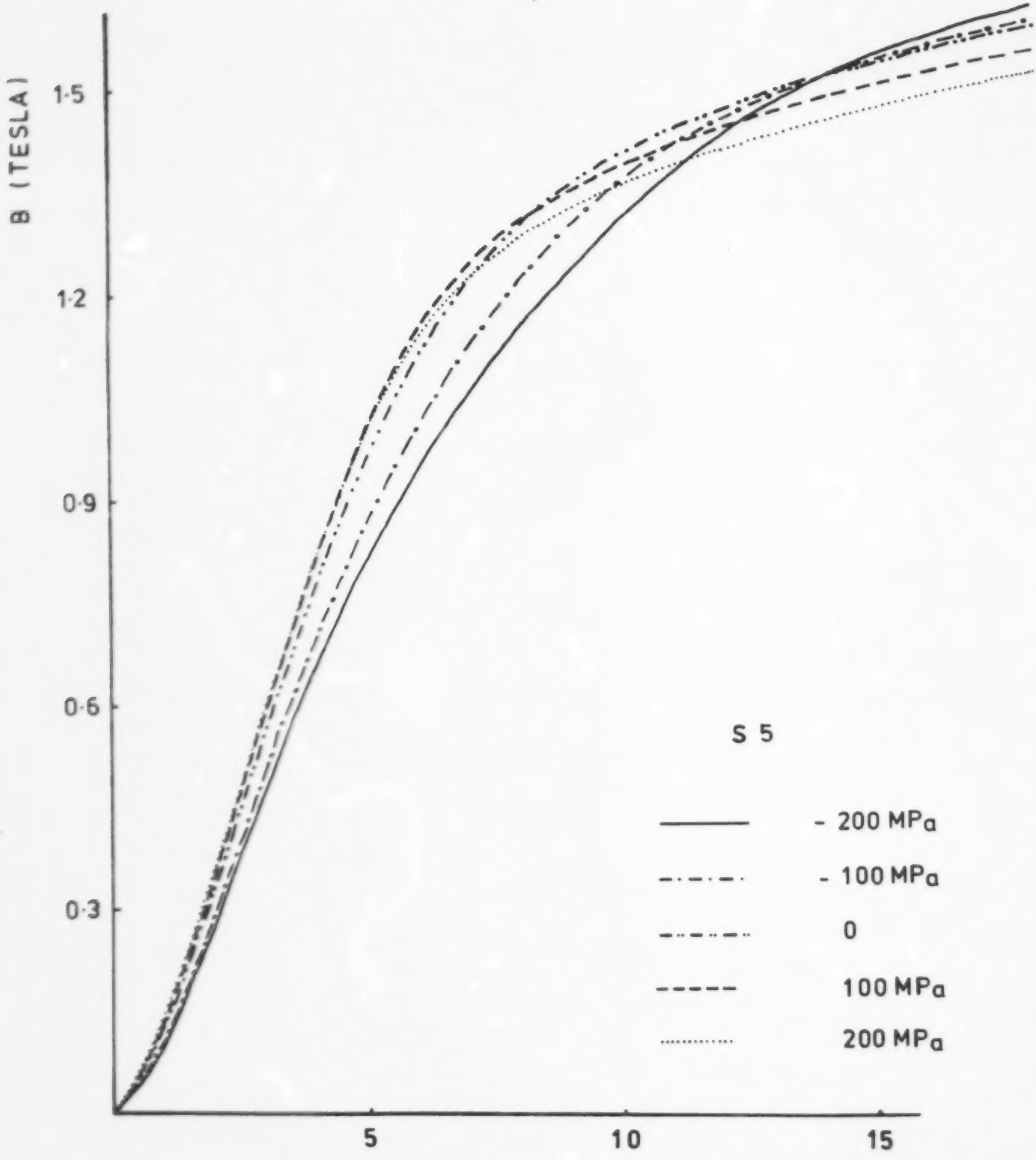
B (TESLA)
1·5
1·2
0·9
0·6
0·3
5
10
15
H (kA/m)
S 5
- 200 MPa
- 100 MPa
0
100 MPa
200 MPa

fig. 29

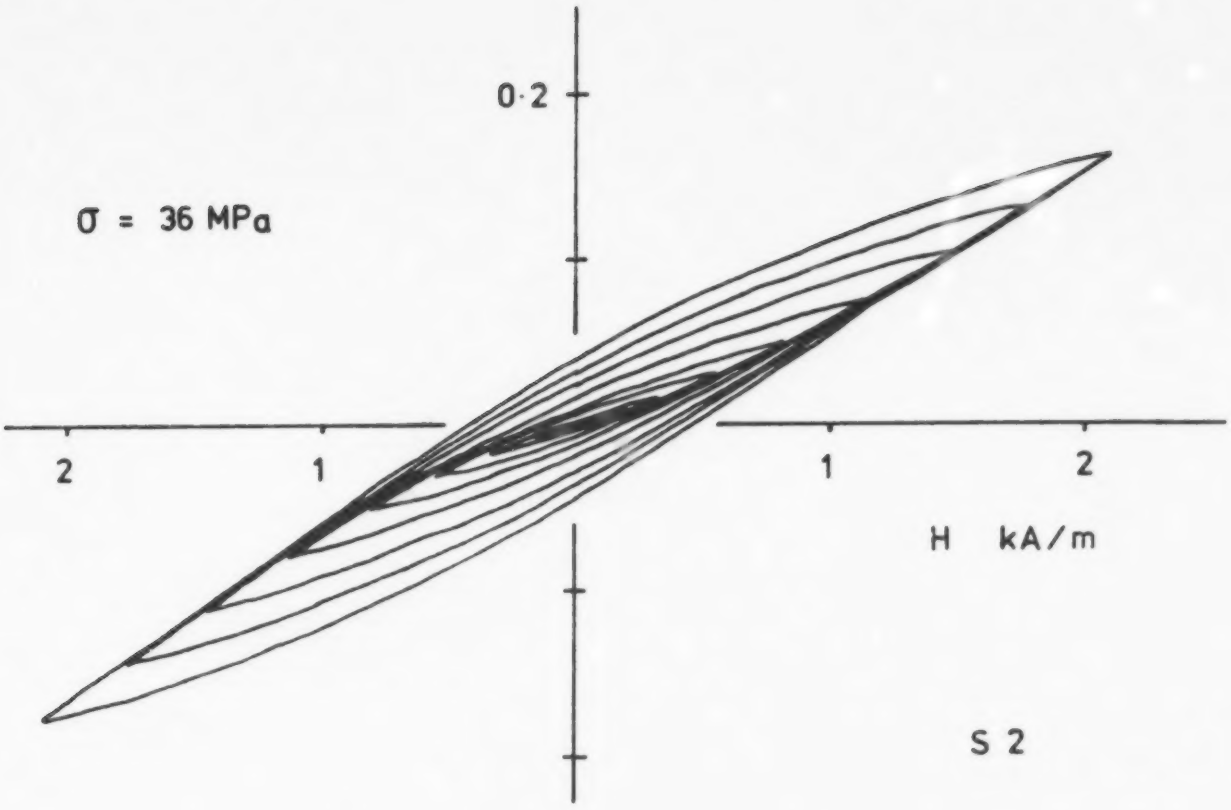

fig. 30

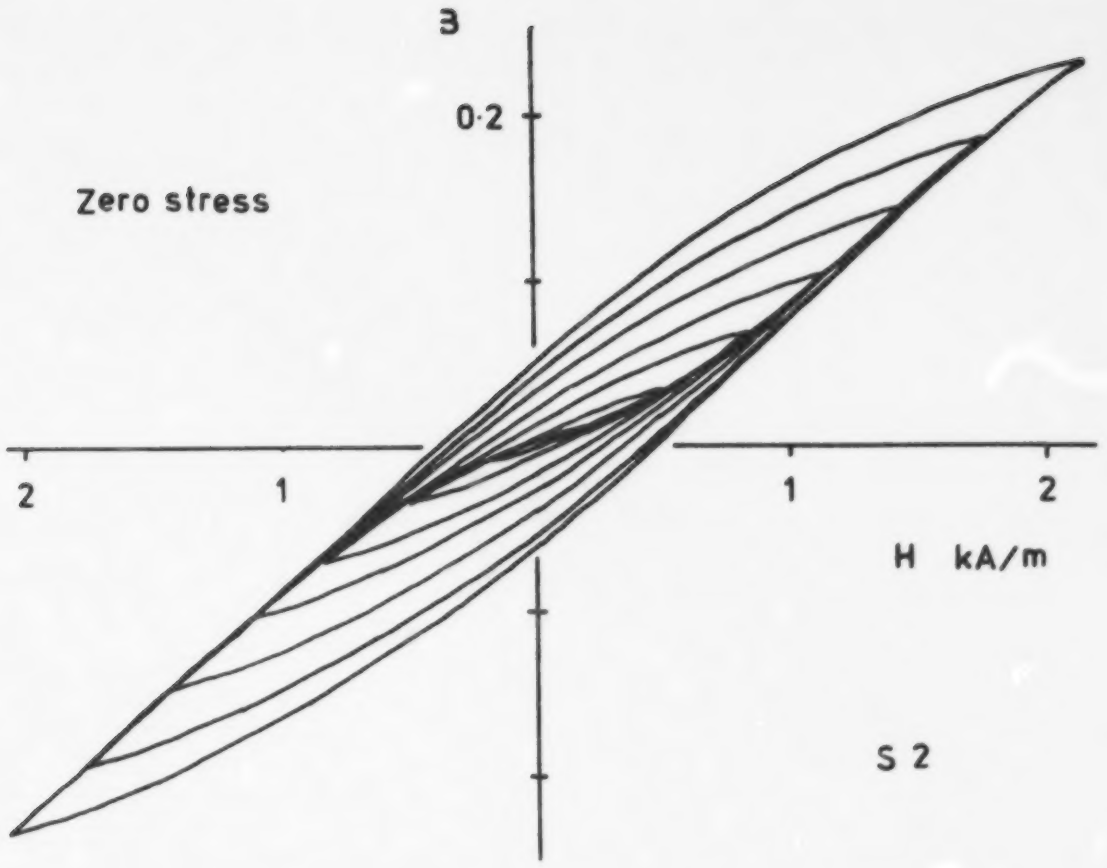

fig. 31

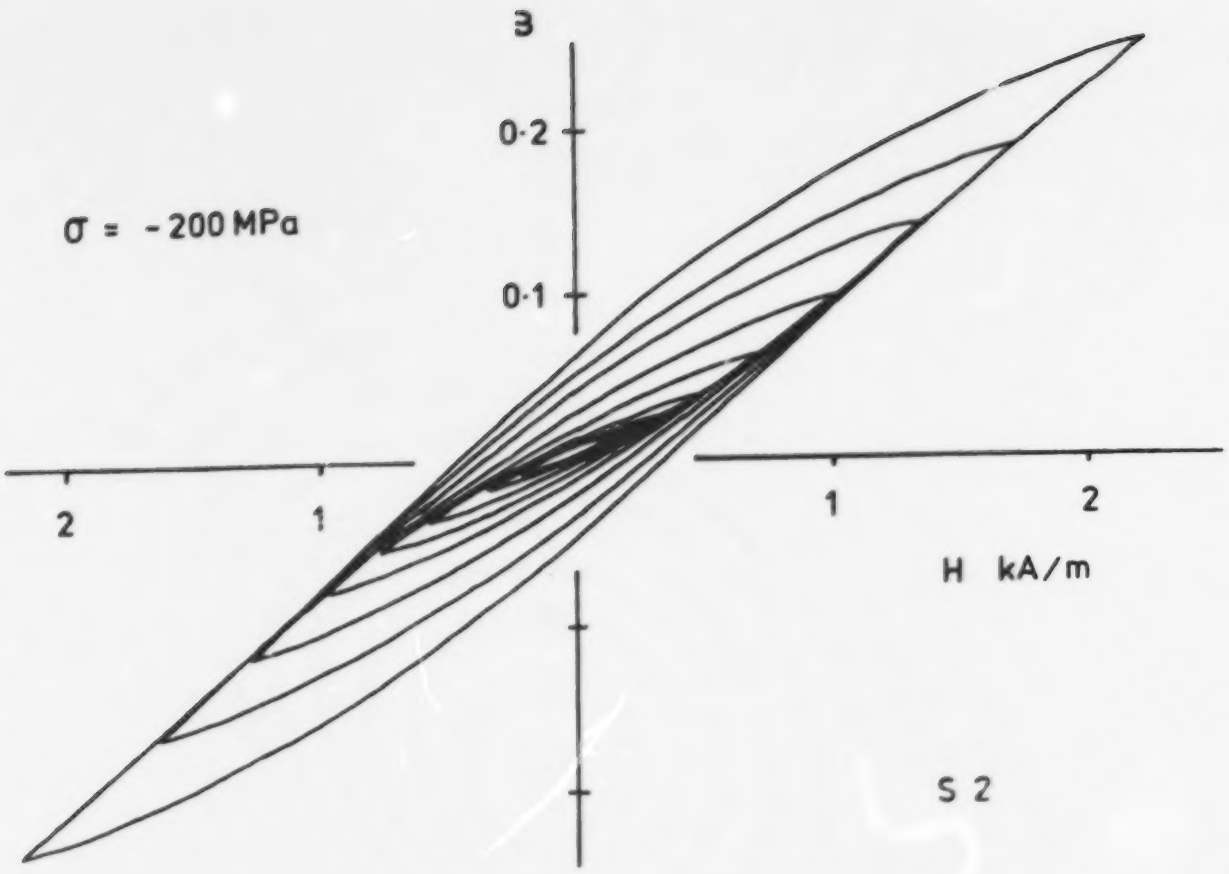

fig. 32

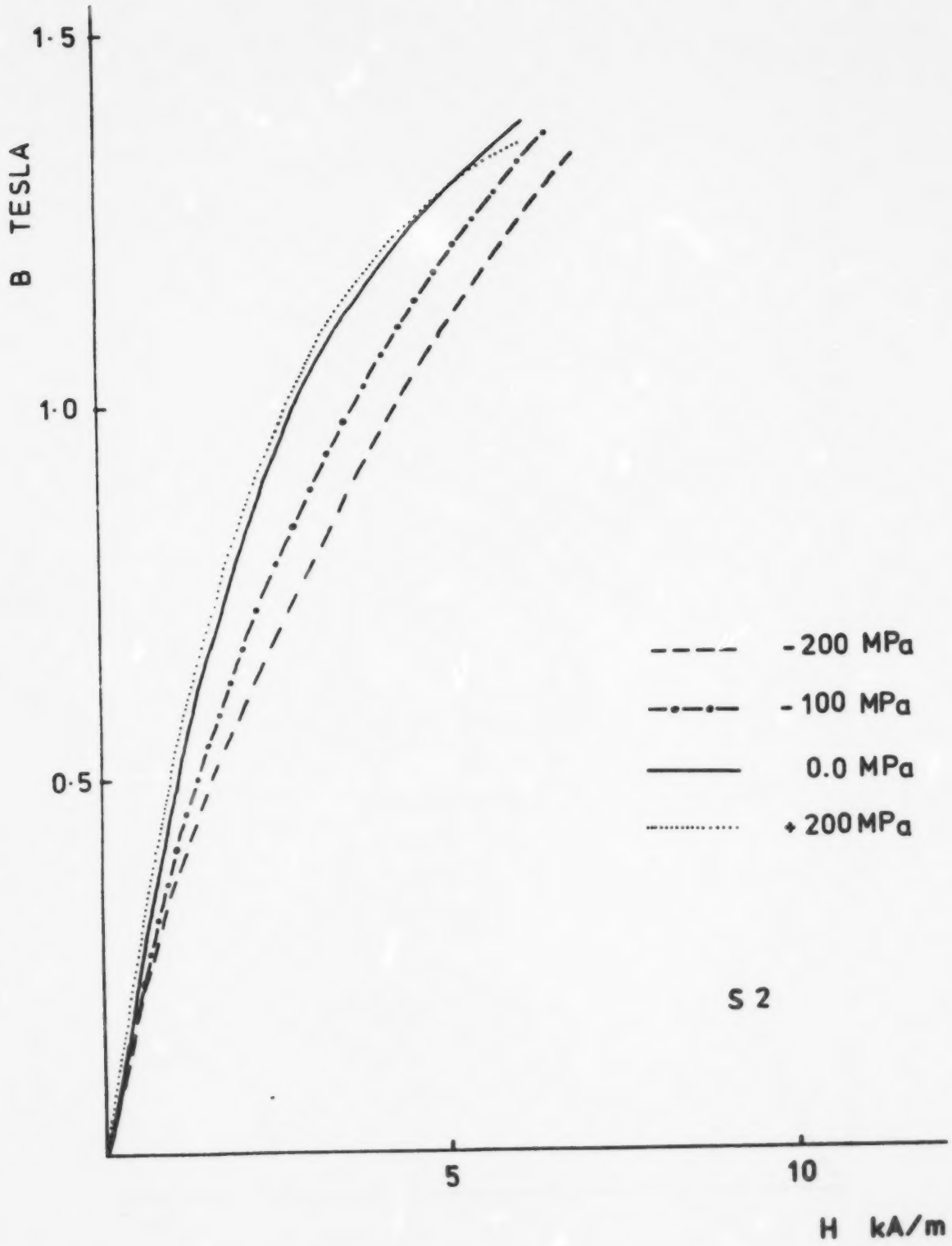

fig. 33

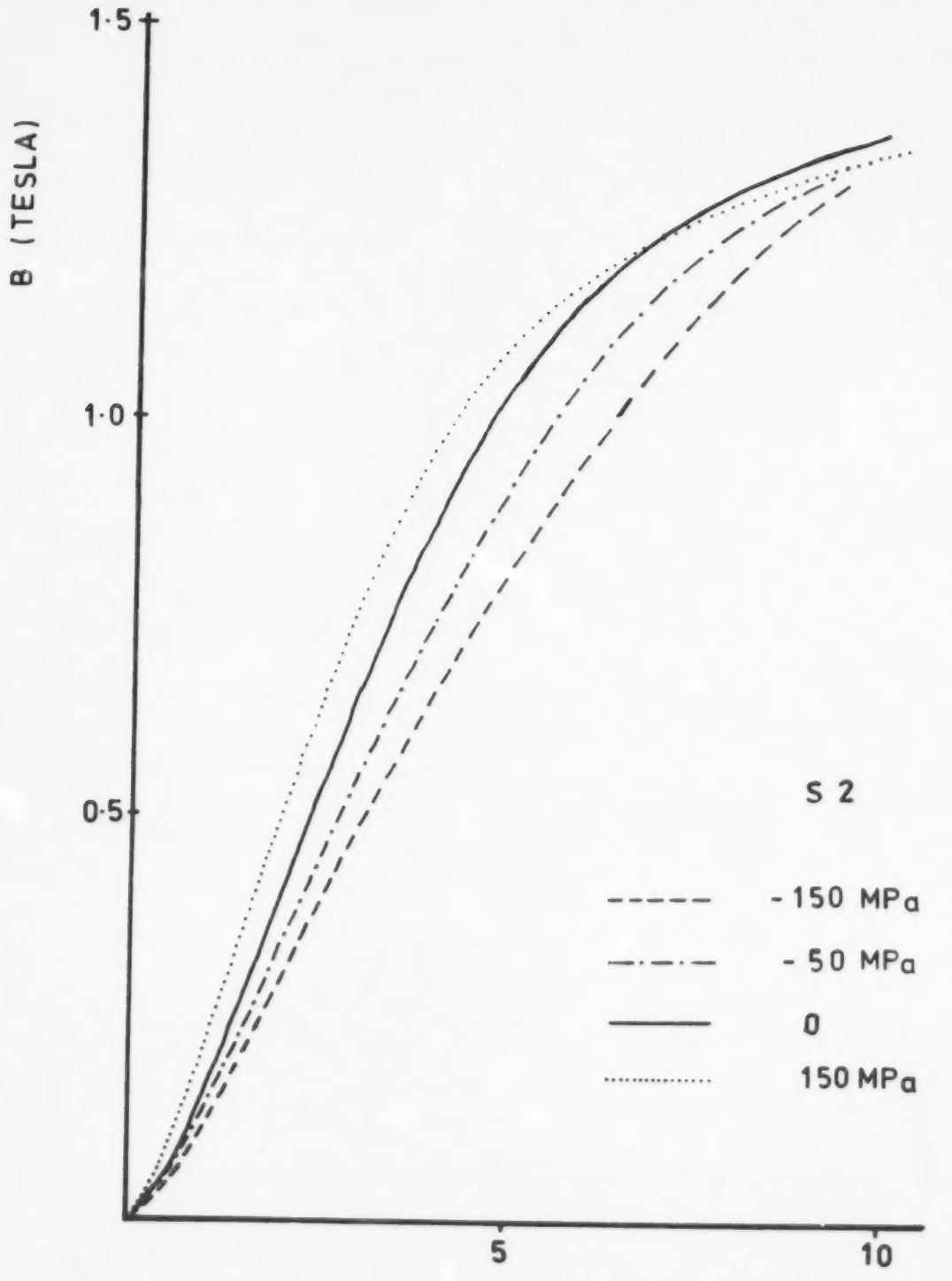

fig. 34

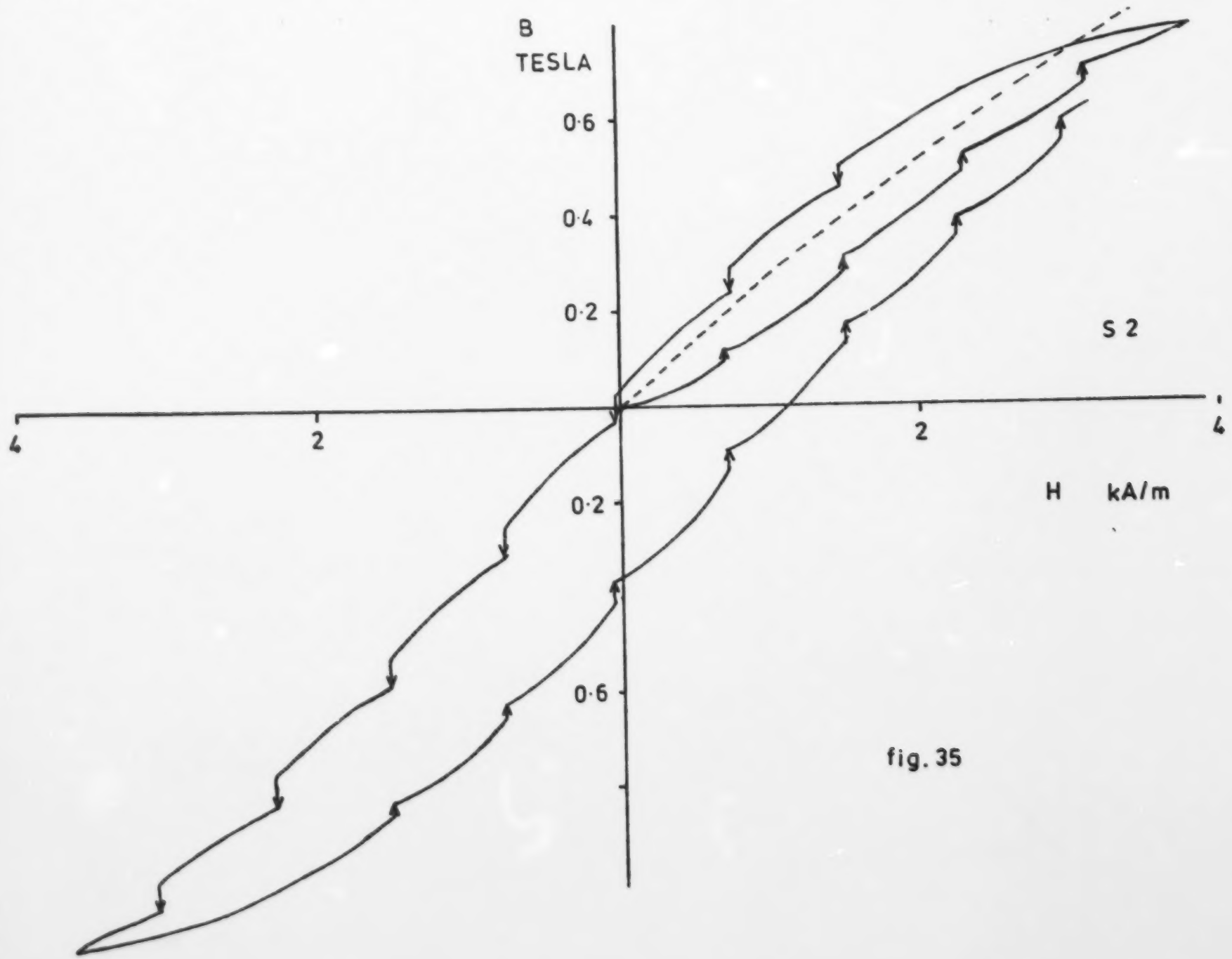

fig. 35

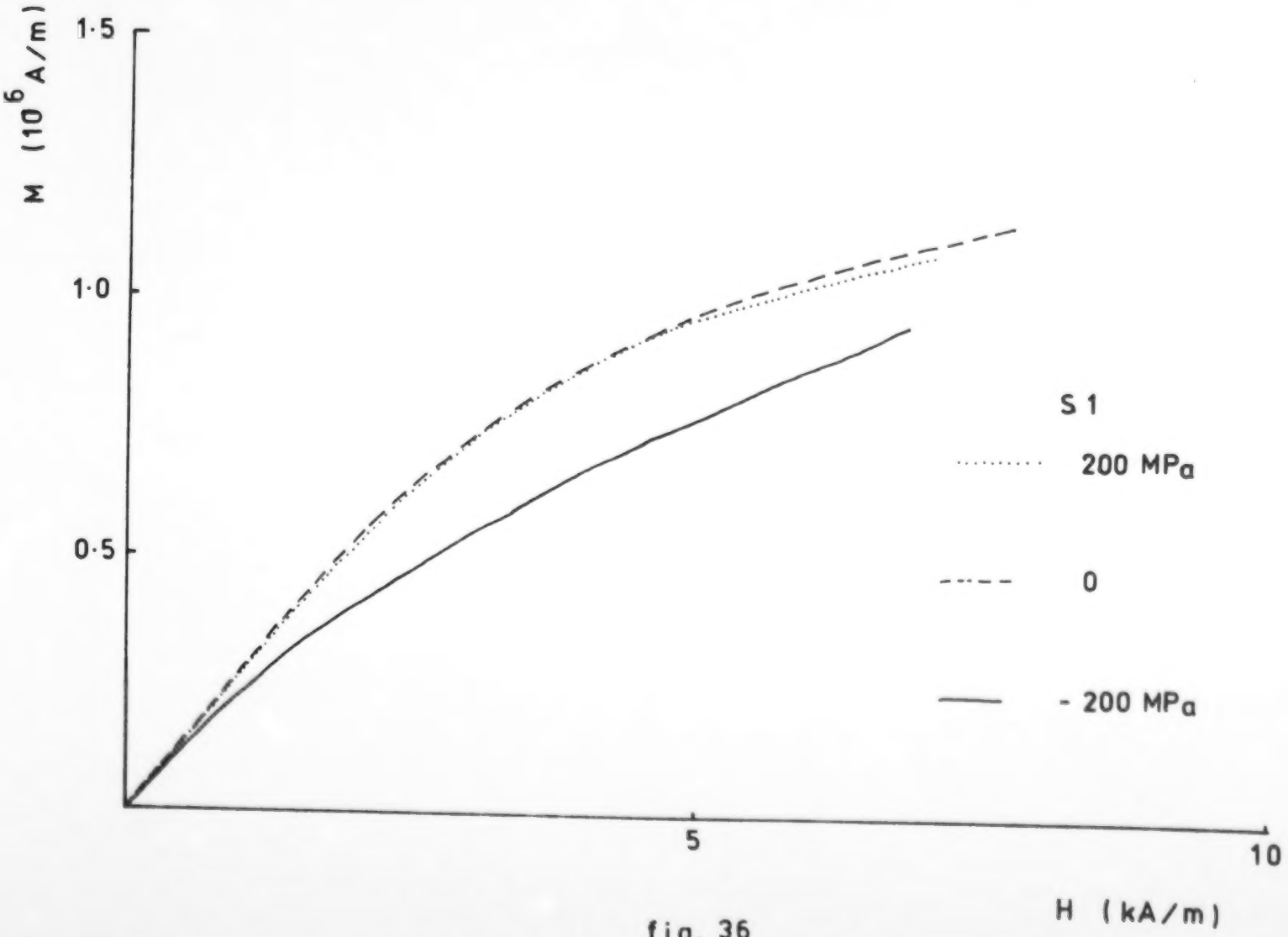

fig. 36

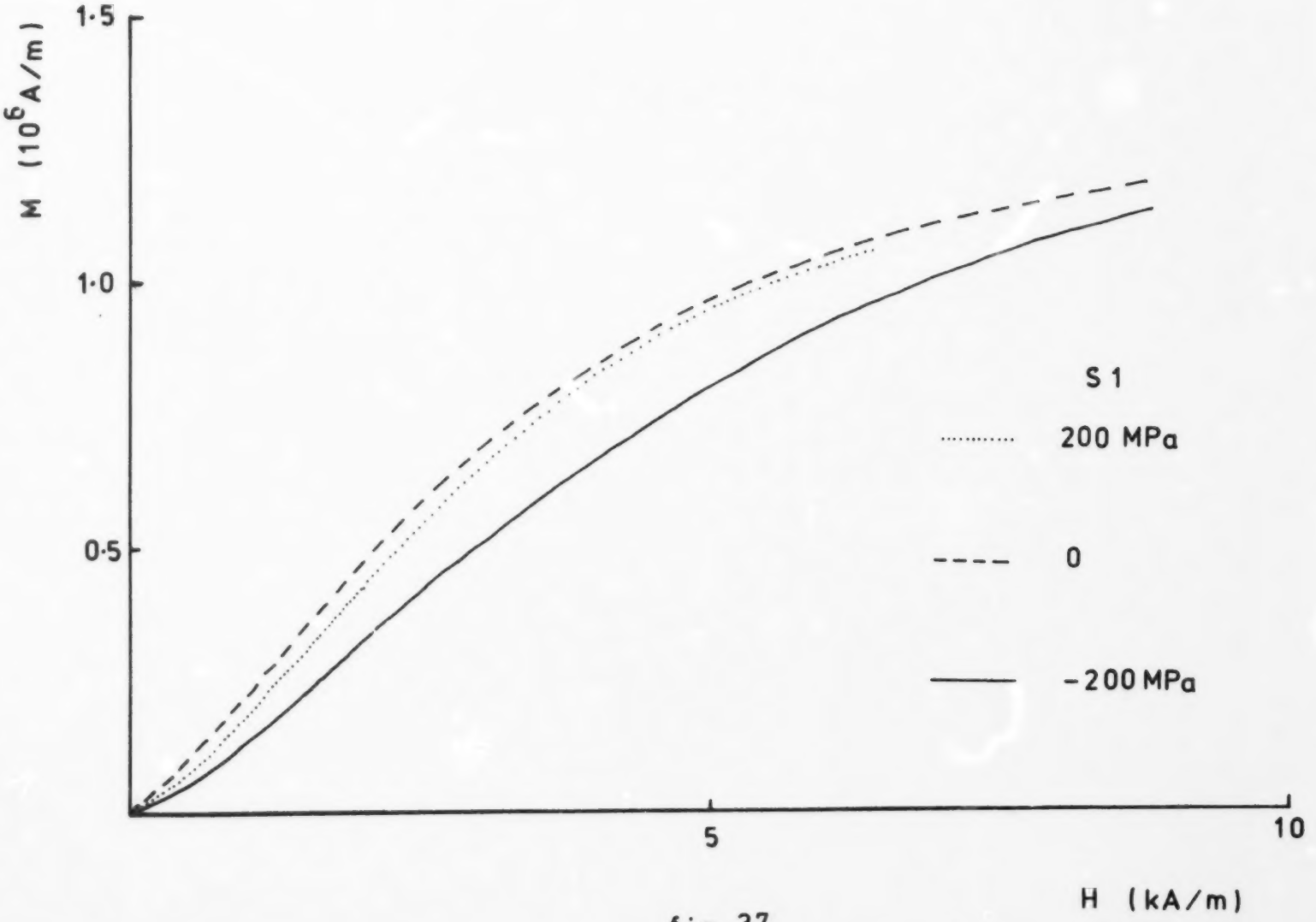

fig. 37

Table 1: Pipeline Sample Data

Sample No.	S 1	S 2	S 5
Source	TCPL	TCPL	EMR
Pipe	1.22m spiral weld	0.76	1.22m spiral weld
YS	480 MPa	460 MPa	610 MPa
UTS	570 MPa	590 MPa	710 MPa
Elongation	37%	28%	34%
Constituents by weight percentage			
C	0.071	0.25	0.08
Mn	1.24	1.08	1.98
S	0.012	0.02	0.08
P	0.005	0.01	0.015
Cu	0.028		0.055
Mo	0.123		0.235

APPENDIX I

Detection of anomalous stresses in gas pipelines by magnetometer survey (invited)

David L. Atherton

Department of Physics, Queen's University, Kingston, Ontario K7L 3N6, Canada

A. Teitsma

Pipeline Monitoring, TransCanada Pipelines, 1320 Ellesmere Road, Unit 3, Scarborough, Ontario M1P 2X9

Pipelines constructed on unstable terrain (e.g., permafrost), submarine lines, etc. may shift, producing stresses which can lead ultimately to rupture. We have used magnetometer surveys to detect bending stresses in buried pipelines and to monitor new construction. The perturbations to the earth's field are large and complex; typically fluctuations of 5–10 kilogamma are found 2 m above 1 m diameter buried line. These signals record initial magnetizations, joints, construction history, etc. and include the results of stress induced magnetization changes. The magnetostrictive effect in steel depends on field, stress, and cyclic history. There is little basic data on the inverse effect, stress induced changes in magnetization. In a pipeline the bending stress distribution is complex so that fringing field changes due to stress magnetization changes are not calculable. However, experience now enables us to interpret some of the features of our magnetometer surveys. Since stress effects are large we are optimistic that we can eventually develop the technique for surveying pipelines for unusual stress concentrations.

PACS numbers: 06.70.Dn, 75.60.Ej

INTRODUCTION

Gas or oil pipelines are normally buried. In-service inspection is performed by pumping an electronic inspection 'pig' through them. This tool is equipped with an array of magnetic detectors, generally working on the magnetic flux leakage principle. Detector outputs are fed to a magnetic tape recorder. Pigs are introduced into the line at a compressor station using a special launcher and are recovered in a trap at the next compressor station typically, 100 Km and 6 or 7 hours away. Unfortunately many lines have been constructed without launchers and traps and pigging operations cannot be performed without interfering with service. Non-intrusive above ground inspection methods would therefore be highly desirable.

Since buried pipelines are readily detected by magnetometers, TransCanada Pipelines made some proton precession magnetometer surveys of buried lines and lines under construction in 1979. Simple preliminary calculations gave estimates of likely maximum field anomalies due to low permeability material at girth welds between 12 m long joints of 0.76 m diameter 10 mm wall pipe as about 50γ (1 gamma = 10^{-9} T) 1m above a buried line (i.e. approximately at ground level) falling to less than 10γ 2m above.

Fig. 1 shows a simple representative survey plot of proton precession magnetometer total field readings 2 m above such a line made during construction. The axial displacement scale is shown in multiples of 12 m because the welds between joints of pipe occur at 12 m intervals in this case. It is readily apparent that since the field fluctuations are several kilogamma the assumptions on which the preliminary estimates were based cannot be valid. Further, although there is clearly some correlation with the welds it is not a direct one. We concluded therefore that the field patterns were not due to anomalously magnetized weld sections. Since some measurements were made whilst the line was still on the skids on which it was welded, before it was placed in the ditch, we considered that uneven skid support might be stressing the pipe and might be responsible for the anomalous magnetic effects. However further consideration showed that these stresses should be small and that there appeared to be no correlation between the observed field patterns and the skid locations. It was also noted that the patterns remained almost unchanged after the pipe has been laid in the ditch. Single joints of pipe produced field patterns suggestive of weak bar magnets. TransCanada performed early experimental studies of the field patterns produced by various configurations of bar magnets. Singularities were noted between these field patterns and the patterns observed above pipelines.

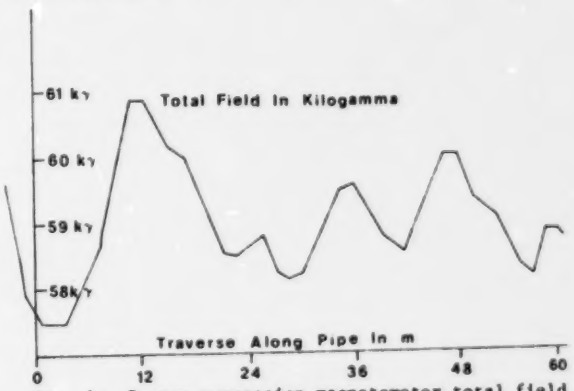

Fig. 1: Proton precession magnetometer total field plot. The traverse is made 2 m above a 0.76 m diameter 10 mm wall pipe. The axial displacement scale is given in multiples of 12 m because the pipe joints from which the line is strung are 12 m long. Note that the field fluctuations are several kilogammas (1 gamma ≡ 10^{-9} T) and that there appears to be some correlation with the welds between joint lengths.

 0021-8979/82/118130-06$02.40 © 1982 American Institute of Physics

In due course we realized that some of the field fluctuations were due to each joint of pipe being magnetized and acting as a weak bar magnet as shown in idealized form in Fig. 2 and in a practical example in Fig. 3. The bar magnet pipe joints are strung together to form a pipeline with their senses aligned or opposed in semi-random fashion. There are many further complications including non-standard joint lengths, construction procedures and also indeed stress effects which are readily detectable where the pipe has been cold bent in the field in order to allow small changes of direction to follow the contour of the land etc.

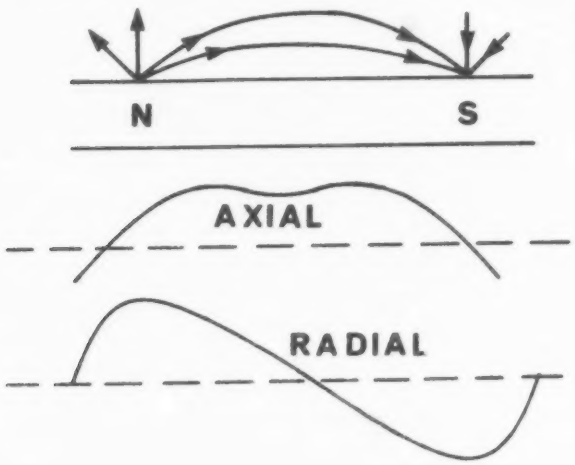

Fig. 2: An idealized isolated pipe joint acting as a simple bar magnet produces axial and radial field components above the joint as shown.

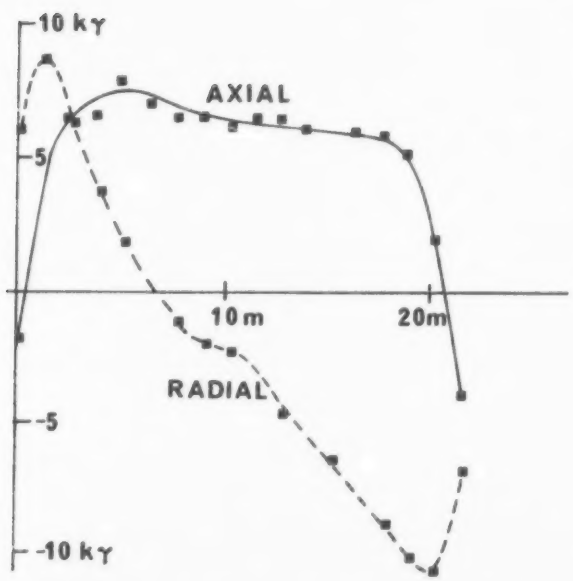

Fig. 3: Fluxgate magnetometer traverses showing the axial and radial field components measured 1.2 m above a 1.2 m diameter isolated pipe joint. These measurements are superimposed on the earths background field of approximately 60 kilogamma.

Figure 4 shows a more typical plot of vertical field components measured using a fluxgate magnetometer 1.2 m above a 1.2 m diameter line during construction. It includes the effects of several field bends superimposed on a complex bar magnet pattern. The overall pattern of field fluctuations is generally rather difficult to interpret but, with several years of experience, we are gaining confidence. Further tests and demonstrations described subsequently have shown conclusively that the effects of stress on these field patterns is easily detectable. The possibility of inverting this process to monitor pipelines for anomalous stress concentrations or changes by non-invasive magnetometer surveys has caused some excitement although we must emphasize that substantial amounts of further basic investigation, development, and experience are needed before this hope can be fully realized.

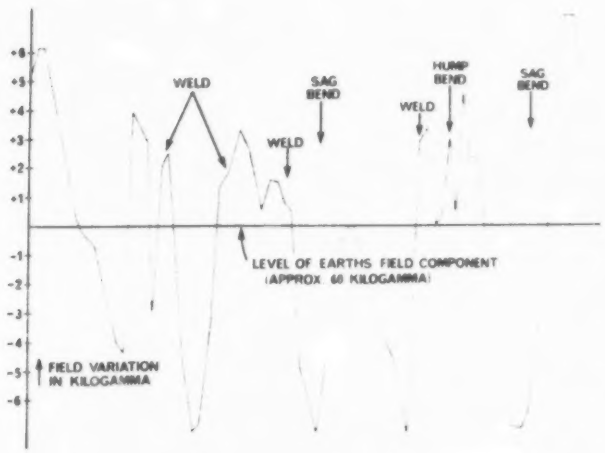

Fig. 4: Fluxgate magnetometer traverse showing the vertical field fluctuations along a 200 m string of welded pipe joints. The traverse is made 1.2 m above a 1.2 m diameter 13 mm wall pipeline during construction immediately prior to lowering it into the ditch in which it will be buried. Several field bends are included in this traverse. Although the field fluctuations are large the general pattern is typically complex.

Stress in Pipelines

Pipelines are subject to stringent codes during construction and operation designed to ensure safety, because gas pressures subject the walls to signficant tensile stresses. During fabrication and construction all welds are rigorously inspected using X-rays and ultrasonics. Line pipe is coated and wrapped and cathodic protection is used to protect it from electrolytic corrosion. Once it is buried, in-service inspection becomes much more difficult and expensive but considerable effort and ingenuity has been devoted to meeting this challenge.

Northern pipelines constructed on permafrost may have footings or support weakened if the permafrost equilibrium is inadvertently destroyed. Unsupported lengths of line will introduce bending stresses and, in extreme cases, this may ultimately lead to failure. River crossings and submarine pipelines are further examples of lines laid on potentially unstable foundation. Geodetic surveys

are used to detect pipeline shifting or bending leading to high bending stresses but simpler methods and techniques for monitoring stress itself are clearly highly desirable, hence our interest in the potential use of magnetometer surveys to detect changes in stress distributions or anomalous stress concentrations.

Other applications of potential interest are magnetic monitoring of stress changes in the legs of offshore platforms after storms or indeed in monitoring stresses in any large steel structure subject to variable loads.

Pipelines as Magnet Arrays

Many school children familiar with iron filing field pattern pictures of bar magnets are aware that the North and South poles are located somewhat inward from the physical ends of the magnet. Despite this simple fact being so well known, there is no magnetician expert enough to be able to calculate the positions of the poles. Simple shape effects for uniform magnetic material in a uniform external field are calculable [1] but in the case of a permanent magnet the material is nonlinear, the self generated field is nonuniform and so is the magnetization. Furthermore hysteresis effects are essential. We would need therefore not just to calculate the final state of the magnet but also the processes by which it arrived there - i.e. the history.

If we take a long bar magnet and divide it the original poles move in somewhat from the ends and two more are formed near the division. If we rejoin it the process is not reversible. The original poles move out again but not as far as the original positions. The poles formed near the division are attracted and tend to neutralize but some evidence of relict poles remains.

Considering a pipeline initially as a string of semirandomly oriented bar magnets is a simple concept but the details and the resulting field patterns are very complex. The fringing field patterns depend not just on the lengths and strength of the bar magnet pipe joints and also on their relative stresses but also on their sequence of assembly etc.

Although we do find sections of magnetometer surveys where the bar magnet pattern interpretation seems relatively straightforward there are others where we are reminded of the potential complexity.

There are other complications to be considered such as other ferromagnetic bodies (wire fences!, water lines, other pipelines etc.), magnetic storms, relative changes in the earths field vector etc. The effects of stress induced changes in magnetization on the fringing fields are superimposed on all these and may not always be readily apparent therefore.

Magnetostriction and Stress Induced Changes in Magnetization

When steel is magnetised there is an accompanying strain magnetostriction. Typical behaviour of the magnetostriction coefficient $\lambda = \frac{\Delta l}{l}$ for iron is shown in Fig. 5 as functions of H for different stresses. For unstressed steel there is an initial expansion at low field which then slows, decreases and eventually becomes a contraction at high fields. Compressive stress increases the initial expansion but this is still reversed at high fields. Increasing tension tends to suppress the initial expansion.

Application of Le Chateliers principle shows that the effect of tension on the magnetization of iron will be to increase the magnetization when the magnetostriction is positive (i.e. at low field) and decrease it when λ is negative as shown in Fig. 6.

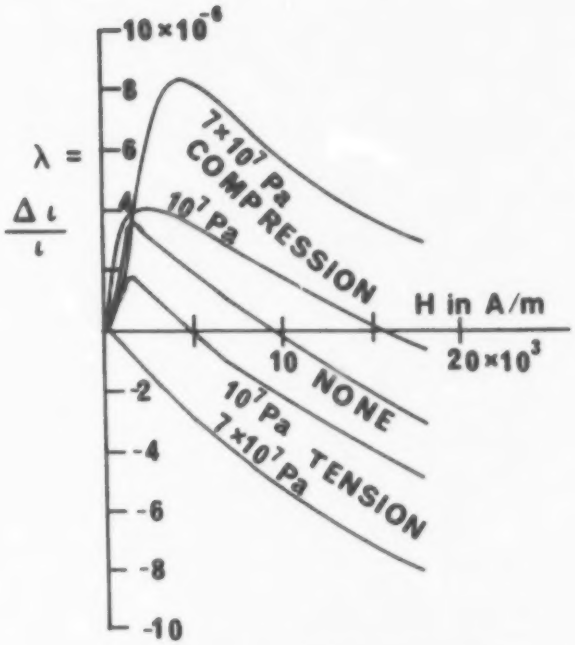

Fig. 5: The effect of tensile and compressive stresses on the magnetostrictive coefficient of iron as functions of H. Based on data of Kuruzar as reported by Cullity [2].

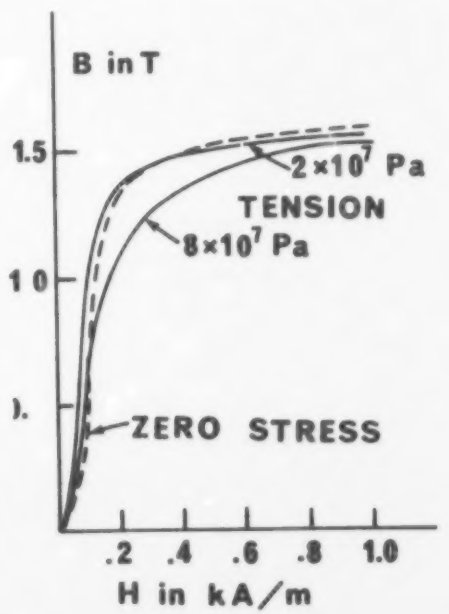

Fig. 6: The effect of tension on the magnetisation of iron. Based on Bozorth and Williams [4]. Le Chateliers principle results in tension tending to increase magnetisation when the magnetostrictive coefficient is positive and vice versa so that Fig. 6 is qualitatively predictable from Fig. 5.

Although measurements on the effect of tension on the magnetization of iron were reported by Ewing [3] nearly 100 years ago there appears to have been very little work reported on the changes in magnetization produced by changes in stress applied to iron which is already magnetized (see however Bozorth and Williams [4], Fig 4). Clearly the situation is severely complicated both by the rather complex magnetostrictive behaviour of iron or steel.

There are also experimental complications in measuring the effect of changing stress on magnetization. Firstly, mechanisms to apply mechanical stresses to samples, particular compressive stresses, are not normally designed so that they may be conveniently placed between the poles of a laboratory electromagnet! Secondly the desire to make mechanical stress cycles at numerous different fixed fields means that the times to complete magnetic cycles become very long. This results in the drift of the voltage integrators used on flux sensing coils becoming a major concern. We believe that we have overcome both of these problems and at Queen's University we are starting a program to make basic measurements on the effects of mechanical stress on the magnetization of pipeline steels in order to help interpret the results of magnetometer pipeline surveys.

Field Testing and Demonstration

Even if there was basic data available on magnetization changes induced by changing stress in pipeline steels it would be very difficult to correlate this directly with the anomalies we have observed in magnetometer surveys because of the complicated 'bar magnet array' non-uniform magnetization of the line which is further compounded by the fact that stresses are also highly non-uniform. In a pipe, simple bending stress varies circumferentially around the pipe as well as axially along it and real pipeline stresses involve more than simple bending stresses. Worse still, we are not measuring magnetization, but rather the relatively weak fringing fields near a massive ferromagnetic body. Clearly then the interpretation of magnetometer survey anomalies is difficult and a great deal of experience will be needed.

We have therefore undertaken various field tests and demonstrations of varying intermediate complexity to gain experience and help to confirm our interpretations.

We have made numerous magnetometer surveys of pipelines during construction including many before and after surveys of joints which have been cold bent in the field in order to allow the final line to change direction slightly so as to conform to the terrain. Cold bending essentially uses a a massive hydraulic bender to stress the pipe joint beyond its yield point so that when the load is removed the pipe relaxes with a permanent deformation. Multiple small bends are used. The resulting stress distribution is of course very complicated.

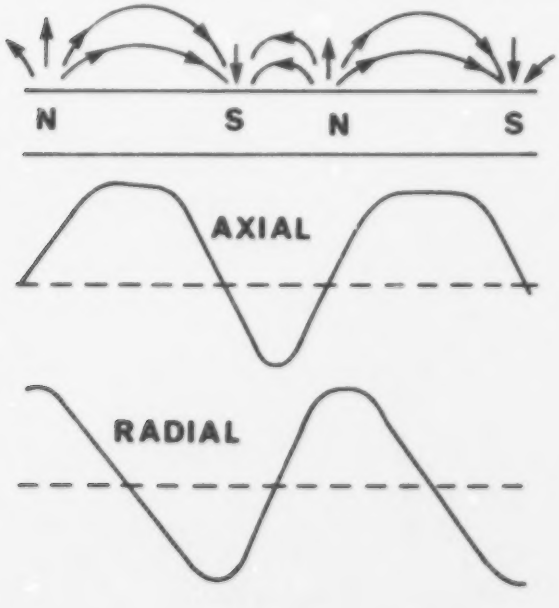

Fig. 7: An idealized pipeline joint which has had a cold bend made in the middle. This has the effect of introducing a short reversed bar magnet at the bend which produces axial and radial field components as shown.

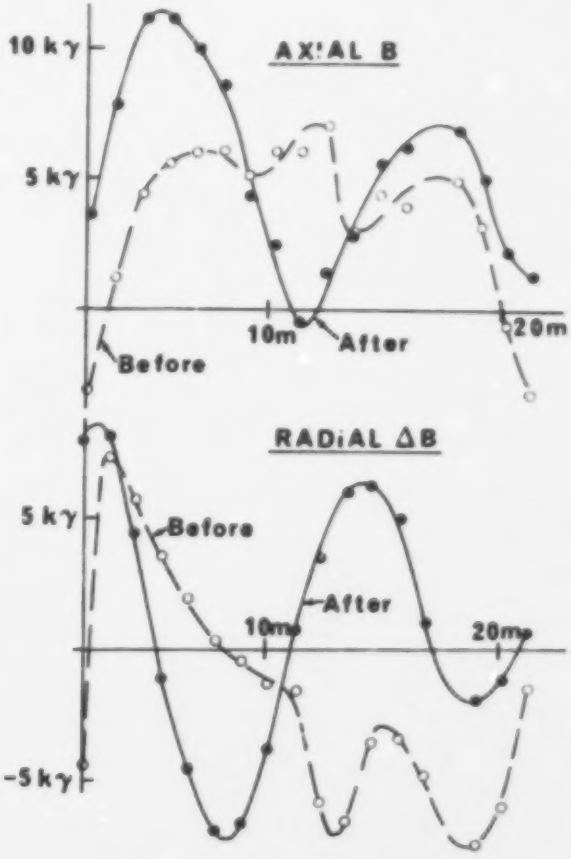

Fig. 8: Measurements of the axial and radial field components made before and after cold bending a 21 m length of pipe to produce a 2° sag (upward) bending. The 21 m length was produced by factory welding two approximately 10 m long joints. Although the before bending plots show that these two original joints appear to have been magnetised in the same direction and to have formed a longer bar magnet when jointed there is a suggestion of relict poles near the middle. The measurements were made 1.2 m above the 1.2 m diameter line.

The effects of cold bends on the magnetometer survey patterns can be summarized most simply by describing them as extra bar magnets added into the string used to represent the pipeline as shown ideally in Fig. 7 for a single joint with a bend made in the middle. Fig. 8 shows actual before and after field measurements for comparison these are of course, slightly more irregular partly because the length surveyed is in fact a double length joint formed by factory welding two standard joints. There is some evidence of 'relict poles' from the original two joint bar magnets towards the middle of the double joint before bending although after bending these have been almost obliterated by the large stress induced changes. These field tests help to identify the causes of some of the anomalies in our pipeline surveys but even simple bends do not generally produce such ideal changes as shown in Fig. 8 as shown by another 'before and after' cold bending example in Fig. 9. Here the simplest summary is just to say that the changes are large and readily detectable.

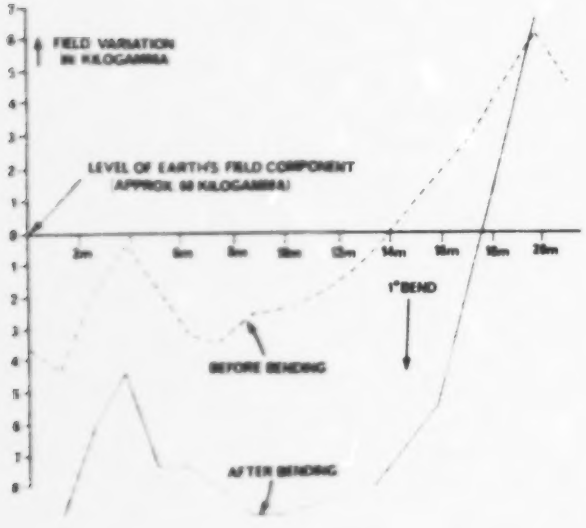

Fig. 9: Before and after making a 1° cold bend vertical field components made with a fluxgate magnetometer 1.2 m above a 1.2 m diameter 13 mm wall isolated pipe joint. These traverses are rather more typical than the simpler example shown in Fig. 8.

We have also made various fluxgate magnetometer measurements near the boom of a 15 ton mobile crane relaxed and under load and also along the boom of a small hydraulic hoist. Some of the results showing the field changes on loading the hoist are shown in Fig. 10, where it would appear that the most significant changes occur near positions of maximum stress concentration.

The results of these before and after stressing tests appear encouragingly simple, perhaps surprisingly so considering the complexities of the stresses and of the magnetostrictive behaviour. But clearly a great deal more experience is needed. We therefore have other tests in progress and planned which are investigating the field changes which occur as the stresses are gradually increased and to examine some of the other potential complicating factors.

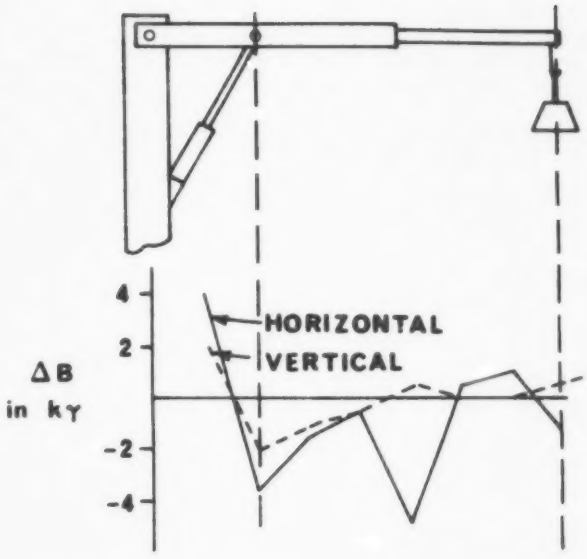

Figure 10: Fluxgate magnetometer field component change measurements made at various positions along the boom of a simple hydraulic hoist. The greatest changes show some possible correlation with the suspected locations of maximum stress.

CONCLUSIONS AND DISCUSSION

The first major conclusions are that there are large stress induced anomalies in the fringing magnetic fields near buried pipelines and that these may be readily detected even above ground. The fringing field patterns are however complex and their interpretation is difficult. This of course suggests that periodic surveys could be made in order to detect changes in stress distributions. This is of course an easier goal than the determination of absolute stress levels but still potentially extremely useful.

We have already won useful experience in interpreting the intricate magnetometer survey patterns and some simple concepts such as the bar magnet string visualization and bend stress magnetic anomalies are already well established and confirmed by test and demonstration. Some other concepts of course have had to be rejected whilst others are in the process of formulation or test.

Despite the current lack of basic data on stress induced magnetization changes, which we hope to remedy shortly, and the anticipated complexity of the effect for iron and steel coupled with the obviously enormous difficulties of applying this basic data to practical stressed engineering structures we have been encouraged that our experimental tests of stress effects have all appeared relatively consistent.

We believe that magnetometer surveys show promise for non invasive monitoring of large pipelines and other large steel engineering structures for changes in stress distributions and possibly for determining stress concentrations etc. Trans Canada has proven the principle and applied for certain patents. Despite this optimism we caution that a great deal has yet to be learnt from basic data and theory, from tests and demonstrations and from experience in interpreting field surveys. There are many years work ahead but the potential applications make this an exciting new field.

REFERENCES

1. R.M. Bozorth and D.M. Chapin "Demagnetizing Factors of Rods', J. Appl. Phys., Vol. 13, No. 5 320-326, May, 1942

2. Data of M.E. Kuruzar reported by B.D. Cullity, 'Fundamentals of Magnetostriction', J. Metals, 35-41, Jan. 1971.

3. J.A. Ewing, "Magnetic Induction of Iron and other Metals', 3rd Ed. p. 210, 'The Electrician' Printing and Publishing Co., London 1900.

4. R.M. Bozorth and H.J. Williams, 'Effect of Small Stresses on Magnetic Properties', Rev. Mod. Phys., Vol. 17, No. 1, p. 72-80, Jan. 1945.

APPENDIX II

Presented at the "International Conference on Pipeline Inspection", Edmonton, Canada, June 1983.

THE DEVELOPMENT OF AN ABOVE GROUND STRESS MEASUREMENT METHOD

David L. Atherton and D.C. Jiles
Department of Physics
Queen's University
Kingston, Ontario
K7L 3N6

and

H.A. French and A. Teitsma
Pipeline Monitoring
TransCanada Pipelines
1320 Ellesmere Road, Unit 3
Scarborough, Ontario M1P 2X9

Abstract

Magnetometer surveys above buried pipelines can be used to detect bending stresses or changes in stress to monitor new construction. Magnetometer pipeline survey logs show that the pipeline joints behave as a string of randomly orientated bar magnets. Superimposed on these complex fringing field patterns are signals produced by stress-induced changes in magnetisation. Cold bends are readily detectable. Laboratory scale magnetometer surveys of stressed pipe have been used to investigate the effects of orientation in the earths magnetic field, the effects of bending stresses within the elastic range and the effects of hydraulically simulated line pressure. Hysteretic effects are important. Fundamental investigations of the effects of mechanical stress on the magnetization of pipeline steels show that the effect of stress cycling A-60 line pipe steel, which is magnetically hard, in an applied field is to reduce the hysteresis i.e., to shift its magnetisation towards the anhysteretic curve. Above ground magnetometer surveys offer the potential of non-invasively monitoring pipelines for anomalous stress due to bending as may occur in regions of permafrost, river crossings etc., where line is laid in unstable terrain and for monitoring stress in the legs of offshore platforms etc.

Introduction

Since approximately 50% of pipelines cannot be inspected by internal tools without removing the lines from service and cutting into them, a method capable of detecting anomalous pipe stresses from above ground and preferably of measuring stress to a reasonable degree of accuracy would be a great advantage. In the case of TransCanada Pipelines Limited, almost all of its lines cannot be pigged without being taken out of service. Fortunately most of its transmission system traverses areas where abnormal stress does not occur but in areas where it can occur such a method would be very desirable. Bending stress concentrations might be likely to occur in lines constructed on unstable terrain such as river crossings, submarine lines, northern pipelines constructed on permafrost where the thermal equilibrium may be inadvertently altered or where pipelines are constructed in swampy ground.

Strain gauging can, of course, be used to measure changes in stress at a predetermined location, however, this has severe practical and economic limitations, futhermore, it does not have the important potential capability of monitoring unanticipated stress concentrations which may develop because of unforseen circumstances in areas where it is not expected. An above ground stress detection method however, has the potentially important advantage of being able to monitor such stresses and without interruption of service.

The stress detection technique being developed by TransCanada Pipelines Limited in collaboration with the Applied Magnetics Group at Queen's University is one of several important outcomes of TCPL's ongoing internal inspection tool development program. The stress detection method is based on measuring changes in the

magnetic fringing field patterns of a pipeline which are caused by changes in mechanical stress in the pipeline. After an initial magnetometer survey subsequent magnetometer surveys may be compared to the initial survey and changes in the field patterns used to indicate stress changes in the pipeline. The magnetometer surveys show large readily detectable anomalies but the patterns are complex and experience is needed to interpret them. Our developments have therefore proceeded along three mutually supportive paths. Firstly by practical magnetometer surveys of existing gas transmission lines and lines under construction and other full scale tests which have established the feasibility of the method. Secondly by laboratory scale magnetometer surveys of stressed pipes under more controllable conditions in order to investigate and demonstrate the significance of some of the various parameters. Thirdly a fundamental experimental and theoretical investigation of the effects of mechanical stress on the magnetization of pipeline steels. We should emphasize that since many of the results we have obtained in each of these three areas of investigation have been contrary to our initial expectations the mutual interaction has contributed very greatly to improving our understanding of the complicated processes involved.

Magnetometer surveys in the field

Since buried pipelines are readily detected by magnetometers TCPL made some proton precession magnetometer surveys of buried lines and lines under construction in 1979. Fig. 1 shows a simple representative survey plot of proton precession magnetometer total field readings 2 m above a 760 mm diameter 10 mm wall line made during construction. Large

fluctuations of several kilogamma in the earth background field of about 60 kilogamma are apparent (1 gamma = 10^{-9} Tesla = 10^{-5} oested). There appears to be some correlation with the 12 m joint length. Preliminary calculations gave estimates of field anomalies due to low permeability material at girth welds of only about 10 γ and were therefore concluded to be irrelevant.

Since some measurements were made whilst the line was still on the skids on which it was welded, before it was placed in the ditch, we considered that uneven skid support might be stressing the pipe and might be responsible for the anomalous magnetic effects. However further consideration showed that these stresses should be small and that there appeared to be no correlation between the observed field patterns and the skid locations. It was also noted that the patterns remained almost unchanged after the pipe had been laid in the ditch. Single joints of pipe produced field patterns suggestive of weak bar magnets. TransCanada performed early experimental studies of the field patterns produced by various configurations of bar magnets. Simularities were noted between these field patterns and the patterns observed above pipelines.

In due course we realized that some of the field fluctuations were due to each joint of pipe being magnetized and acting as a weak bar magnet as shown in idealized form in Fig. 2 and in a practical example in Fig. 3. The bar magnet pipe joints are strung together to form a pipeline with their senses aligned or opposed in semi-random fashion. There are many further complications including non-standard joint lengths, construction procedures and also indeed stress effects which are readily

detectable where the pig has been cold bent in the field. We consider that it may ultimately be desirable to string pipe joints in a deliberate pattern of magnetisation in order to provide auxilliary simple location markers for investigative digging.

Fig. 4 shows a more typical plot of vertical field components measured using a fluxgate magnetometer 1.2 m above a 1.2 m diameter line during construction. It includes the effects of several field bends superimposed on a complex bar magnet pattern. The overall pattern of field fluctuations is generally rather difficult to interpret but, with several years of experience, we are gaining confidence. Further tests and demonstrations, described subsequently, have shown conclusively that the effects of stress on these field patterns is easily detectable. The possibility of inverting this process to monitor pipelines for anomalous stress concentrations or changes using non-invasive magnetometer surveys has caused some excitement although we must emphasize that substantial amounts of further basic investigation, development, and experience are needed before this hope can be fully realized.

Considering a pipeline initially as a string of semi-randomly oriented bar magnets is a simple concept but the details and the resulting field patterns are very complex. The fringing field patterns depend not just on the lengths and strengths of the bar magnet pipe joints but also on their sequence of assembly etc. Although we do find sections of magnetometer surveys where the bar magnet pattern interpretation seems relatively straightforward there are others where we are reminded of the potential complexity.

There are other complications to be considered such as other ferromagnetic bodies (wire fences!, water lines, other pipelines etc.), magnetic storms, relative changes in the earth field vector etc. The effects of stress induced changes in magnetization on the fringing fields are superimposed on all these.

We have therefore undertaken various field tests and demonstrations of varying intermediate complexity to gain experience and to help to confirm our interpretations.

We have made numerous magnetometer surveys of pipelines during construction including many before and after surveys of joints which have been cold bent in the field. The stress distribution left after cold bending is, of course, very complex but the effects of cold bends on the magnetometer survey patterns can be summarized most simply by describing them as extra bar magnets added into the string used to represent the pipeline as shown ideally in Fig. 5 for a single joint with a bend made in the middle. Fig. 6 shows actual before and after field measurements for comparison; these are of course, slightly more irregular partly because the length surveyed is in fact a double length joint formed by factory welding two standard joints. There is some evidence of 'relict poles'[1] from the original pair of joint bar magnets towards the middle of the double joint before bending although after bending these have been almost obliterated by the large stress induced changes. These field tests help to identify the causes of some of the anomalies in our pipeline surveys but even simple bends do not generally produce such ideal changes as shown in Fig. 6 as shown by another 'before and after' cold bending example in Fig. 7. Here the simplest summary is just to say that the changes are large and readily detectable.

Laboratory scale magnetometer surveys of stressed pipes

Full scale field surveys above buried lines or during construction are conducted under less than ideal well controlled conditions. They have given very encouraging results but have raised many further questions including the possible effects of orientation with respect to the earths

field, line pressure, and the effects of varying stress within the elastic range rather than before and after cold bending.

We have therefore constructed a rather more versatile and controllable laboratory scale test rig shown in Fig. 8. It consists of two 114 mm diameter 3.3 m long steel pipes (2.1×10^9 Pa = 30 Kpsi yield strength) which are stressed in bending by clamping them at one end and near the centre and springing the other ends together. Stresses are measured by strain gauges and verified by calculations both from deflections and from loads. The system is pivoted like a childs teeter-totter and can be orientated in any direction with respected to the earths field.

We have used this to demonstrate that the stress induced changes in magnetic fringing fields do not appear to be a strong function of orientation and that it appears that greater stresses induce greater changes. Figs. 9 and 10 show the changes in axial and radial field components measured 100 mm outside one of the pipes using a fluxgate magnetometer for peak bending stresses of 35 MPa, 70 MPa, 105 MPa and 140 MPa with the pipes aligned horizontally E-W and also at 140 MPa with the pipes aligned and dipping along the earths field. Although the results are somewhat irregular they show that greater stresses induce greater changes and that the orientation with respect to the earths field does not appear to be a major influence. The changes confirm the general description of adding an additional bar magnet pattern but it should be noted here that the stress induced bar magnet seems significantly longer than the extent of the stress. Figs. 11 and 12 again show the changes in radial and axial field components under similar bending stresses but here the changes with increasing stress are much more regular; these surveys

were made as the stress was directly increased to each successively higher peak bending stress whereas in the previous surveys, the bending stress was relaxed to zero between each progressively higher stress. The differences between the two sets of survey results are attributed primarily to stress induced changes in magnetic hysteresis. The significance of magnetic hysteresis in determining stress induced magnetization changes was first realized during our fundamental investigation of the effects of mechanical stress on the magnetization of pipeline steels (see below) and indicates that the magnetometer survey logs of pipelines depend not only on magnetic history and stress but also on stress history.

Pipelines are subject to axial and hoop stress due to line pressure as well as possible axial stress due to bending. We have investigated some of the effects of line pressure by hydraulically pressurizing our model test pipes. Figs. 13 and 14 show the changes in radial and axial field components during and after hydraulically pressurizing to 100 MPa (14K psi) giving wall stresses of 100 MPa (14K psi).
The changes are rather similar to those induced by bending stress but in this particular case most of the change remains when the stress is relaxed, indicating again that there has been a change in the stress induced hysteresis. We have also started investigations of the results of combining line pressure and bending stress; the results so far are complex probably again due to stress induced changes in magnetic hysteresis.

Fundamental investigations of the effects of mechanical stress on the magnetization of pipeline steels

When iron or steel is magnetised there is an accompanying change in length or strain, this is known as the magnetostrictive effect. Although magnetostriction has been studied extensively relatively little work has

been done on the inverse effect namely the change in magnetization due to mechanical stress (or strain). The magnetostrictive behaviour of iron is complex but for materials studied previously the stress induced changes in magnetization would seem to be largely explicable from the magnetostrictive behaviour by applying Le Chateliers principle. Thus, for a positive magnetostrictive coefficient (expansion with magnetization) tension should increase magnetization thus tending to reduce the applied stress whereas with negative magnetostrictive coefficient (contraction on magnetization) tension should decrease magnetization and compression increase it.

In the case of pipeline steel we find both tension and compression can increase magnetization. We believe that the reason for this very different behaviour is that the steel is magnetically hard and that we are seeing primarily stress induced changes in the magnetic hysteresis whereas previously studied materials have been magnetically soft.

Fig. 15 shows a family of major B-H loops for an A-60 line pipe steel sample. The relative permeability is low (less than 100) and the hysteresis large indicating magnetically hard material. The application of a constant mechanical stress modifies these loops. In our case a tensile stress tends to tilt the hysteresis loops downward indicating negative magnetostrictive coefficient. Stress cycling at a constant applied field tends to reduce the magnetic hysteresis. Fig. 16 shows a major B-H loop approaching saturation together with the initial magnetization curve which is obtained by increasing H applied to an initially demagnetized sample and also the anhysteretic magnetization curve. The anhysteretic magnetization curve is obtained rather similarly to demagnetizing a sample, by applying AC of

steadily decreasing amplitude but superimposing this on a DC cffset; it represents therefore magnetization with hysteretic effects suppressed. The differences between the initial and anhysteretic magnetization curves are small for magnetically soft material but large for hard material.

For magnetically soft material the effect of mechanical stress, which is attributable to magnetostriction, is to tilt the anhysteretic curve (and therefore also the initial curve and B-H loops) to give greater magnetization for positive magnetostrictive coefficient and applied tension or vice versa. This effect also occurs for magnetically hard material but in addition, when the stress is cycled with a constant applied field the hysteresis is reduced which means that the magnetisation will shift towards the anhysteretic curve (which itself is stress dependent). The magnetisation can increase or decrease depending on the relative positions of the original and anhysteretic magnetizations.

The stress induced changes in magnetic hysteresis are probably the major factor governing the different changes in magnetization with different procedures for the laboratory scale pipe bending demonstration. The basic data and understanding obtained from these fundamental investigations is helpful in improving our understanding of our pipe bending demonstrations and our field magnetometer surveys but there is of course a great increase in complexity between considering the magnetization changes of a uniformly stressed small sample and in considering surveys of the external fringing fields of a non-uniformly stressed pipe in proximity to other ferromagnetic pipe.

Conclusions and Discussion

We have demonstrated that stress effects produce readily detectable effects in the fringing fields observed by magnetometer survey above buried pipelines. The fringing field patterns and their relationship to stress are complex but we have already learnt a lot about their interpretation through our field surveys, demonstrations and fundamental investigations. We have gained much useful experience although there remains much to be learnt still.

At this stage we feel that the technique offers excellent potential for monitoring pipelines for changes in bending stress and that the effects are large enough for it to be used non-invasively above the ground. There are also numerous other important applications such as monitoring stress changes in the support legs of offshore platforms etc.

A major question is of course can we measure actual stress levels rather than just detecting changes in stress. Our basic studies suggest that this is possible in principle and we are working on the challenge of whether we can do this in a practical fieldworthy technique.

Figure Captions

Fig. 1: Proton precession magnetometer total field plot. The traverse is made 2 m above a 0.76 m diameter 10 mm wall pipe. The axial displacement scale is given in multiples of 12 m because the pipe joints from which the line is strung are 12 m long. Note that the field fluctuations are several kilogammas (1 gamma = 10^{-9}T) and that there appears to some correlation with the welds between joint lengths.

Fig. 2: An idealized isolated pipe joint acting as a simple bar magnet produces axial and radial field components above the joint as shown.

Fig. 3: Fluxgate magnetometer traverses showing the axial and radial field components measured 1.2 m above a 1.2 m diameter isolated pipe joint. These measurements are superimposed on the earths background field of approximately 60 kilogamma.

Fig. 4: Fluxgate magnetometer traverse showing the vertical field fluctuations along a 200 m string of welded pipe joints. The traverse is made 1.2 m above a 1.2 m diameter 13 mm wall pipeline during construction immediately prior to lowering it into the ditch in which it will be buried. Several field bends are included in this traverse. Although the field fluctuations are large, the general pattern is typically complex.

Fig. 5: An idealized pipeline joint which has had a cold bend made in the middle. This has the effect of introducing a short reversed bar magnet at the bend which produced axial and radial field components as shown.

Fig. 6: Measurements of the axial and radial field components made before and after cold bending at 21 m length of pipe to produce a 2^{o} sag (upward) bend. The 21 m length was produced by factory welding two approximately 10 m long joints. Although the 'before' bending plots show that these two original joints appear to have been magnetized in the same direction and to have formed a longer bar magnet when joined there is a suggestion of 'relict poles' near the middle. The measurements were made 1.2 m above the 1.2 m diameter line.

Fig. 7: Before and after making a 1^{o} cold bend vertical field components made with a fluxgate magnetometer 1.2 m above a 1.2 m diameter 13 mm wall isolated pipe joint. These traverses are rather more typical than the simpler example shown in Fig. 6.

Fig. 8: The 'teeter-totter' test rig for examining the effects of bending stresses on 114 mm diameter 3.3 m long steel pipes. There are two pipes separated by a central aluminum saddle tied at one end and sprung together at the other. These are supported on a non-magnetic wooden structure. A fluxgate magnetometer is being used to survey the magnetic fringing fields.

Fig. 9: Changes in radial field components 100 mm above one of the teeter-totter pipes for peak bending stresses of 35 MPa, 70 MPa, 105 MPa and 140 MPa with the pipes aligned horizontally E-W and also 140 MPa with the pipes aligned with and dipping along the earths field.

Fig. 10: Changes in axial field components measured concurrently with the radial field changes shown in Fig. 9.

Fig. 11: Radial field changes under increasing stresses similar to Fig. 9 except that instead of relaxing the bending stress between each successively higher peak bending stress as was done in the tests for Fig. 9 here the bending stress was increased directly to the next higher stress.

Fig. 12: Axial field changes obtained concurrently with the radial field changes shown in Fig. 11.

Fig. 13: Radial field changes due to hydraulically stressing the pipe to 100 MPa and after releasing.

Fig. 14: Axial field changes occurring with the radial field changes shown in Fig. 13.

Fig. 15: A family of major B-H loops for A-60 line pipe steel.

Fig. 16: A major B-H loop, the initial magnetization curve and the anhysteretic magnetization curve. The anhysteretic curve is obtained by applying ac of steadily decreasing amplitude on a superimposed dc. It represents magnetization with the hysteretic effects suppressed and is therefore reversible.

References

(1) D.L. Atherton and A. Teitsma, "Detection of Anomalous Stresses in Gas Pipelines by Magnetometer Survey", J. Appl. Phys. Vol. 53, No. 11, pp. , November 1982.

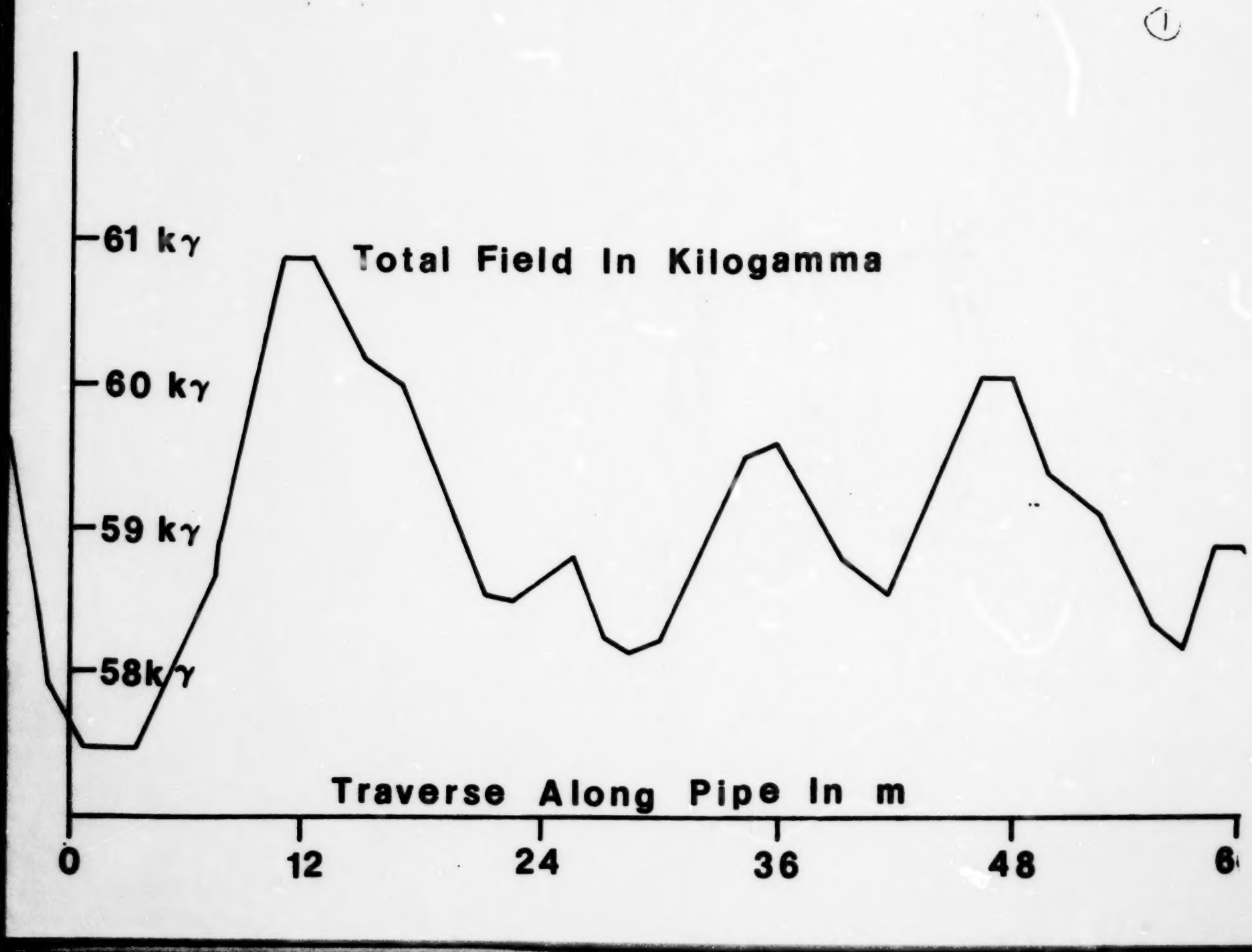
61 kγ
60 kγ
59 kγ
58kγ
Total Field In Kilogamma
Traverse Along Pipe In m
0
12
24
36
48

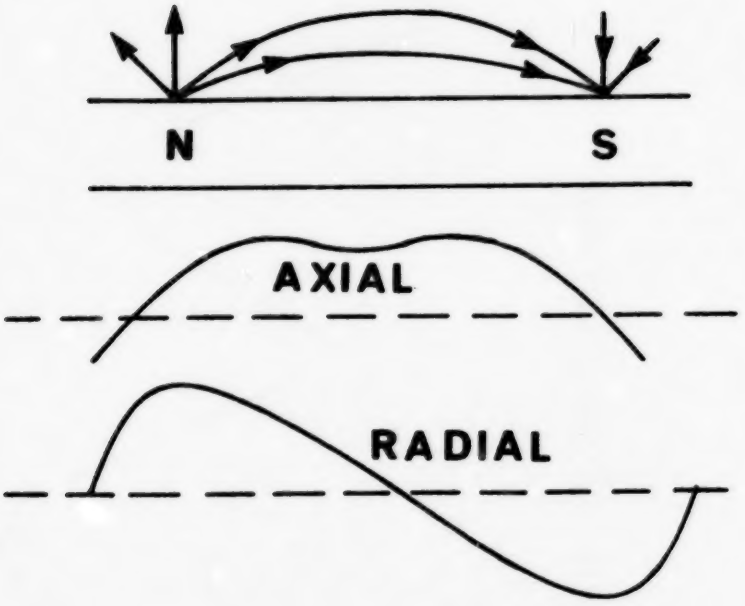
N
S
AXIAL
RADIAL

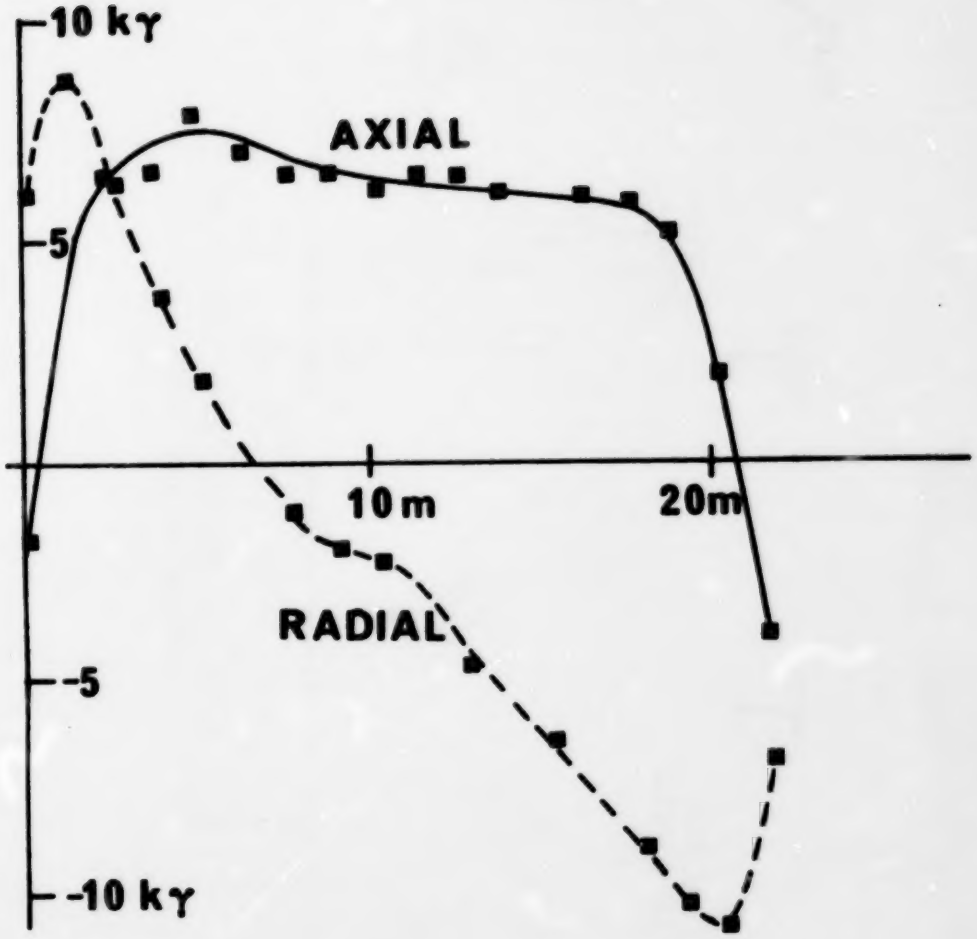
10 kγ
AXIAL
5
10 m
20m
RADIAL
-5
-10 kγ

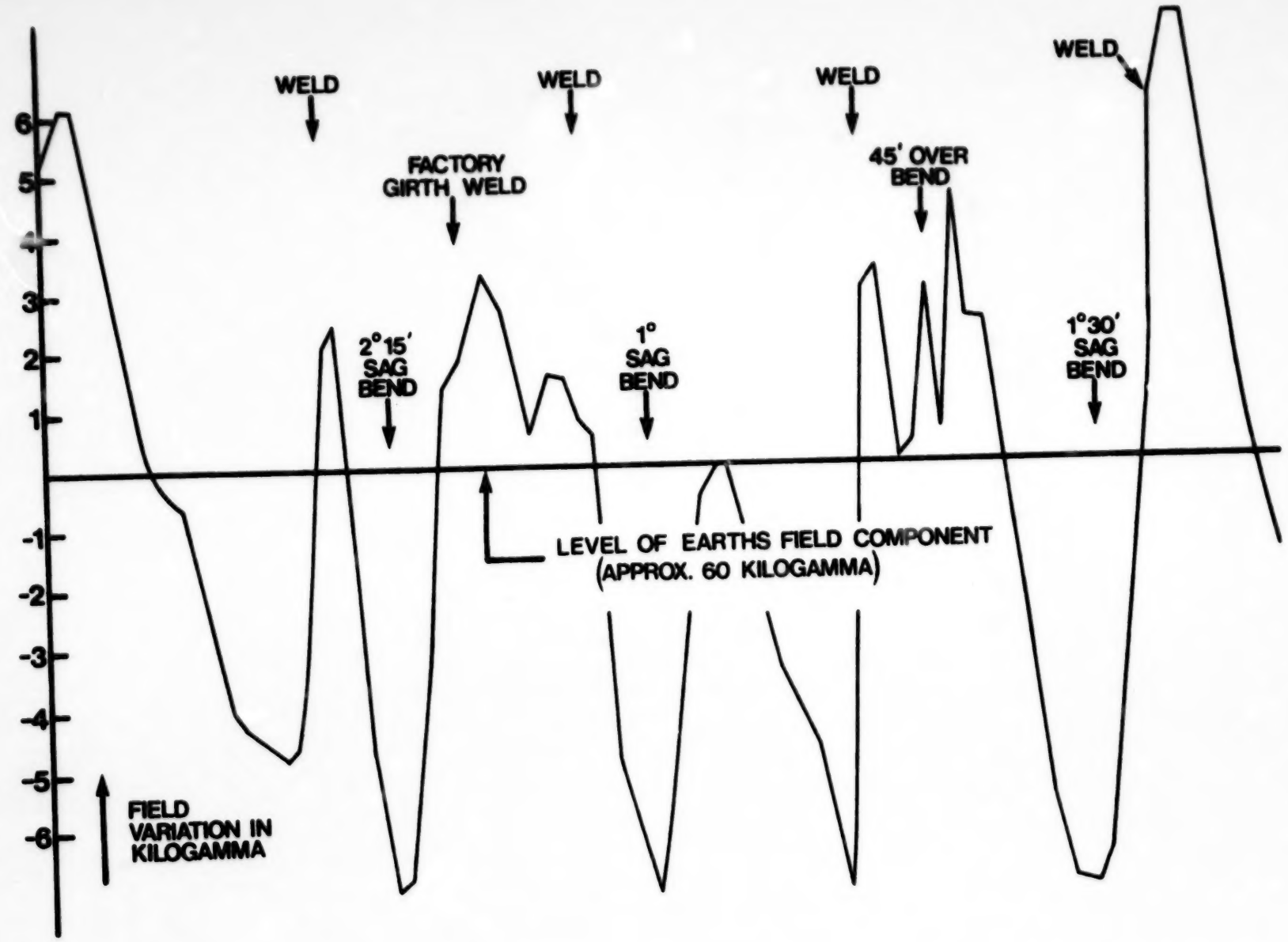
WELD
WELD
WELD
WELD
FACTORY GIRTH WELD
45' OVER BEND
2°15' SAG BEND
1° SAG BEND
1°30' SAG BEND
6
5
4
3
2
1
-1
-2
-3
-4
-5
-6
LEVEL OF EARTHS FIELD COMPONENT (APPROX. 60 KILOGAMMA)
FIELD VARIATION IN KILOGAMMA

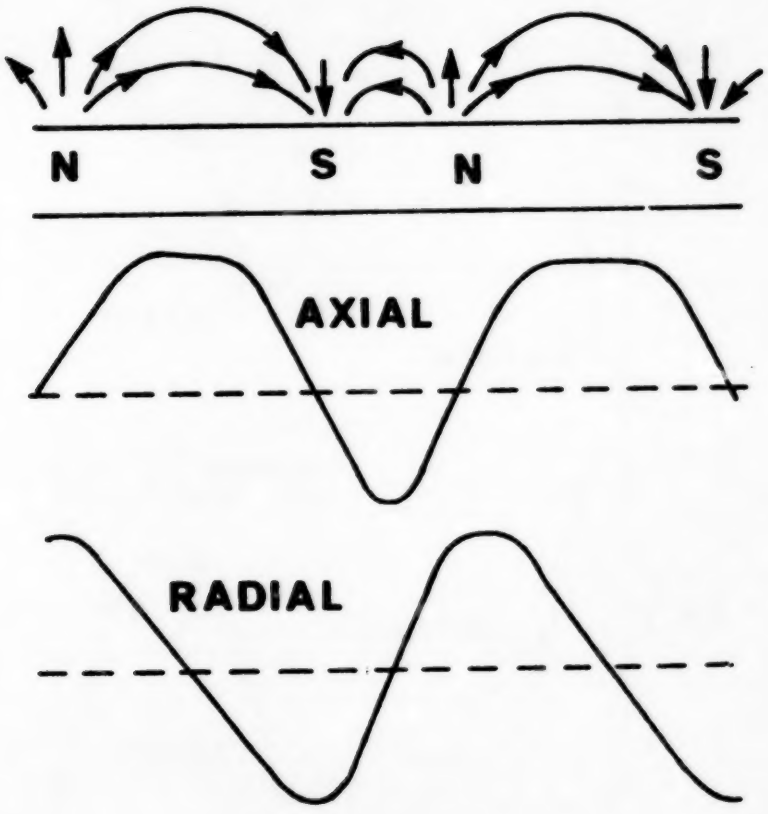
N
S
N
S
AXIAL
RADIAL

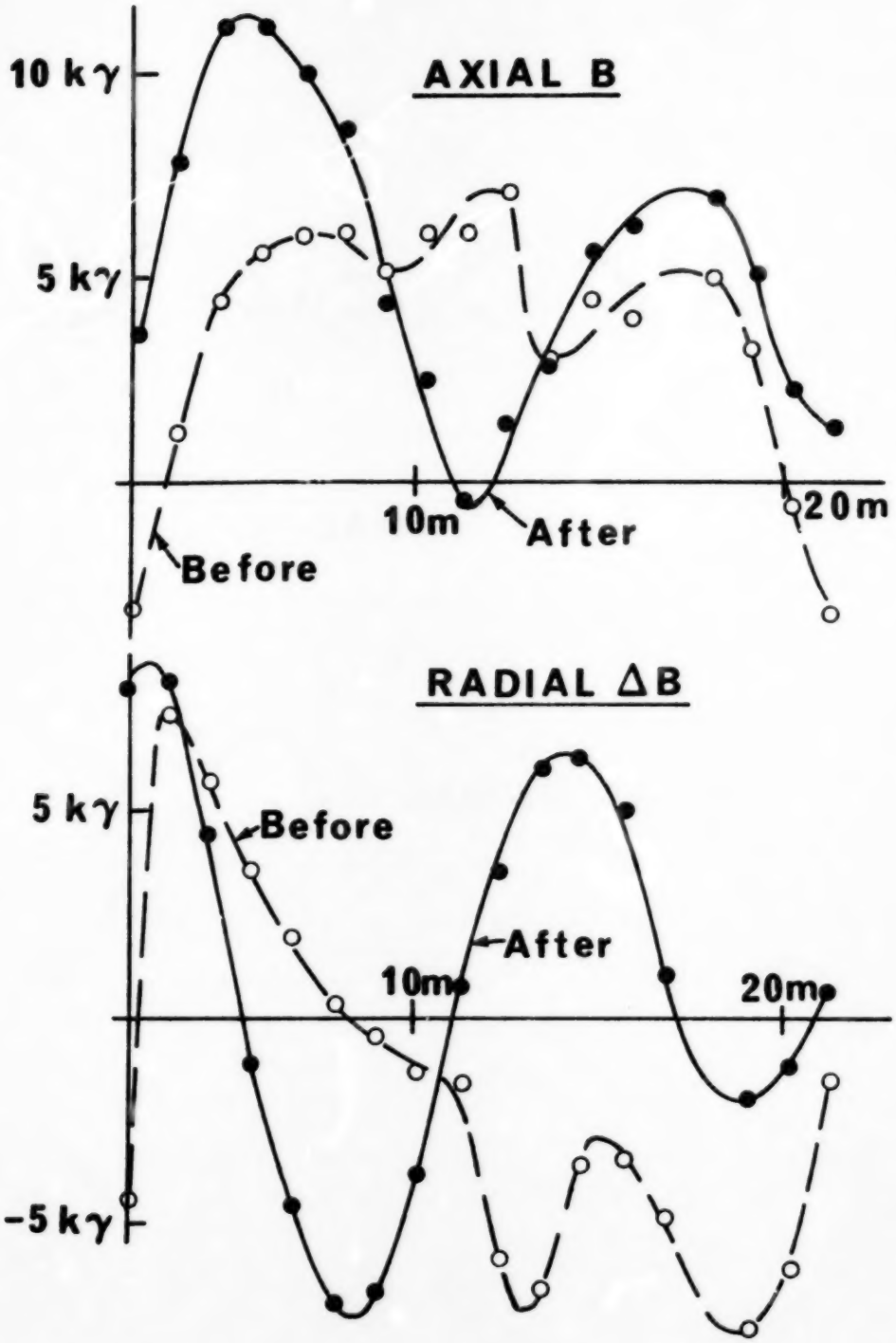
10 kγ
AXIAL B
5 kγ
10m
After
20m
Before
RADIAL ΔB
5 kγ
Before
After
10m
20m
-5 kγ

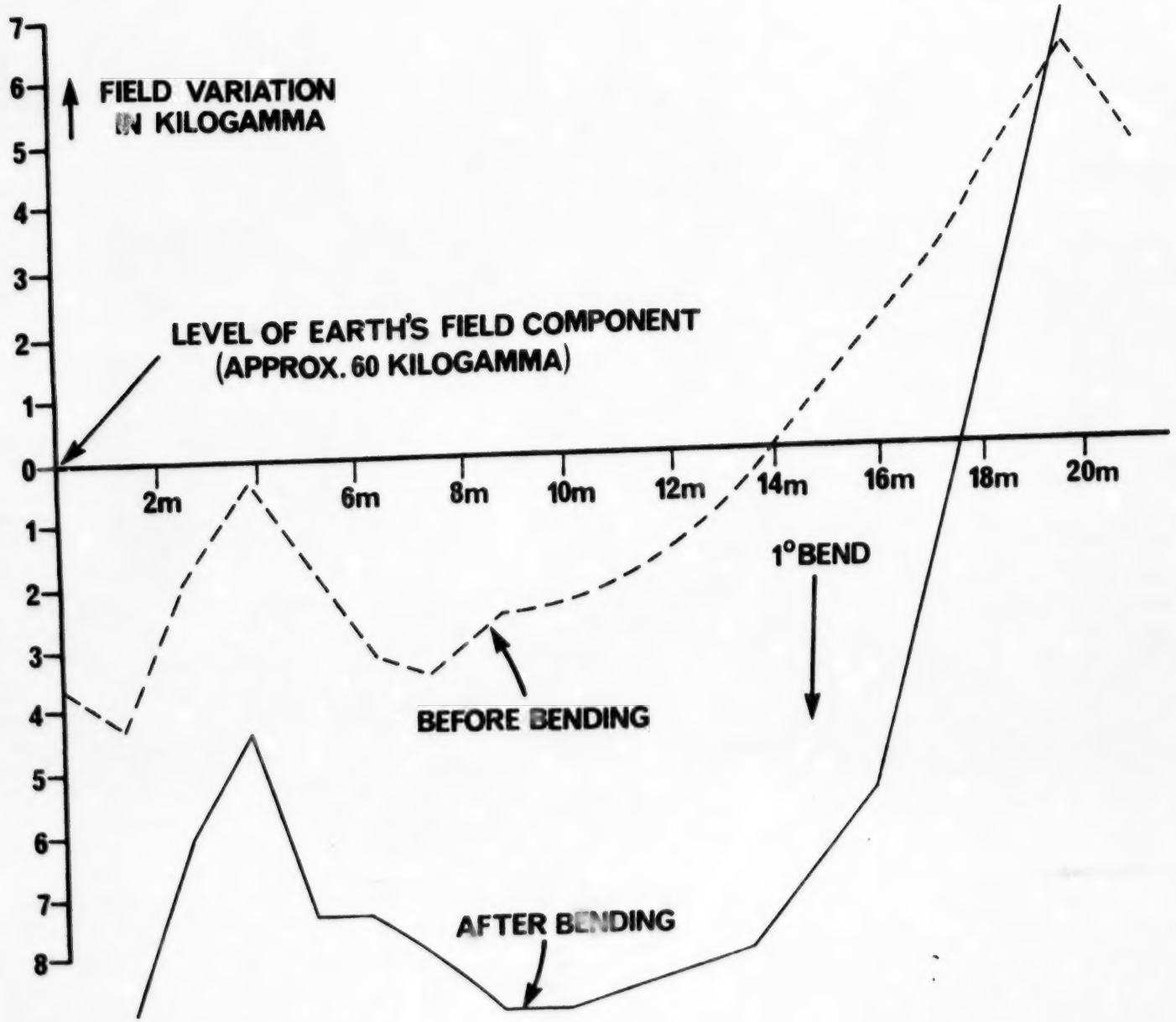
FIELD VARIATION
IN KILOGAMMA
LEVEL OF EARTH'S FIELD COMPONENT
(APPROX. 60 KILOGAMMA)
7
6
5
4
3
2
1
0
1
2
3
4
5
6
7
8
2m
6m
8m
10m
12m
14m
16m
18m
20m
1°BEND
BEFORE BENDING
AFTER BENDING

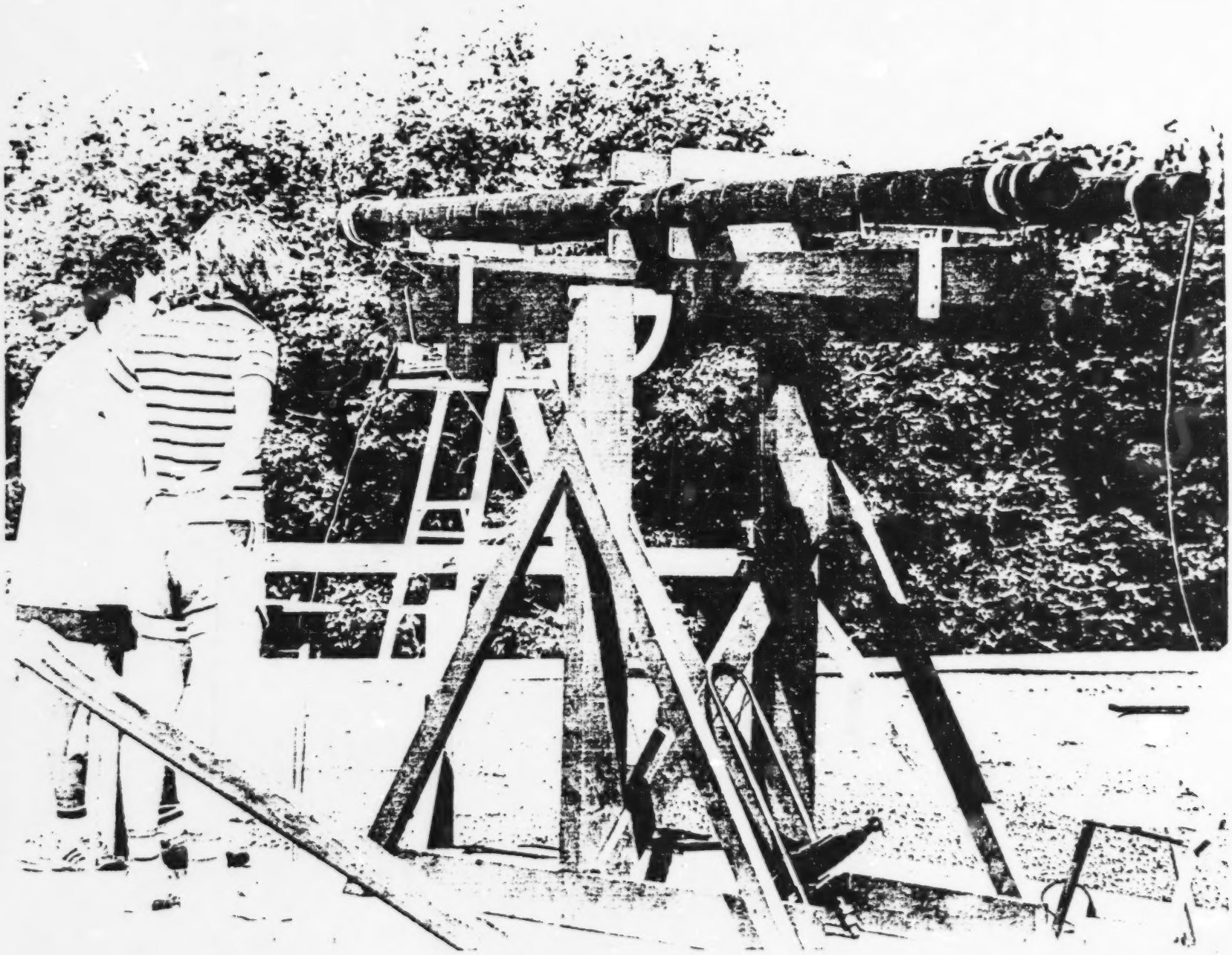

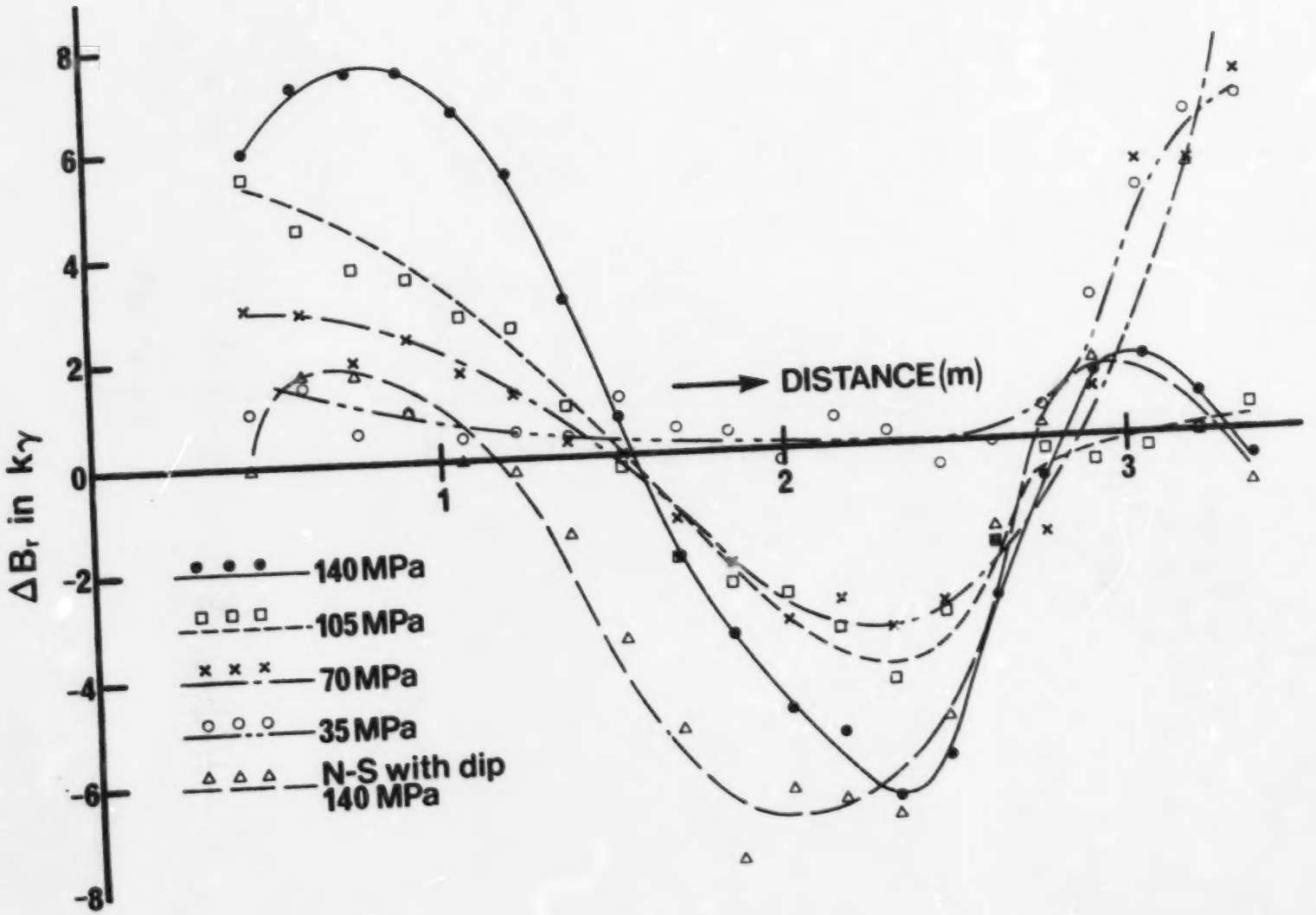
8
6
4
2
0
-2
-4
-6
-8
ΔBr in kγ
DISTANCE (m)
1
2
3
140 MPa
105 MPa
70 MPa
35 MPa
N-S with dip
140 MPa

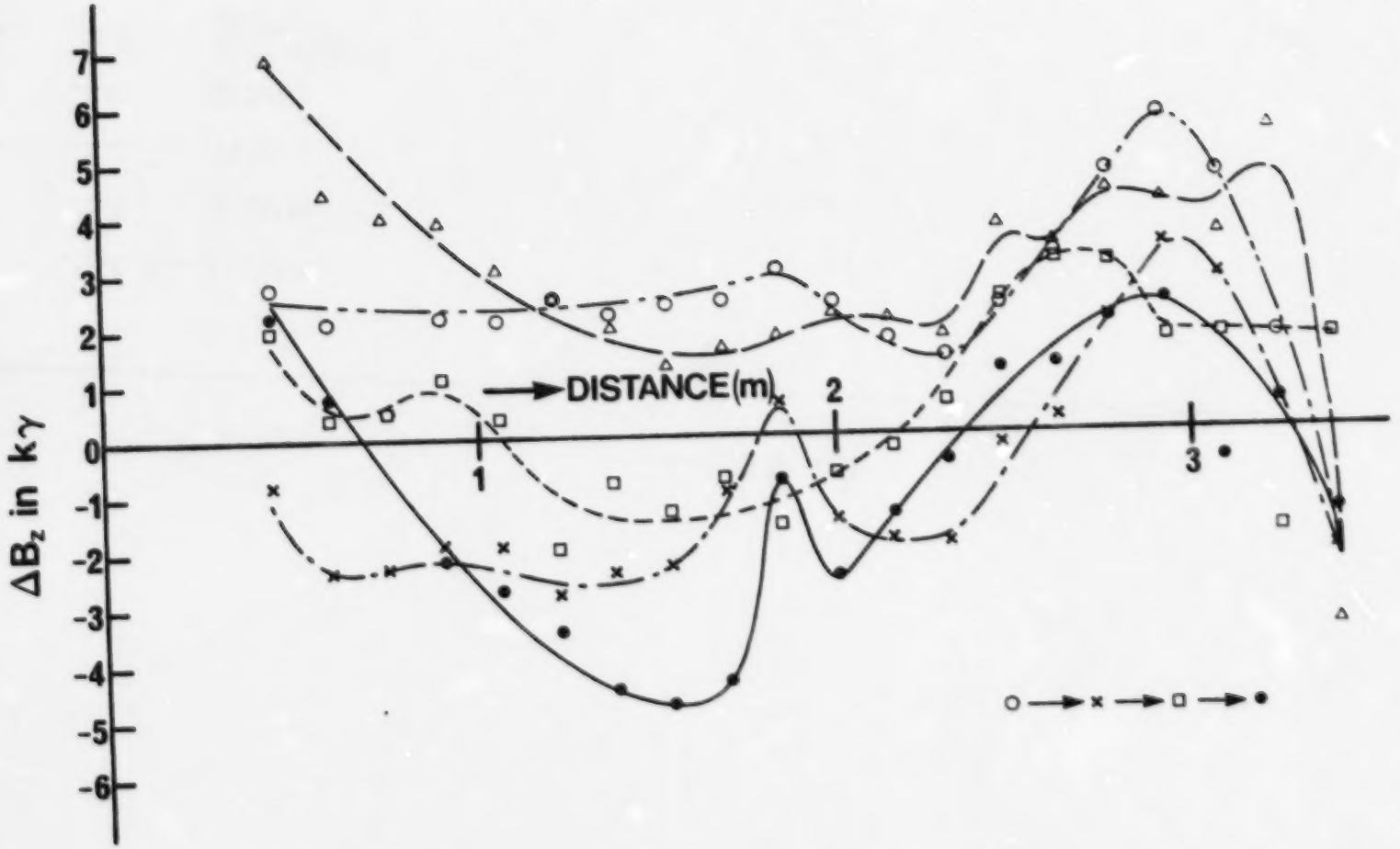
7
6
5
4
3
2
1
0
-1
-2
-3
-4
-5
-6
ΔBz in kγ
DISTANCE(m)
1
2
3

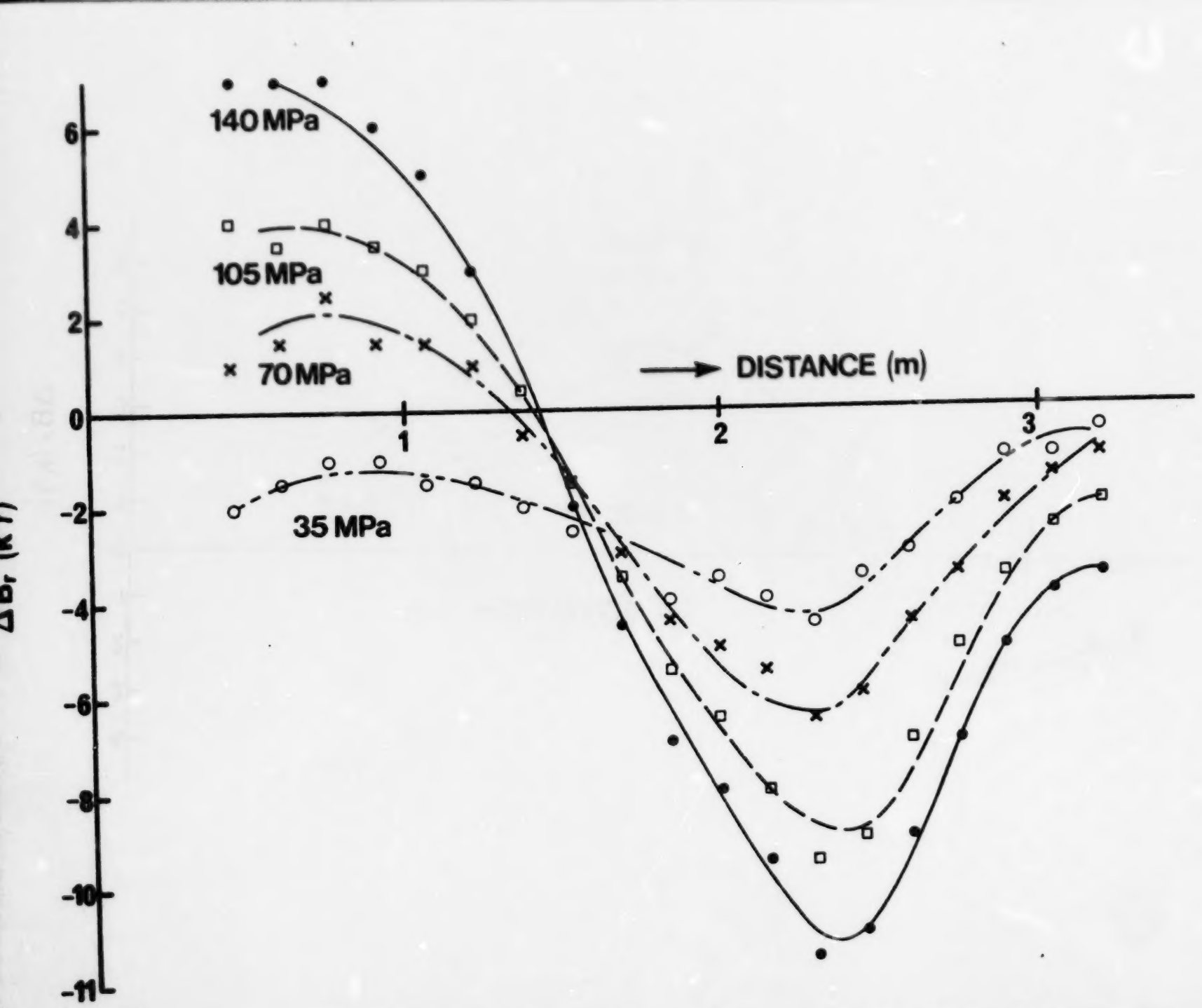
140 MPa
105 MPa
70 MPa
35 MPa
DISTANCE (m)
ΔBr (KT)
6
4
2
0
-2
-4
-6
-8
-10
-11
1
2
3

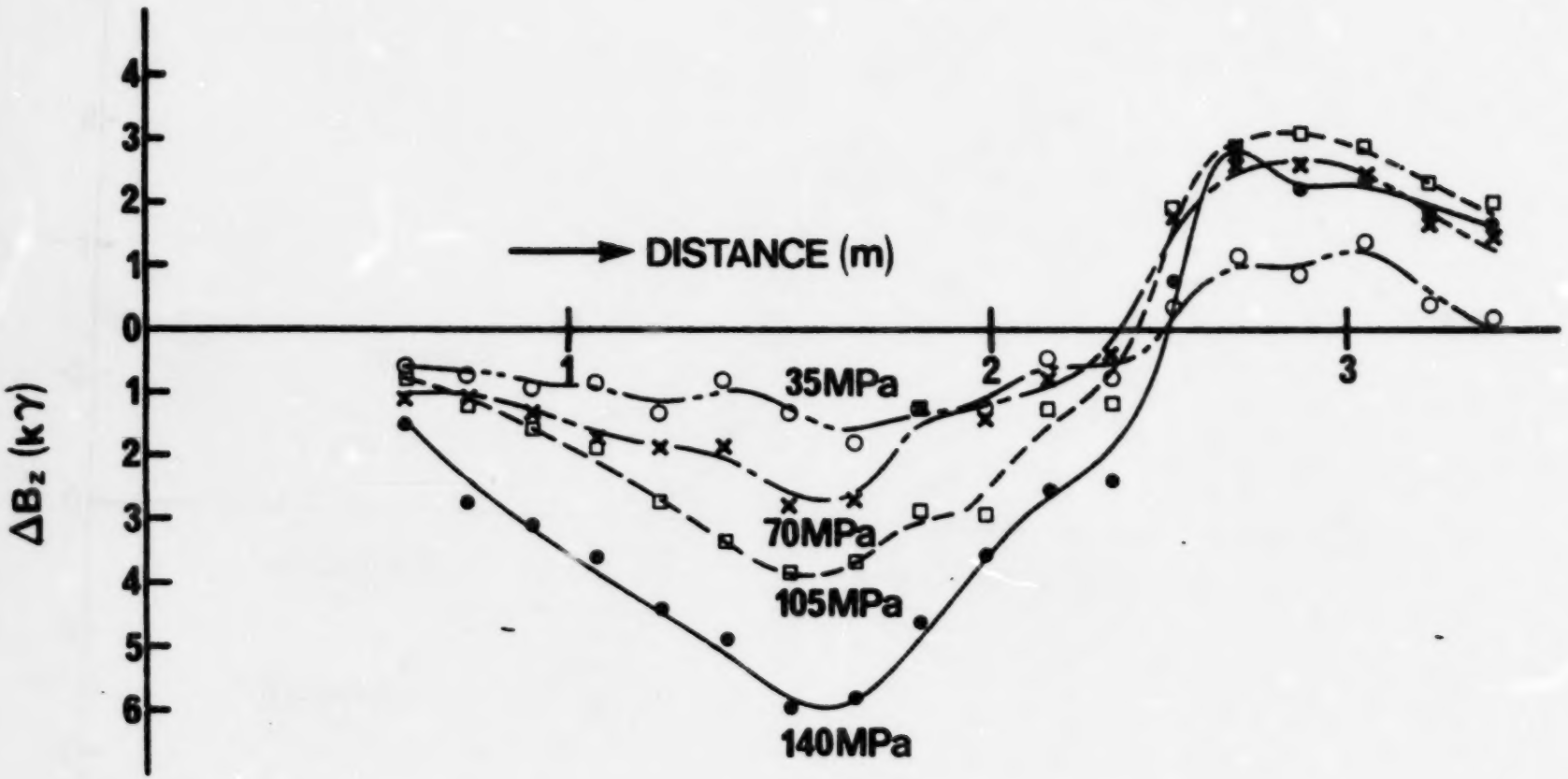
4
3
2
1
0
1
2
3
4
5
6
DISTANCE (m)
1
2
3
35MPa
70MPa
105MPa
140MPa
ΔBz (kγ)

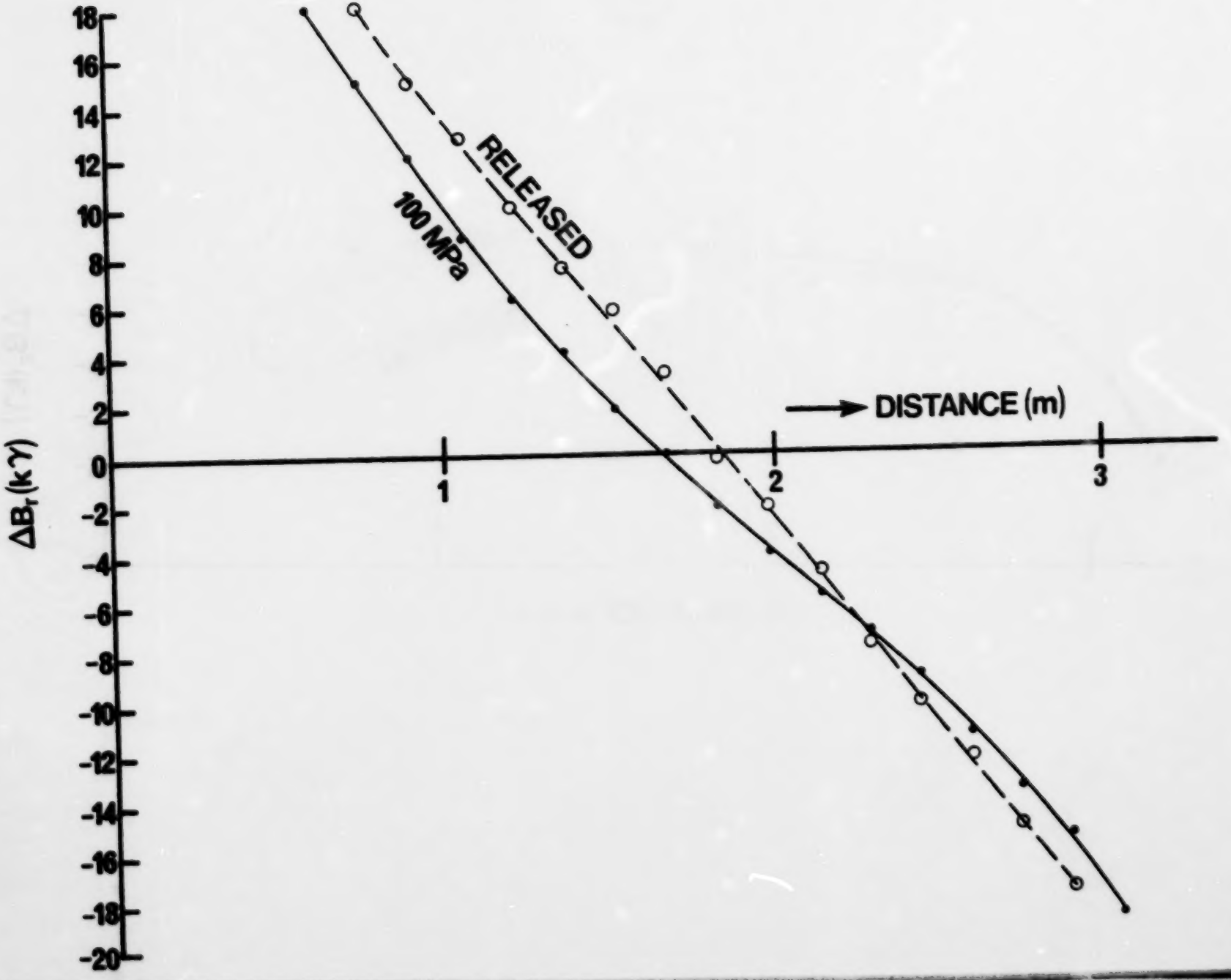
18
16
14
12
10
8
6
4
2
0
-2
-4
-6
-8
-10
-12
-14
-16
-18
-20
ΔBr(kγ)
RELEASED
100 MPa
DISTANCE (m)
1
2
3

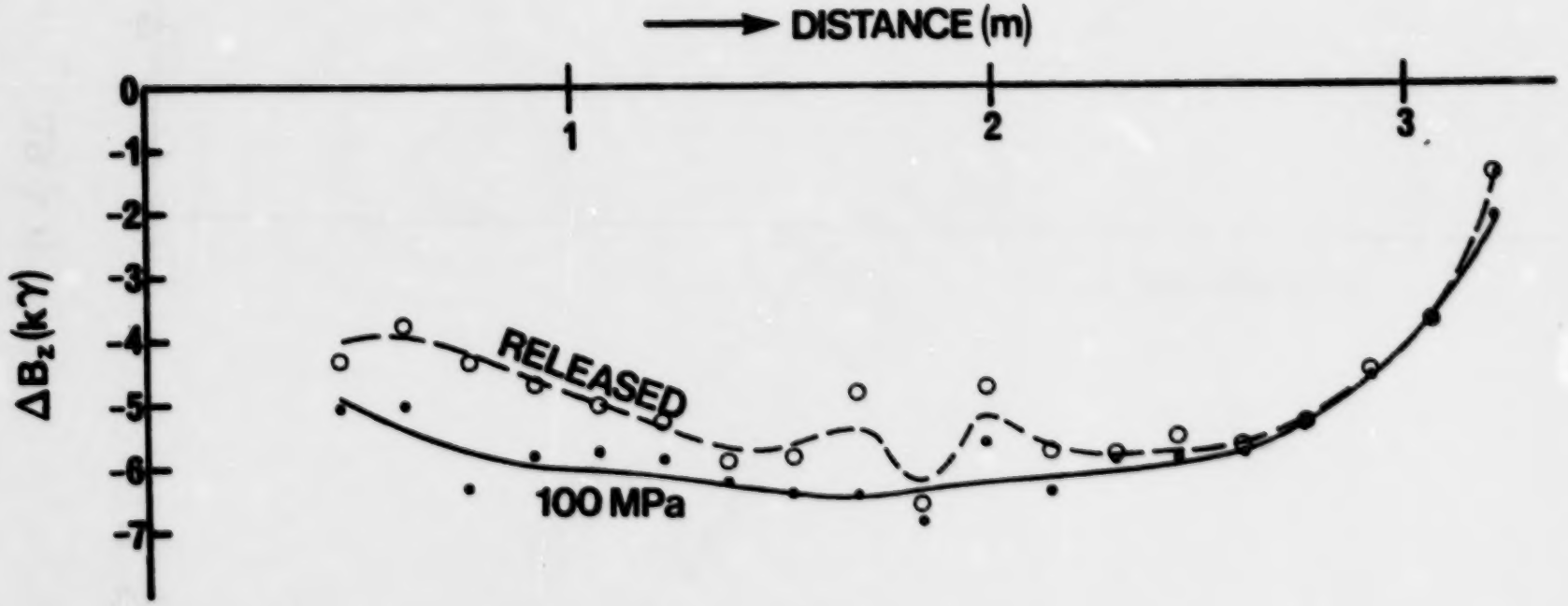
DISTANCE (m)
0
1
2
3
-1
-2
-3
-4
-5
-6
-7
ΔBz(kγ)
RELEASED
100 MPa

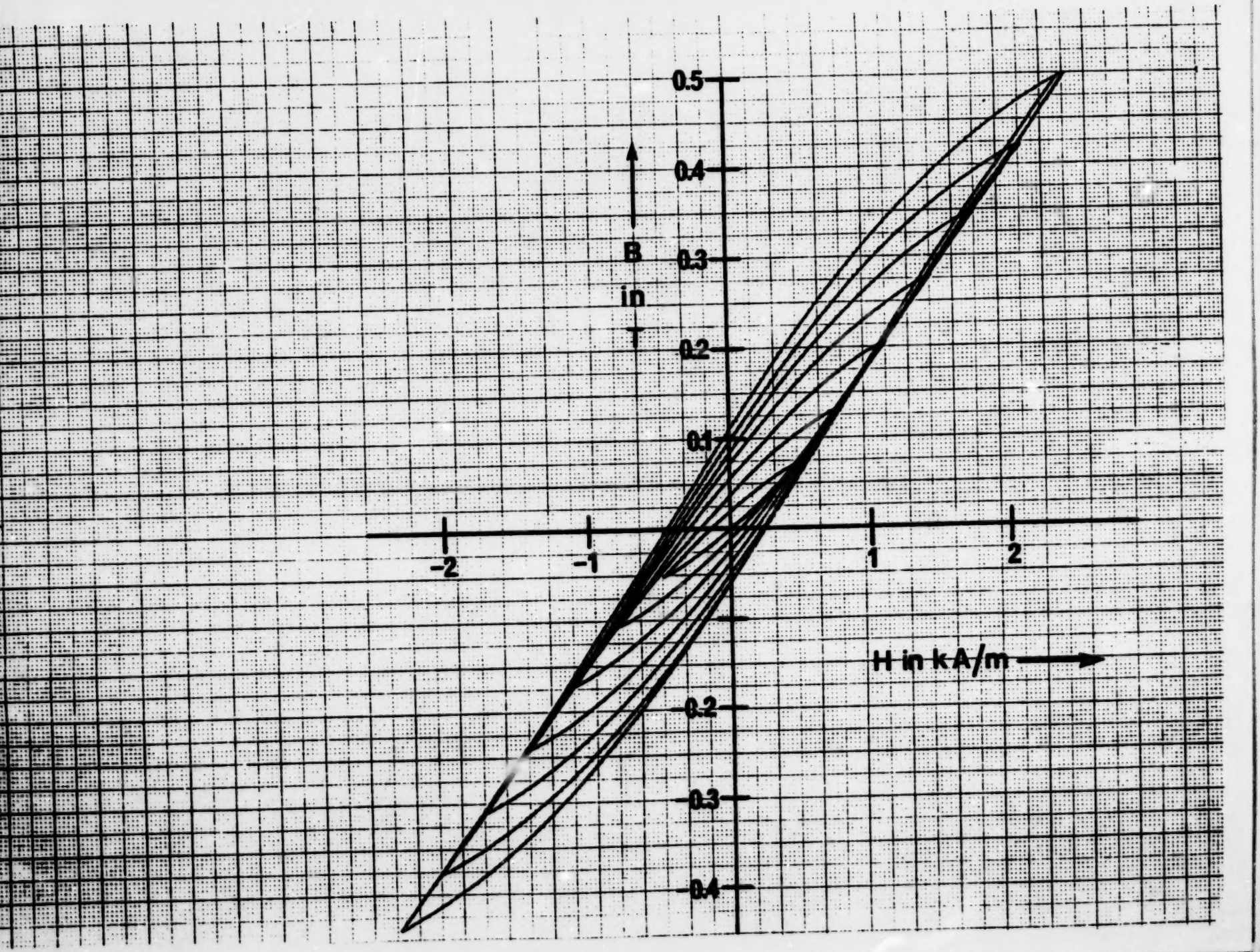
0.5
0.4
B
in
T
0.3
0.2
0.1
-2
-1
1
2
H in kA/m
0.2
0.3
0.4

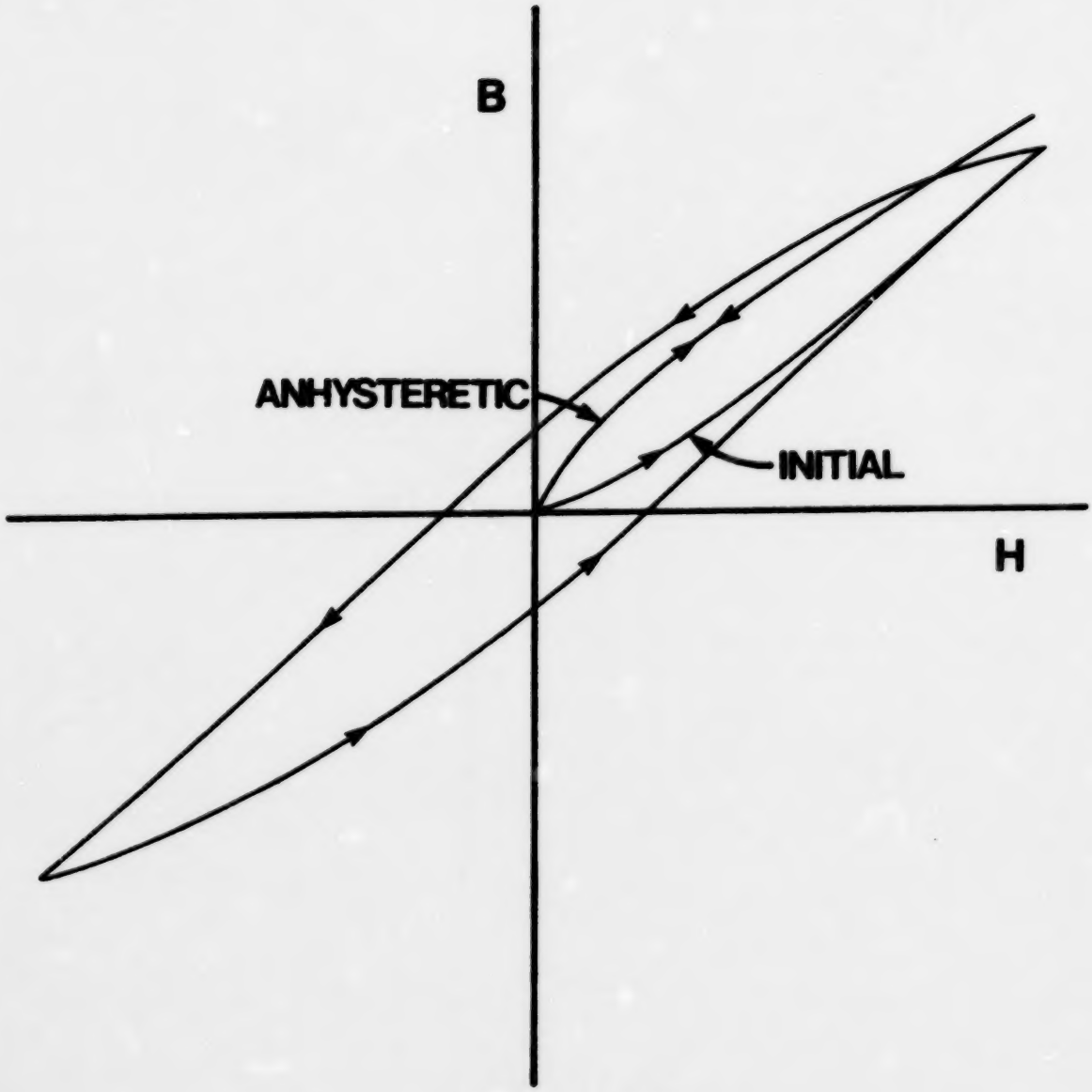
B
ANHYSTERETIC
INITIAL
H

Stress-shadow magnetic inspection technique for far-side anomalies in steel pipe

D.L. Atherton

A two-step process for obtaining strong magnetic leakage flux signals from far-side anomalies in steel pipe is described. The pipe is magnetized by a magnetic pig while it is stressed by line pressure. Anomalous local stresses on the near side of the steel caused by far-side corrosion produce anomalies in the residual magnetization. These near-side residual field anomalies due to the stress shadows from exterior corrosion are then readily detectable. Initial laboratory tests are described.

Keywords: magnetic measurement, non-destructive testing + stress, steel pipe + corrosion

Gas pipelines are, typically, buried. Since they are effectively pressure vessels they are carefully inspected both during construction and at intervals during their operational life. Pipeline inspection must normally be performed by pumping an inspection tool, known as a pig, through the pipe. The inspection pig is normally fitted with anomaly detectors using either magnetic leakage flux or eddy-current techniques. Both of these types of detectors can respond well to interior defects such as corrosion pits and cracks, but skin depth and magnetic diffusion limitations mean that signals from the far side or exterior of the steel pipe-wall are much less satisfactory and are likely to give very poor signal-to-noise ratios because of the small signals and the microphonic noise generated in magnetic leakage flux detectors. In fact, it might appear that far-side signals obtained by magnetic inspection techniques are almost inevitably bound to be much weaker than near-side signals. Unfortunately, for gas pipelines where the product has been properly cleaned the major concern is inspection for exterior metal loss which may occur at 'holidays' (damaged sections in the protective wrapping) where there is galvanic corrosion due to improper electrolytic protection *etc.*

Here, we describe the concept and initial testing of a new technique devised specifically to obtain strong signals from far-side or exterior defects in steel pipe-walls such as corrosion, cracks *etc.*

Conceptual description

The strain or change in length of steel when it is magnetized is known as the magnetostrictive effect and is well understood and documented. The inverse effect, namely the change in magnetization with strain, has not been as widely investigated but is presently attracting renewed attention[1]. Our technique exploits the stress-dependence of magnetization.

In our technique the pipeline is pressurized by the internal operating line pressure, and is magnetized whilst under pressure by passing a magnetic pig through it. Subsequently a detector pig fitted with residual field anomaly detectors is passed through the line. This is therefore a two-step process.

In the first step, the line is magnetized whilst it is pressurized with a typical gas transmission-line operating pressure of the order of 4 MPa, which produces a stress of about 150 MPa in the steel pipe-wall due to hoop tension. It is magnetized whilst under stress using a magnetic pig fitted with either electromagnets or permanent magnets.

Where there are anomalies in the pipe wall such as hard spots, cracks or pipe-wall thinning due to corrosion *etc*, there will be local stress anomalies which will, in general, give rise to anomalies in the residual magnetization remaining after the pipe has been magnetized. Exterior corrosion and cracks which are not aligned with the direction of stress will tend to give local anomalously high stresses on the interior of the pipe wall and consequent surface anomalies in the residual magnetization. Interior corrosion or cracks, on the other hand, will tend to give residual magnetization surface anomalies on the outside of the pipe. The leakage fluxes arising from these local surface magnetic anomalies resulting from stress will tend to be mostly inside the pipe for exterior metal loss and outside the pipe for internal corrosion, since the pipe wall itself will act as a low reluctance magnetic shunt. The corrosion pits themselves may also be considered as magnetic anomalies due to missing magnetized material and it is this effect which is the basis of the magnetic flux leakage method illustrated in Figure 1.

The magnetic flux leakage method produces excellent signals from near-side corrosion whereas stress-produced magnetization anomalies are on the opposite side to the corrosion and will therefore tend to emphasize far-side anomalies. The first step in our process is therefore the development of a suitable magnetic anomaly picture using, effectively, the stress shadows cast on the interior of the pipe wall by metal loss on the exterior.

0308-0126/83/030145-05 $03.00 © Butterworth & Co (Publishers) Ltd

The second step in the process is to read the magnetic anomaly pattern by sensing the anomalous stress-shadow leakage fluxes or fringing fields. A variety of detectors or gradiometers can be used for this, such as moving or vibrating coils, fluxgates or Hall probes (all of which we have tested).

The use of a two-step process has a major potential advantage in noise reduction compared with conventional magnetic flux detectors or eddy-current detectors. Magnetic leakage flux detectors often use dynamically induced signals in a sense coil located between the poles of a magnet, as shown in Figure 1, and are very susceptible to vibration-induced microphonic noise; eddy-current detectors also use drive and sense coils in close proximity and tend also to be susceptible to lift off and vibration-induced noise. Our two-step process isolates the relatively noisy magnetic development process from the subsequent read process and allows each process to be optimized separately.

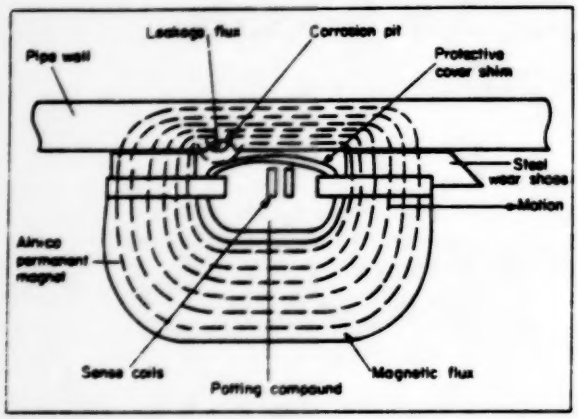

Fig. 1 Principle of operation of typical magnetic leakage flux anomaly detector. A region of the pipe wall is magnetized by the permanent-magnet. The magnetic leakage flux in the vicinity of an anomaly, such as the corrosion pit shown, induces a signal voltage in the sense coils as the detector moves by. The magnetic flux paths are greatly simplified here for clarity: in particular the leakage flux density in the air is small; there is considerable direct leakage flux across the permanent magnet; the flux density on the near side of the pipe wall will be greater than on the far side; and the flux pattern will be swept back somewhat as a result of the detector motion and magnetic diffusion times

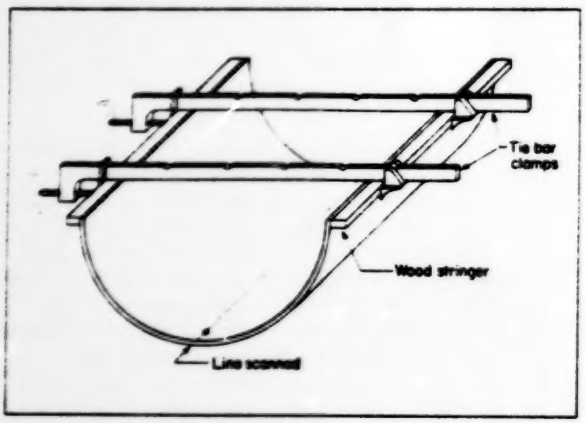

Fig. 2 The pipe and stress mechanism

Experimental testing

For convenience, and also to allow better control, we used simulated line pressure stress in our initial testing. Stress was produced by taking a semi-circular half-section of line pipe and bending it by using tie rods across its diameter as shown in Figure 2. It will be noted that this is not an exact simulation since it gives tensile stresses on the outside and compressive stresses on the inside rather than the uniform-hoop tensile stress which should be generated by line pressure; nevertheless, for external surface corrosion it is a reasonable simulation.

The pipe section used was a nominal 762 mm diameter A-60 steel pipeline (0.25%C, 1%Mn, 0.01%P, 0.02%S, 430 MPa yield strength and 590 MPa ultimate tensile strength) with a 9.5 mm wall thickness. Local corrosion was simulated by milling round- and square-bottom holes of various sizes and wall penetrations. Stresses at the external surface of the pipe were measured using a strain gauge and verified by calculation from the measured pipe deflections. All stresses assume normal, non-corroded pipe wall thickness without additional allowance for stress concentration near the corroded regions.

Field profiles were recorded using a special Hall probe configuration, scanning slowly along the line of synthetic defects indicated in Figure 2. The simulated defect types and locations are shown schematically in Figure 3. Many tests were made, and Figures 4–8 are representative of the results. Since only slow scanning was possible there is no vibration-induced noise. Scans were made with the pipe both unstressed and stressed in bending to a peak stress of 200 MPa, and with the pipe both magnetized and not magnetized. The pipe was magnetized along the defect line using the permanent-magnet assembly of a magnetic-flux leakage defect detector which was moved along the pipe by hand. It was 'demagnetized' by sweeping the detector magnet along the pipe in alternate directions at successively greater distances from the pipe wall.

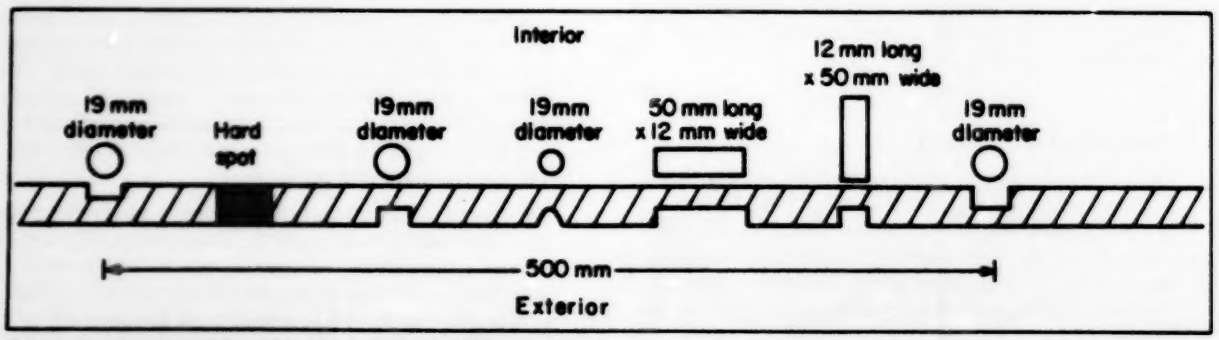

Fig. 3 A schematic representation of the synthetic defect line scanned

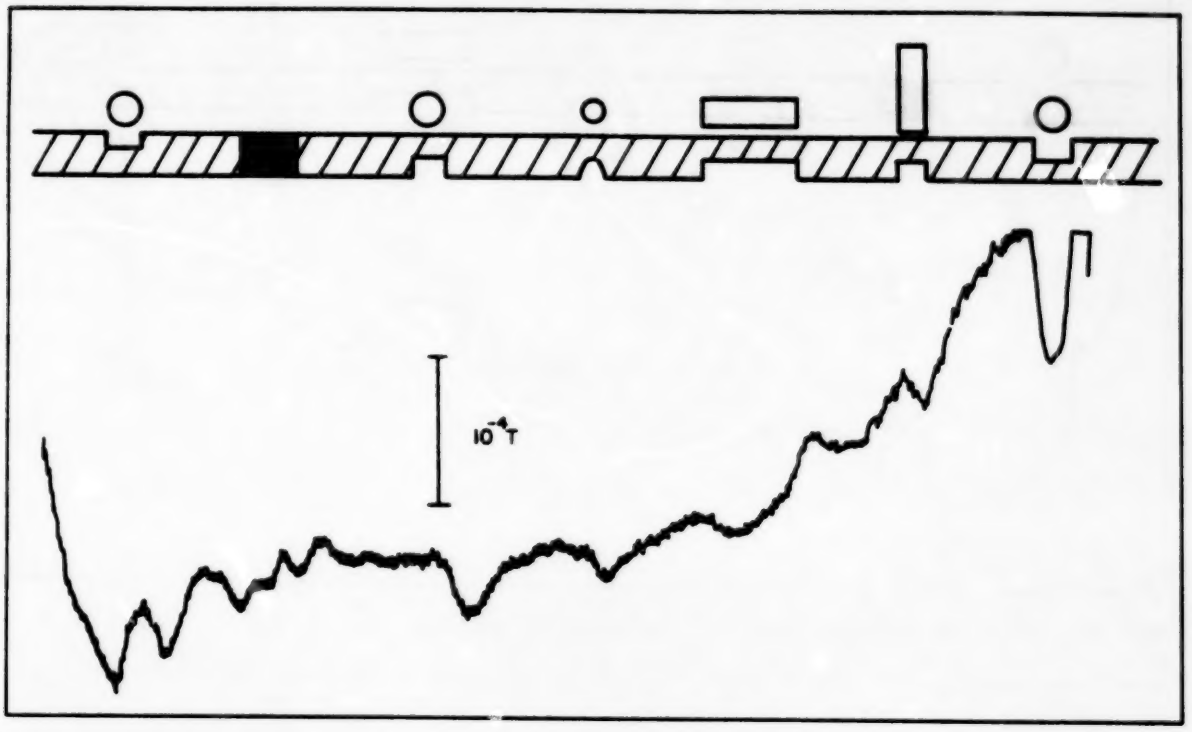

Fig. 4 A high sensitivity radial field profile made with the pipe unstressed and not magnetized

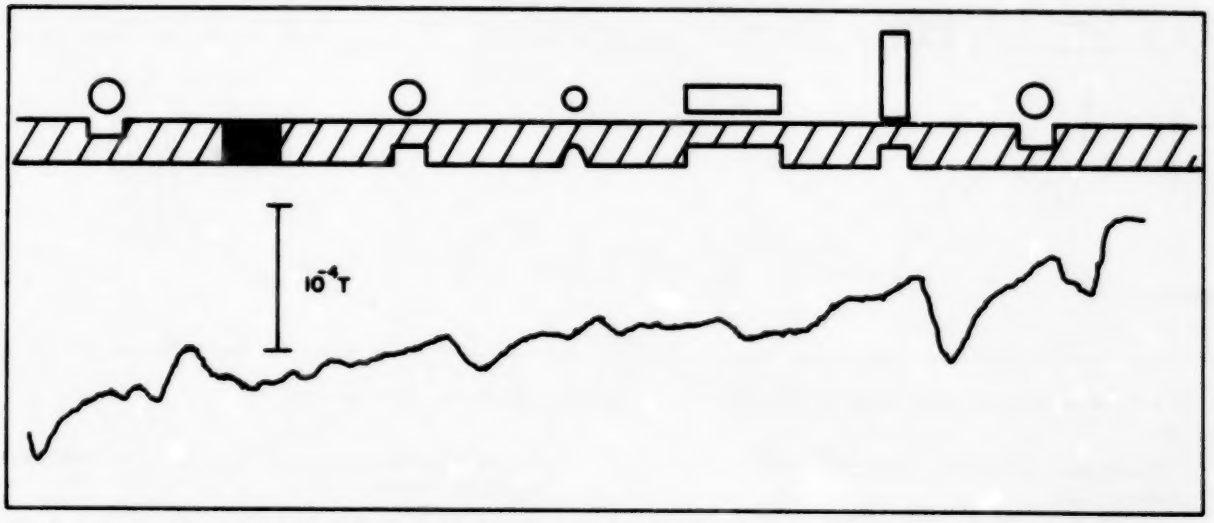

Fig. 5 A high sensitivity radial field profile made with the pipe stressed to 180 MPa peak and not magnetized

These techniques, of course, only altered a strip of pipe wall along the defect line, although they were selected to represent the effects of magnetic pigging. As in real pigging operations, the results were not fully reproducible due to air gap and speed variations, end and side effects *etc.* The approximate maximum flux density generated in the pipe wall by the detector magnet was 0.7 T.

Figures 4 and 5 show radial field profiles of unstressed and stressed pipe which is nominally not magnetized. At this high sensitivity there is still evidence of residual pipe magnetization, indicated by the general slope, and of field fluctuations, particularly near the ends of the pipe, which always tend to be noisy. These are not generally well-correlated with defects and represent mostly noise due to irregular pipe demagnetization, although interior metal loss may give small signals where local demagnetization has been incomplete.

Figure 6 is a radial field profile made with sensitivity reduced by a factor of 5 from the previous profiles and with the pipe unstressed but magnetized. There are possible signals correlated with the interior anomalies, namely the hard spot and interior pits (although these tend to be obscured by end

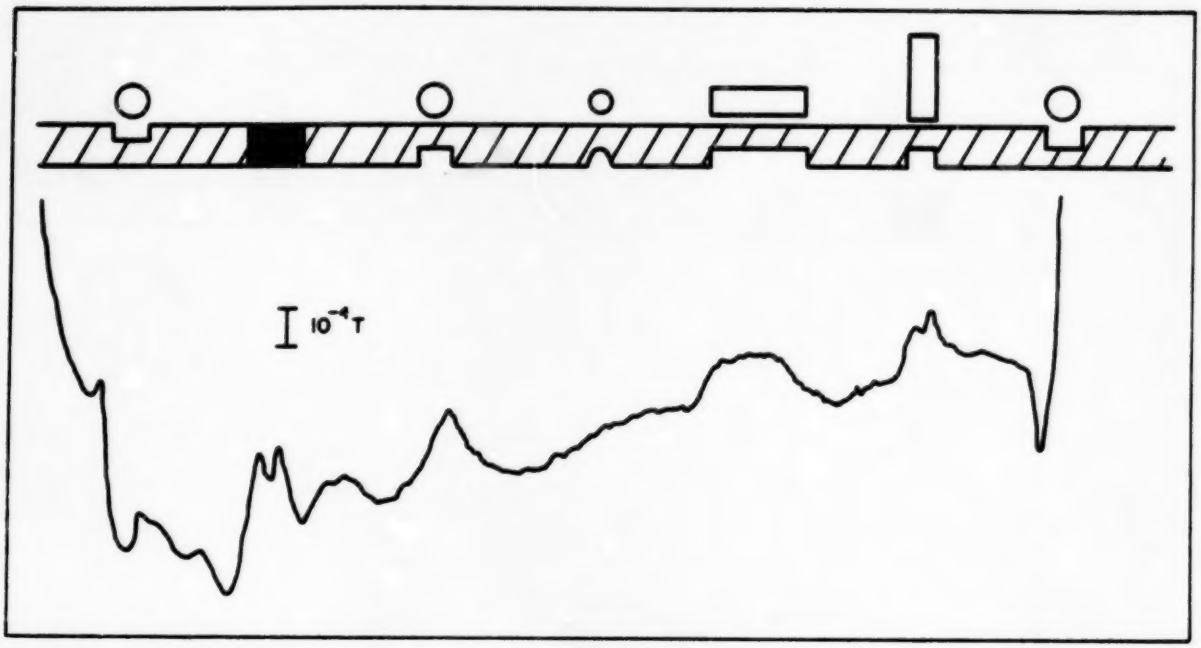

Fig. 6 A low sensitivity radial field profile made with the pipe unstressed but magnetized

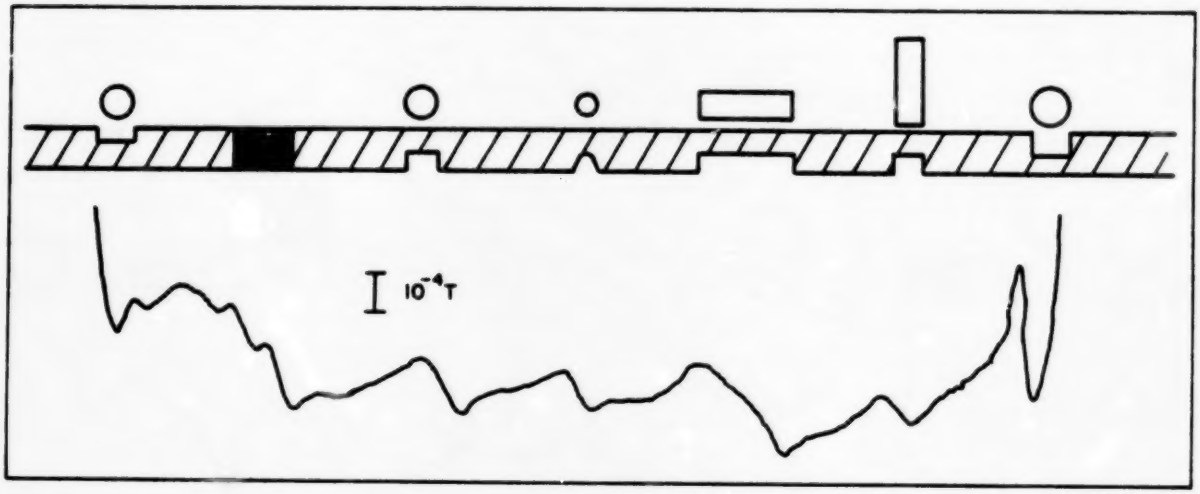

Fig. 7 A low sensitivity radial field profile made with the pipe stressed to 180 MPa peak and the pipe magnetized

effects), and questionable signals from some of the large external pits.

Figure 7 is a further low sensitivity radial-field scan made after the pipe has been stressed and then magnetized. There are excellent signals from all the external pits each with a similar, clear signal form consisting of a full period sinusoid fundamental indicative of local anomalous magnetization. Figure 8 is a similar axial-field plot showing, again, excellent signals with, as expected, a typical half-period fundamental. It is interesting to note that the exterior pitting appears to produce larger signals than the interior pitting here.

We have also investigated the effects of different stress levels and conclude that higher stress-levels tend to produce clearer signals from exterior metal loss. If the stress is relaxed after magnetization, the signals are reduced somewhat but are still discernible.

Conclusions

Our concept and initial tests of the stress-shadow technique for detecting exterior metal loss from the inside of a pipeline have been most encouraging and we are proceeding to further tests, including noise effects and the development of special detectors. It is interesting to note that concerns regarding exterior corrosion of gas pipelines are not generally directly related to the corrosion and resultant porosity and leakage, but rather with the resultant local stress concentrations which might, in extreme cases, lead to rupture. The detection of stress is therefore of greater significance than corrosion itself.

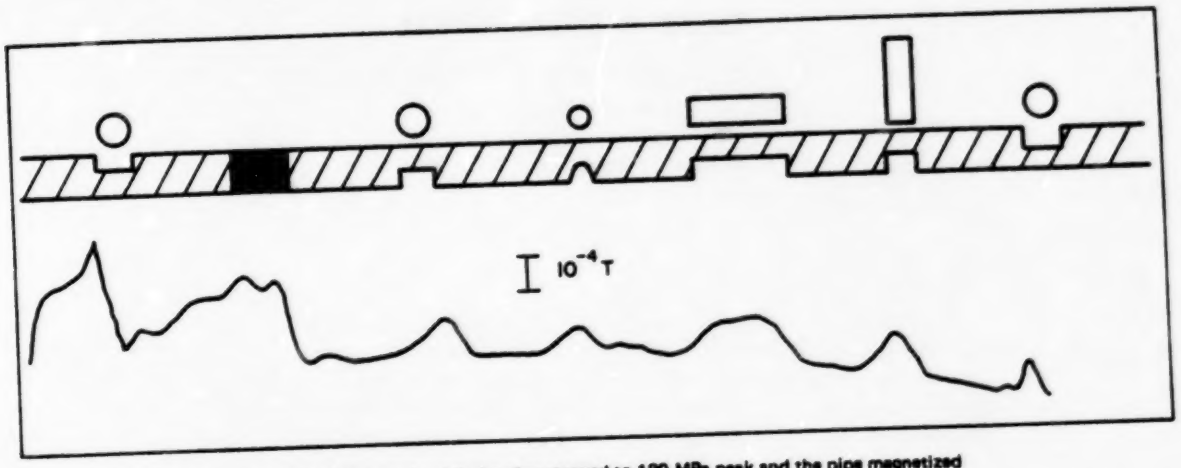

Fig. 8 A low sensitivity axial field profile made with the pipe stressed to 180 MPa peak and the pipe magnetized

Our two-step process, in which we first-of-all develop a near-side anomalous magnetization pattern by magnetizing whilst the pipe wall is under stress and read the pattern subsequently, has important potential advantages for inservice use. It enables the magnetization and anomaly sensing devices to be optimized independently, and by separating them removes a major source of noise tending to obscure the anomaly signals.

Acknowledgements

The work was supported by the Canadian Natural Sciences and Engineering Research Council. I am grateful to H.A. French of TransCanada Pipelines Limited for many stimulating discussions and to S. Allen for careful experimental testing.

Author

Professor Atherton is in the Department of Physics, Queen's University, Kingston K7L 3N6, Canada.

Reference

1 **Atherton, D.L. and Jiles, D.C.** 'Effects of stress on the magnetization of steel', Intermag conference, Philadelphia (April 5–8, 1983)

Presented at the "International Conference on Magnetics", Philadelphia, April 1983 and IEEE Transactions on Magnetics, September 1983.

APPENDIX IV

FERROMAGNETIC HYSTERESIS

D.C. Jiles and D.L. Atherton
Department of Physics
Queen's University
Kingston, Ontario K7L 3N6
Canada

Abstract

An equation describing the initial magnetisation curve and hysteresis loops of ferromagnetic materials has been derived theoretically based on a mean field approximation. The mutual interaction of the moments is expressed as a coupling coefficient and a restraining force on the motion of the domain walls, caused by the pinning of the walls at defect sites, is expressed as a pinning coefficient. The resulting equation of state for the model is a first order linear differential equation incorporating the two parameters and a scaling parameter λ which represents the ratio of the coupling to the two fields H and M.

Introduction

In the majority of applications of ferromagnetic materials, the magnetic properties are most conveniently expressed as magnetisation curves or hysteresis loops. In the present paper a model of the hysteresis behaviour of a ferromagnet is presented based on a mean field approximation.

The ideas of Maxwell [1] and Ewing [2] concerning the mutual interactions of the magnetic moments were applied to large numbers of moments and hence formulated into a mathematical theory of paramagnetism by Langevin [3]. The method of Langevin was then used by Weiss [4] with slight modifications and applied to groups of strongly interacting moments which he called domains. Although the Weiss theory requires the assumption of an unrealistically high internal field, and is therefore only a phenomenological theory nevertheless it can be used as the basis for an equally phenomenological model of hysteresis in which the physically interpretable parameters may be determined empirically.

Mutual Magnetic Interactions. The Coupling Coefficient

Considering only the interactions of a system of moments with the field $\underline{B} = \mu_o(\underline{M} + \underline{H})$ such that the energy of a moment $\underline{m}$ is $E = -\underline{m}.\underline{B}$ leads to the Langevin equation [3] for the field dependence of the magnetisation $\underline{M}$. However Weiss [4] discovered that the field experienced by a ferromagnet could not be expressed by the classical $\underline{B}$ but rather as an effective field $\underline{B_e}$ given by $\underline{B_e} = \mu_o(\underline{H} + \alpha\underline{M})$. Replacing $\underline{B}$ in the Langevin equation with B_e gives the Weiss mean field equation

$$M = M_s \left[\coth\left(\frac{\mu_o \underline{m} \cdot (\underline{H} + \alpha \underline{M})}{kT} \right) - \frac{kT}{\mu_o \underline{m} \cdot (\underline{H} + \alpha \underline{M})} \right] \quad (1)$$

where solutions of this equation for various values of the parameters are shown in fig. 1.

Domain Wall Motion: The Pinning Coefficient

Most of the early workers in ferromagnetism considered that the hysteresis properties of these materials were due to a kind of frictional resistance. These ideas can be traced back to Weber [5] and Maxwell [1] but seem to have been due mainly to Weidemann [6]. At the time of Wiedmann's work the understanding of magnetism was at a far more primitive state than today. The concept of magnetic domains was unknown and he was concerned with "molecular magnetic dipoles" whose rotation into the field direction was envisaged as being inhibited by a kind of viscous friction.

It was not until many years later that the interpretation of changes in magnetisation in terms of domain wall motion was given by Kersten [7,8] and Becker and Doring [9]. The motion of domain walls in a ferromagnet is impeded by the existence of defects in the solid, which cause the domain walls to remain pinned to the defects until sufficient energy has been provided to break away from the pinning site, usually by increasing the applied field, although alternatively the sample could be stressed to cause changes in the energy required to overcome the defect and hence needed to break from the pinning site. The pinning of domain walls therefore presents a restraining force which inhibits changes in magnetisation, and when considering the aggregate effect, behaves much as a frictional force.

Let the density of pinning sites be n per unit volume and the average pinning energy per site be E_p. Then the total energy lost against pinning, per unit volume swept out by a domain wall, will be $n.E_p$, and hence,

$$\frac{dE_{loss}}{dx} = n.E_p . A \quad (2)$$

where A is the area of a particular domain wall and x is the distance through which it is moved. The change in magnetisation is proportional to the volume swept out by the moving domain wall, $dM = A.dx$, and therefore,

$$\frac{dE_{loss}}{dM} = k \quad (3)$$

where k ($= nE_p$) is a constant.

The total energy supplied to the ferromagnet may be split into two terms, the energy dissipated against pinning (hysteresis loss) and the change in energy due to the change in magnetisation of the solid which may be considered reversible.

Under an applied field H the domain walls are acted upon by a force which tends to move them in such a way that the bulk magnetisation approaches its anhysteretic value. In the absence of pinning this energy is reversible and so

$$\int M.dB_e = \int f\left(\frac{M+\lambda H}{a}\right) dB_e \qquad (4)$$

where f(x) is the Langevin function and the parameter λ and a are such that, $\frac{\lambda}{a} = \frac{\mu_o m}{kT}$ and $\frac{1}{a} = \frac{\alpha\mu_o m}{kT}$ from equation (1).

If there is any hysteresis loss then

$$\int f\left(\frac{M+\lambda H}{a}\right) dB_e = \int M.dB_e + \int k.dM \qquad (5)$$

and differentiating with respect to B_e gives the basic differential equation of the model

$$M = f\left(\frac{M+\lambda H}{a}\right) - k\,\frac{dM}{dB_e} \qquad (6)$$

Examples for different values of the parameters are given in fig. 2 and 3 showing the generation of families of major hysteresis loops as the field amplitude H_{max} is increased. Furthermore the model can be extended to include minor loops (assymmetric loops) as shown in figs. 4 and 5.

Conclusions

A phenomenological model of magnetic hysteresis was proposed by Weiss and Freudenreich [10] and later by Preisach [11] whereby a ferromagnet was considered to be composed of elementary domains each of which had two possible magnetisation states parallel or antiparallel to the field. The model was further refined by Neel [12]. In this model the domains of the model ferromagnet can be classified into phases where all domains with the same orientation are considered to belong to one phase. This allows thermodynamic analysis of the magnetic properties without undue consideration of the spatial distribution of the domains.

The present model also dispenses with the need for a knowledge of the spatial distribution of the different domain orientations. Instead it treats the problem as a statistical thermodynamic distribution of a large number of domains with different orientations. It is based on a modification of the Weiss mean field model in which the changes in magnetisation due to the motion of domain walls under an applied field are accounted for and in particular the hindrance posed by pinning sites in the solid is taken into consideration in the final equation.

References

1. Maxwell, J.C., "Electricity and Magnetism, Clarendon, Oxford 1873.
2. Ewing, J.A., Phil. Mag., 5, 205, 1890.
3. Langevin, M., Ann de Chem. et Phys., 5, 70, 1905.
4. Weiss, P. J. de Physique, 6, 661, 1907.
5. Weber, W., "Abhand. der Kg. Sachs-Gesellschaft der Wissens", 572, 1852.
6. Wiedemann, G., Phil. Mag., 52, July 1886.
7. Kersten, M., "Problem der Technischer Magnetisierungskurve", Springer Verlag, 1938.
8. Kersten, M., "Grundlagen Theorie der Ferromagnetischer Hysterese und der Koerzitivkraft", Hirzel, 1943.
9. Becker, R. and Doring, W., "Ferromagnetismus", Springer-Verlag, 1939.
10. Weiss, P. and Freudenreich, J., Arch. Sci., 42, 449, 1916.
11. Preisach, F., Z. Physik, 94, 277, 1935.
12. Neel, L., J. de Phys. Rad., 5, 241, 1944.

Figure Captions

Fig. 1 Solutions of equation 1 for various values of the parameters. The equation is expressed in the form, $\frac{M}{M_s} = \coth\left(\frac{M+\lambda H}{a}\right) - \left(\frac{a}{M+\lambda H}\right)$. The solutions represent the anhysteretic curves.

Fig. 2 Solutions of the model equation for the given values of the parameters.

Fig. 3 Experimentally determined hysteresis loop for a sample of 1% manganese steel.

Fig. 4 Solutions of the model equation for the given values of the parameters.

Fig. 5 Solutions of the modified equation showing minor hystersis loops.

Fig. 6 Solutions of the modified equation showing minor hystersis loops.

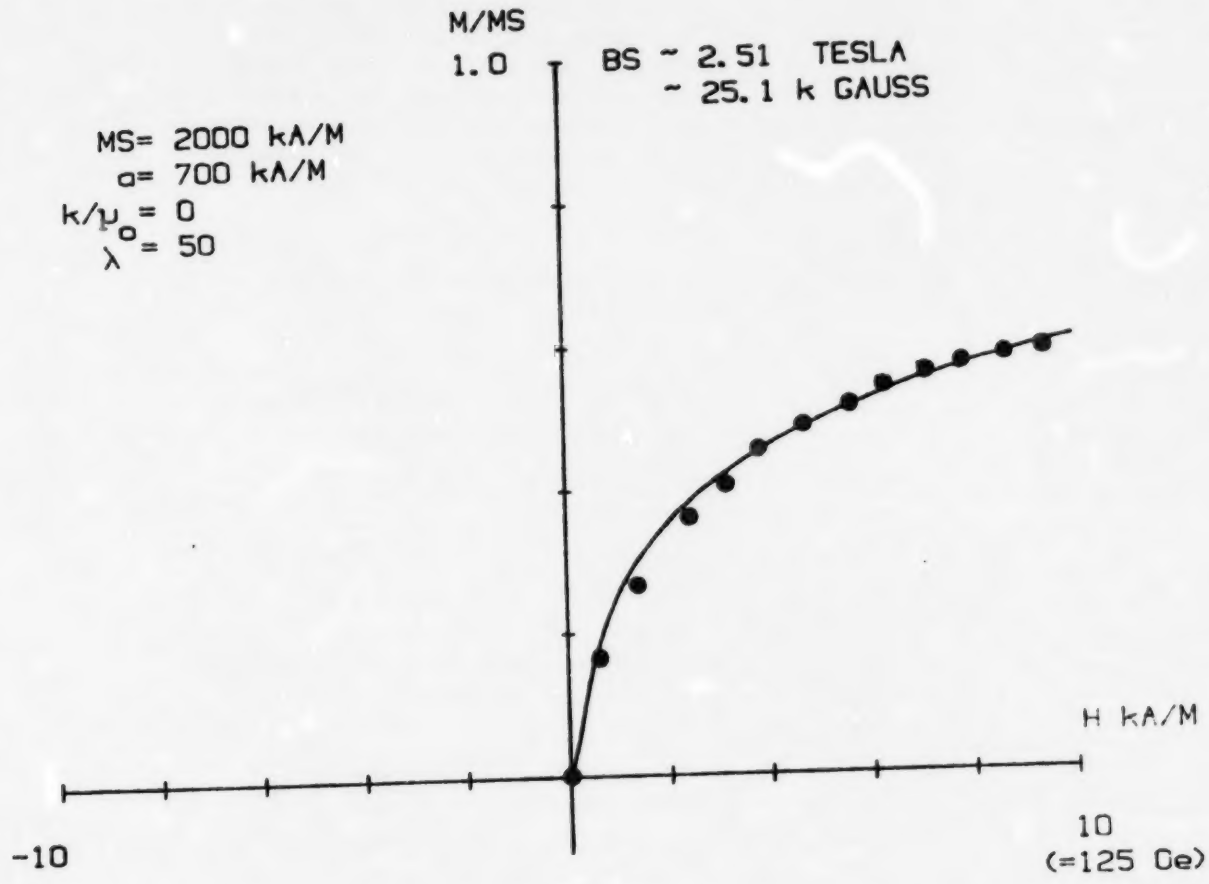
M/MS
1.0
BS ~ 2.51 TESLA
~ 25.1 k GAUSS
MS= 2000 kA/M
a= 700 kA/M
k/μo = 0
λ = 50
H kA/M
-10
10
(=125 Oe)

fig.1

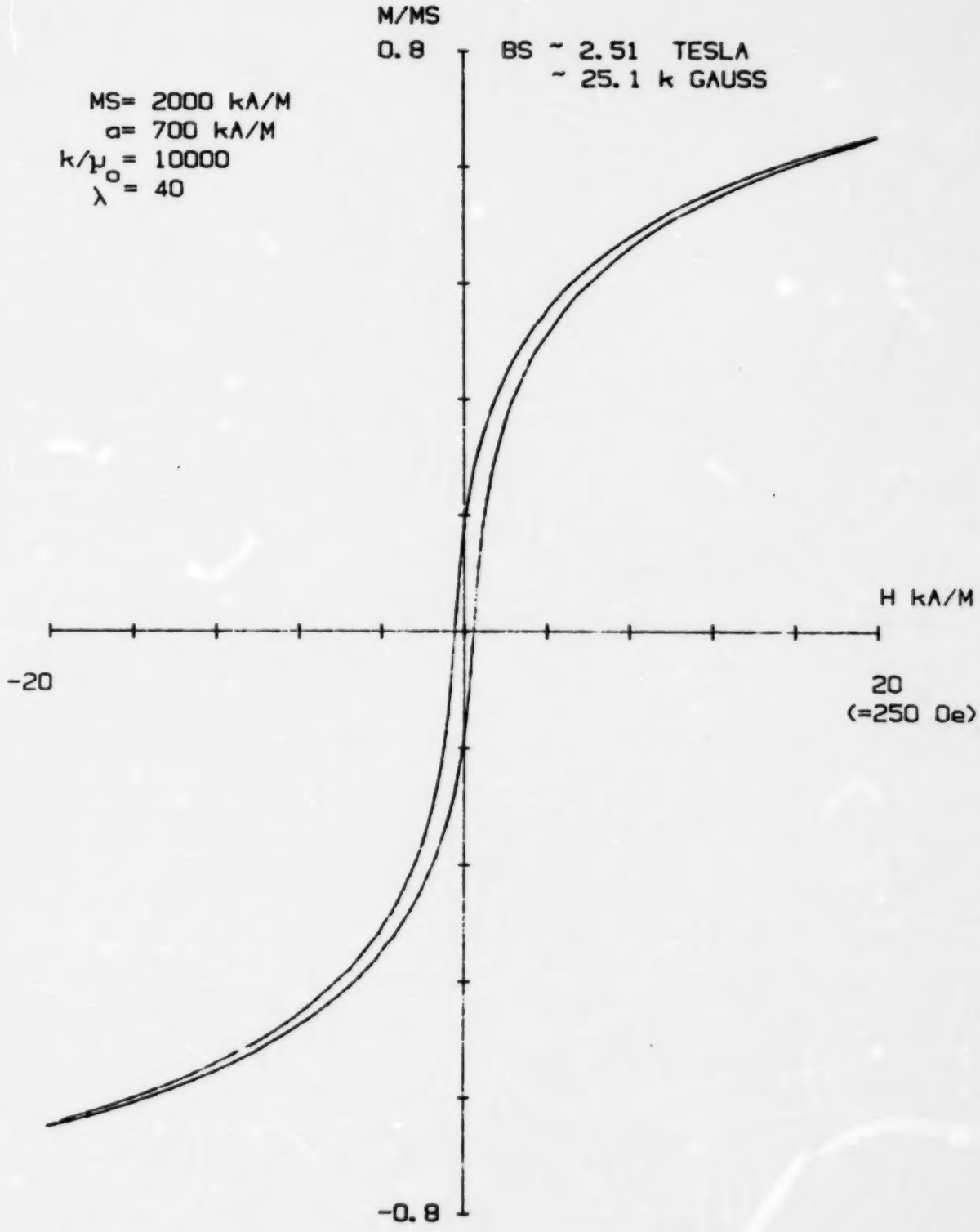
M/MS
0.8
BS ~ 2.51 TESLA
~ 25.1 k GAUSS
MS= 2000 kA/M
a= 700 kA/M
k/μo = 10000
λ = 40
H kA/M
-20
20
(=250 Oe)
-0.8

fig. 2

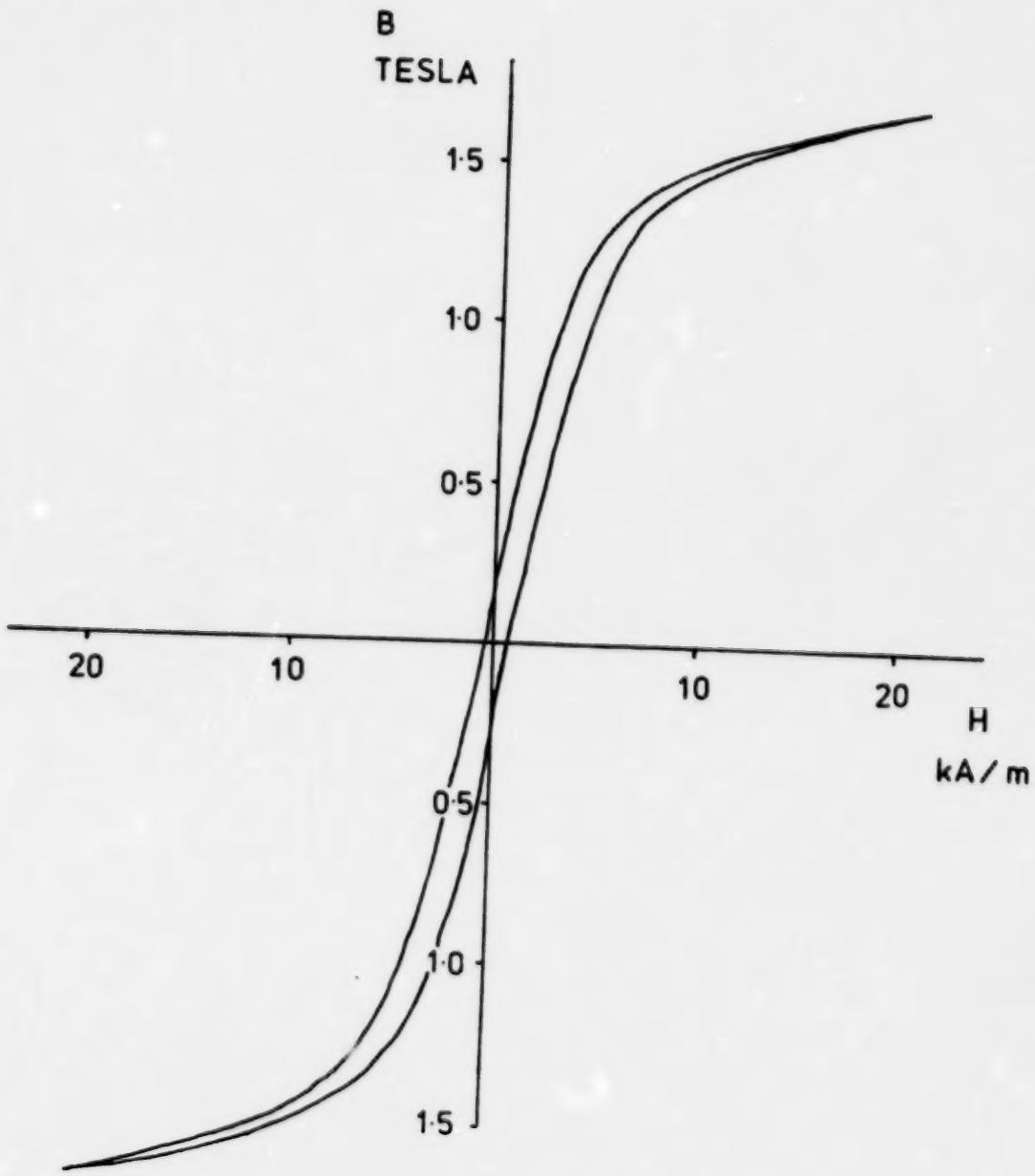

fig. 3

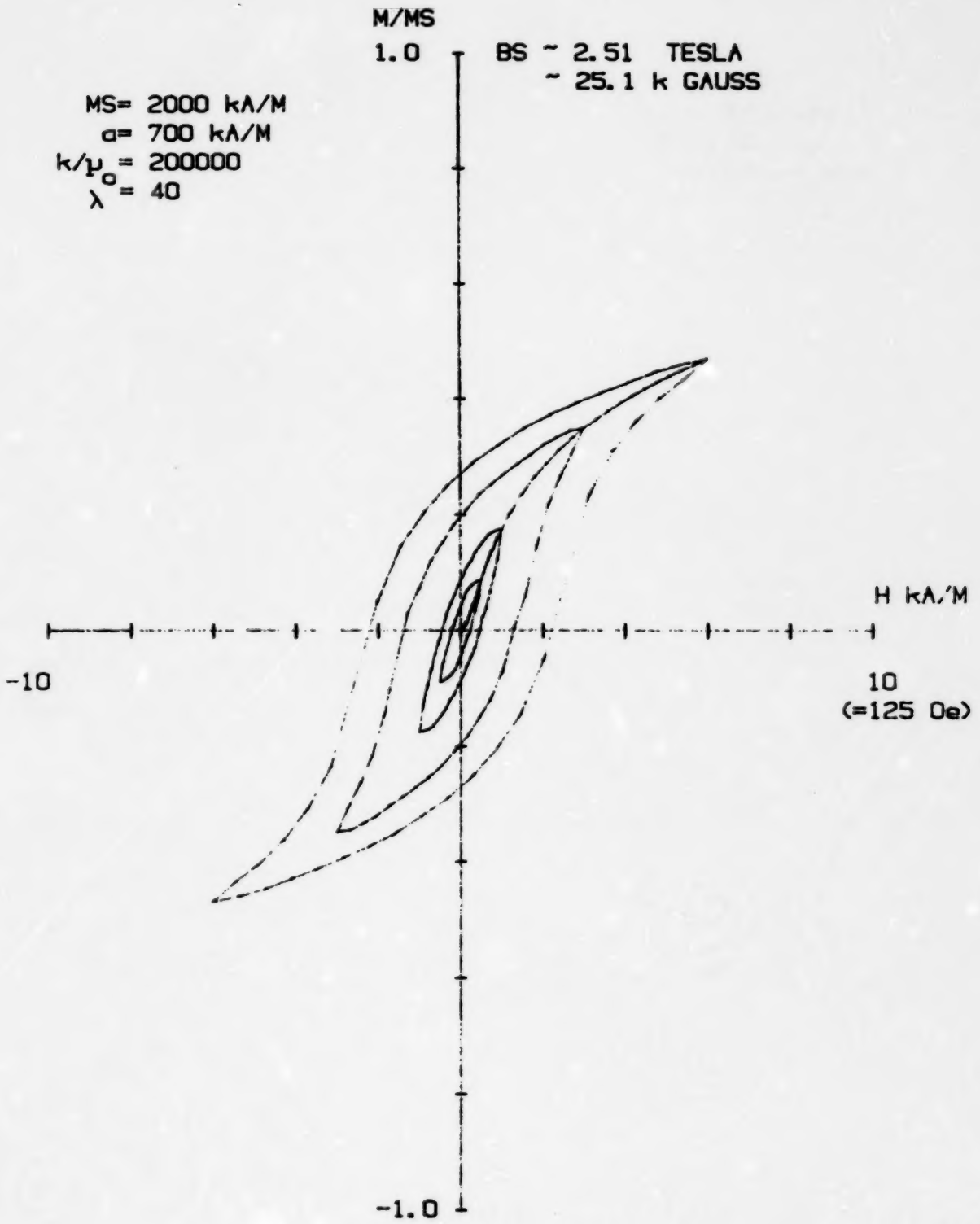
M/MS
1.0
BS ~ 2.51 TESLA
~ 25.1 k GAUSS
MS= 2000 kA/M
a= 700 kA/M
k/μo = 200000
λ = 40
H kA/M
-10
10
(=125 Oe)
-1.0

fig. 4

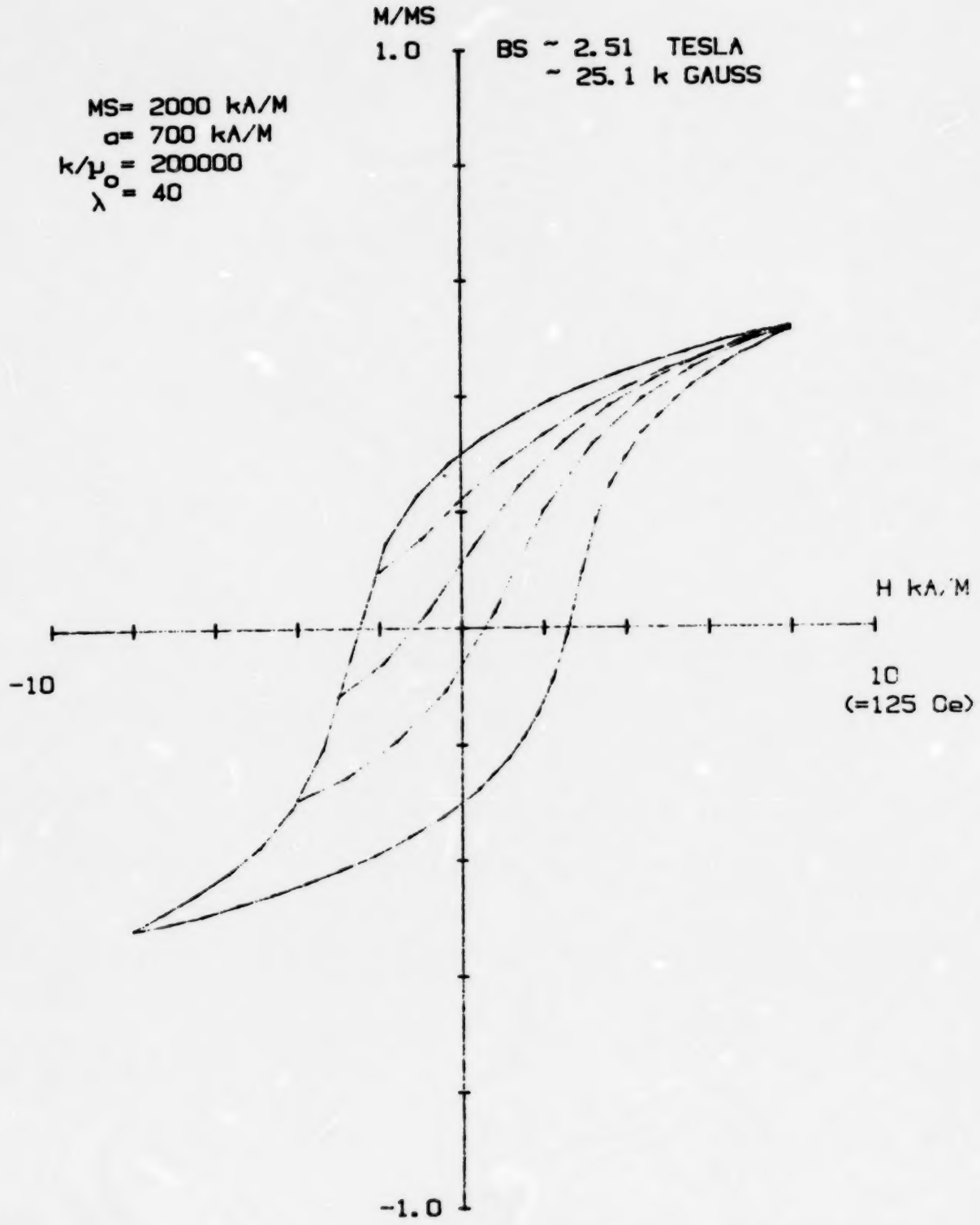
M/MS
1.0
BS ~ 2.51 TESLA
~ 25.1 k GAUSS
MS= 2000 kA/M
a= 700 kA/M
k/μo= 200000
λ= 40
H kA/M
-10
10
(=125 Oe)
-1.0

fig. 5

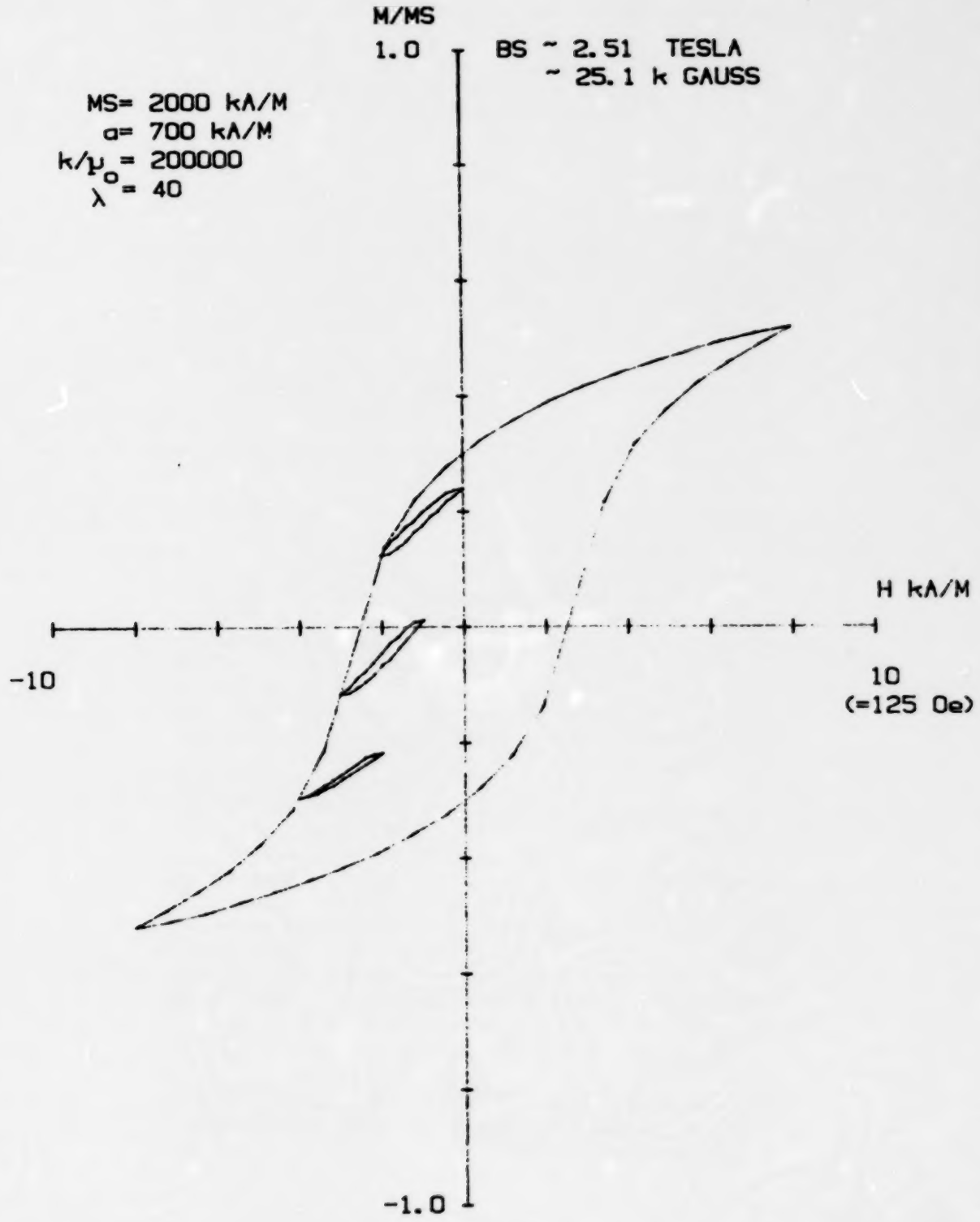
M/MS
1.0
BS ~ 2.51 TESLA
~ 25.1 k GAUSS
MS= 2000 kA/M
a= 700 kA/M
k/μo = 200000
λ = 40
H kA/M
-10
10
(=125 Oe)
-1.0

fig 6

Presented at the "International Conference on Magnetics", Philadephia, April 1983 and IEEE Transactions on Magnetics, September 1983.

APPENDIX V

EFFECTS OF STRESS ON THE MAGNETIZATION OF STEEL*

D.L. Atherton and D.C. Jiles
Department of Physics
Queen's University at Kingston
Kingston, Ontario K7L 3N6
Canada

Abstract

The application of stress cycling to 1% manganese steel at low magnetic fields causes an irreversible shift in the magnetization towards the anhysteretic due to domain walls breaking away from their pinning sites under stress. The change in flux density ΔB caused by a single stress cycle of fixed amplitude σ_{max} has been found to be proportional to the difference between the initial flux density B_i and the anhysteretic flux density B_{an} at the same field, H. The change in flux density as a function of stress has been found to be approximately proportional to σ.

Introduction

It has been known for many years that the application of stress to a ferromagnet can cause changes in the magnetization. In fact it has been stated (1) that stress, σ, ranks with field strength, H, and temperature, T, as one of the primary factors affecting magnetization. The phenomenon has been the subject of investigations since the work of Ewing (2, 3) and has been receiving increasing attention from those interested in applying it to the determination of residual stress in magnetic materials.

According to McCaig (4) the effects of stress on magnetization can be adequately explained by considering the magnetostriction coefficient λ and the sign of the applied stress, whether negative (compression) or positive (tension). In this way it would be expected that the magnetization of a material with positive magnetostriction ceofficient would increase with tension and decrease with compression.

Results in the present work have indicated that this interpretation is oversimplified. Measurements have shown that the changes in magnetization with stress can be of the same sign whether under tension

*This work was supported by the Department of Energy, Mines and Resources (CANMET) and National Research Council of Canada (IMRI).

or compression given the same initial conditions of M and H. This type of behaviour was also predicted theoretically by Brown (5) and by Brugel and Rimet (6). Furthermore results by Craik and Wood (7) have confirmed this, although the magnitude of the changes in two cases are generally rather different. Present results have also indicated that the change in magnetization under tension for example, can have different sign depending on the location of the initial conditions on the hysteresis loop.

A theoretical description of the magnetization process in ferromagnetic materials has been developed (8) based on existing ideas of domain rotation and domain wall motion. It has been found that the magnetization approaches the anhysteretic curve when a ferromagnet is subjected to stress. The change of magnetization with stress can not be predicted solely on the basis of the magnetostrictive coefficient except in special cases when the initial (zero stress) conditions of magnetization lie on the anhysteretic curve. This condition is satisified approximately at higher fields. In the low field region the normal magnetization curve lies well below the anhysteretic curve.

The motion of domain walls under the influence of an applied magnetic field is impeded by the presence of pinning sites in the lattice. This leads to smaller initial permeability and larger coercive forces. Becker and Doring (9) suggested that inhomogeneous internal stresses in a solid, which affect the wall energy, were responsible.

While Kersten (10, 11) considered that imperfections such as non magnetic inclusions or voids, present in the lattice cause a reduction in wall energy when the wall encounters them.

These concepts have been utilized in the present work in conjunction with the idea of Kersten (12) that the changes in the wall energy are balanced by the changes in the mutual energy of the field H and the magnetization M.

Domain Wall Motion

Heck (13) has stated that pinning sites are always present. Therefore when an external field is applied the walls will move but they do so against an internal resistive force. The motion of the domain wall, whether hindered by one type of pinning site or the other may be discussed however in terms of the variation of a single energy term with the magnetization, or alternatively with the wall displacement, according to Cullity (14).

According to Chikazumi (15) in order to have reversible wall displacement, as would occur in an ideal (or unpinned) specimen, it is necessary to invoke a potential which increases with the magnetization. The domain boundary will then come to rest when the work done by the field is balanced by the magnetization energy of the sample as indicated by Hoselitz (16), and when the field is removed the domain wall will return to its original position.

In the case of an ideal "Weiss ferromagnet", (17) the magnetization is given classically by the modified Langevin function $f\left(\frac{B}{\mu_o a}\right) = \coth\left(\frac{\alpha M + H}{a}\right) - \left(\frac{a}{\alpha M + H}\right)$. Consequently the total work done per unit volume by a magnetic field on the magnetic material is

$$\int M dB = \int f\left(\frac{B}{\mu_o a}\right) dB$$

where B is not the classically expected field but an "effective" field $B = \mu_o(\alpha M + H)$.

In the absence of pinning the domain walls of a ferromagnet are acted upon by what might be envisaged as a pressure which tends to move them in such a way that the magnetization reaches equilibrium at the corresponding value of the modified Langevin function (18)

$$M = f\left(\frac{B}{\mu_o a}\right).$$

When considering a real ferromagnet the consequences of domain wall pinning must in included in the energy equation. This leads to irreversible changes in the magnetization with field and hence to hysteresis in the magnetization.

Consider a pinning site on a domain wall between domains with magnetization $\underline{m}$ and $\underline{m}'$ where $\underline{m}$ is aligned parallel to the field and is the growing domain while $\underline{m}'$ is aligned at some arbitrary angle θ to the field and hence to $\underline{m}$. The energy required to overcome the pinning site will depend on two factors, the nature of the pinning site itself and the relative orientations of the magnetizations in the domains. Suppose the energy required to overcome the pinning site is proportional to the change in energy per unit volume of the $\underline{m}'$ domain caused by rotating its moment into the field direction and hence parallel to $\underline{m}$.

$$\Delta E = \underline{m} \cdot \underline{B} - \underline{m}' \cdot \underline{B} = mB(1 - \cos\theta)$$

and consequently if ε_{pin} the pinning energy of a pinning site is proportional to ΔE

$\varepsilon_{pin} \propto mB\,(1 - \cos\theta)$.

If the pinning energy of the site for 180° domain walls is ε_π (π radians) and $\varepsilon_\pi \propto 2mB$.

Therefore, the pinning energy of the one typical site can be expressed as

$$\varepsilon_{pin} = \frac{\varepsilon_\pi}{2}\,(1 - \cos\theta).$$

and taking $\langle\varepsilon_\pi\rangle$ as the average pinning energy of all the sites for 180° walls, and assuming a uniform density of pinning sites of n per unit volume,

$$\langle\varepsilon_{pin}\rangle = \frac{\langle\varepsilon_\pi\rangle}{2}\,(1-\cos\theta)$$

$$E_{pin}(x) = \int_0^x n\,\frac{\langle\varepsilon_\pi\rangle}{2}\,(1 - \cos\theta)\,A\,dx$$

where E_{pin} is the total energy lost through pinning when a domain wall of area A is moved through a distance x, between domains whose magnetizations lie at an angle θ.

The net change in magnetization of the ferromagnet (by symmetry there will be a number of domains at an angle θ to the field direction such that the component of magnetization perpendicular to the field due to these domains will sum to zero) will be,

$$dM = m(1 - \cos\theta)\,A.dx$$

and substituting for A.dx in the equation for energy leaves,

$$E_{pin} = \int \frac{\langle\varepsilon_\pi\rangle}{2m}\,dM$$

which is independent of the relative orientations of the domains. That is although the energy required to move a domain wall through a more unfavourably oriented domain is greater, the change in magnetization achieved by doing so is also proportionally greater.

Replacing the terms on the right hand side by the constant k

$$E_{pin} = k\int dM \qquad \text{where } k = \frac{n\langle\varepsilon_\pi\rangle}{2m}$$

Hence under the assumptions of a uniform distribution of pinning sites, and treating each one as having the average pinning energy, the total work done against pinning is proportional to the change in

magnetization. This then leads to the equation of state as given previously (8).

$$M = f\left(\frac{B}{\mu_o a}\right) - k\left(\frac{\partial M}{\partial B}\right)_\phi$$

Effects of Stress on Magnetization

Measurements taken in the present work have indicated that the anhysteretic curve, and hence the coefficient a, are stress dependent. For the sample of 1% manganese steel used in the present investigations it was found that the anhysteretic value of magnetization increased under tension and decreased under compression. It is clear that the change in the anhysteretic magnetization with stress is of different sign under compression or tension. Furthermore given the magnetostriction coefficient λ of the ferromagnet, the change in magnetization of the anhysteretic M_{an} should obey LeChatelier's principle, giving the following conditions governing the change in magnetization with stress

for $\lambda > 0$ then $\frac{d\sigma}{d\sigma} < 0$ and $\frac{dM_{an}}{d\sigma} > 0$ and conversely for $\lambda < 0$.

Effects of Stress in the Low Field Region

In general the sign of $\frac{dM}{d\sigma}$ does not depend solely on the magnetostriction coefficient. That is to say a ferromagnet with positive λ, which will elongate when the magnetization is increased, will not necessarily undergo an increase in magnetization when subjected to tension. Experimental results, as indicated in fig. 1, have shown that the direction of change in magnetization can be the same whether the sample is subjected to tension or compression. The critical factor here is whether the change in magnetization due to domain wall motion, when the domain walls overcome their pinning sites, is the dominant mechanism affecting the bulk magnetization.

In the low field region, the domain wall motion dominates. Under these conditions the direction of change of magnetization is to a first approximation independent of the sign of the stress. When the initial magnetization lies above the anhysteretic value, application of stress of either sign causes a decrease in magnetization. Conversely when the initial magnetization lies below the anhysteretic curve application of stress causes an increase in magnetization. Therefore it is the location of the

initial conditions in relation to the anhysteretic curve, together with the dependence of the anysteretic curve on stress (the anhysteretic surface) which define the magnetic behaviour of a ferromagnet under stress.

The results in fig. 2 show the changes in flux density B, caused by application of a cyclic stress of 140 MPa tension. at different points around the hysteresis loop. These show that the changes in magnetization are towards the anhysteretic curve.

Dependence of $\frac{dM}{d\sigma}$ on the Initial Conditions

Measurements were taken of the change in magnetization caused by a stress cycle of σ_{max} = 140 MPA at different points along the initial magnetization curve. The locus of the anhysteretic curve was also measured and it was found that the change in flux density $\Delta B(\sigma_{max},H)$ was proportional to the difference between the anhysteretic value of flux density $B_{an}(H)$ and the initial value $B_i(H)$ at a given field strength H. The results are shown in fig. 3 and the graph of $\Delta B(H)$ against σ is given in fig. 4. These results seem to indicate the following relationship

$$\Delta B(\sigma_{max},H) \propto B_{an}(H) - B_i(H).$$

It can be seen from fig. 4 that to a first approximation also,

$$\Delta B(\sigma,H) \propto \sigma$$

although the general behaviour under compression and tension is slightly different with $\frac{dB}{d\sigma}$ having different values depending on the direction of stress.

Conclusions

It seems that the guiding principle in these cases is that the application of stress, of either sign, causes the magnetization to approach the anhysteretic value. Again it is necessary to emphasize that the anhysteretic curve itself changes with stress, so for example, if a ferromagnet with $\lambda>0$ is subjected to a compressive stress when the initial conditions of (M, H) are on the normal magnetization curve, below the anhysteretic then a change in M will be positive at first since M will approach the anhysteretic. If the magnitude of stress is sufficiently large however, the anhysteretic level of magnetization, which decreases with compression, will eventually reach the level of

the sample magnetization causing M to decrease with further stress since it will, according to the above principle move towards the anhysteretic.

References

1. Bozorth, R.M. and Williams, H.J. Revs. Mod. Phys., 17, 72 (1945).
2. Ewing, J.A. Phil. Mag. 5th Series, 30, 205, (1980).
3. Ewing, J.A. "Magnetic Induction in Iron and Other Metals", The Electrician (1900).
4. McCaig, M. "Permanent Magnets in Theory and Practice", Wiley (1977).
5. Brown, W.F. Phys. Rev. 75, 147 (1949).
6. Brugel, L. and Rimet, G. J. Phys. Radium, 27, 589 (1966).
7. Craik, D.J. and Wood, M.J. J. Phys. D., 3, 1009 (1970).
8. Jiles, D.C. and Atherton, D.L., "Ferromagnetic Hysteresis", Intermag Conference (1983).
9. Becker, R. and Doring, W. "Ferromagnetismus", Srpinger (1939).
10. Kersten, M. "Problem der Technischer Magnetisierungskurve", Springer (1938).
11. Kersten, M. "Grundlagen einer Theorie der Ferromagnetischen Hysterese und Koerzitivkraft", Hirzel (1943).
12. Kersten, M. Z. Physik, 124, 714 (1948).
13. Heck, C. "Magnetic Materials and Their Applications", Butterworths (1974).
14. Cullity, B.D. "Introduction to Magnetic Materials" Addison-Wesley (1972).
15. Chickazumi, S. "Physics of Magnetism", Wiley (1964).
16. Hoselitz, K. "Ferromagnetic Properties of Metals and Alloys", Oxford (O.U.P) (1952).
17. Weiss, P. J. de Phys. Radium, 6, 661 (1907).
18. Langevin, P. Ann. de Chem. et. Phys. 5, 70 (1905).

Figure Captions

Fig. 1: Change in flux density through a sample of 1% manganese steel as a function of stress σ, both in compression and tension.

Fig. 2: Changes in flux density with a single stress cycle of 140 MPa tension at various different points around a hysteresis loop.

Fig. 3: Changes in flux density against stress σ at different points around a hysteresis loop. Open circles are from the initial magnetization curve, closed circles from the anhysteretic magnetization. The solid line is $B_a(H) - B_i(H)$.

Fig. 4: Changes in flux density against the difference in flux density between the initial magnetization curve and the anhysteretic curve, for a stress cycle of 140 MPa tension. Starting conditions were on the initial magnetization curve.

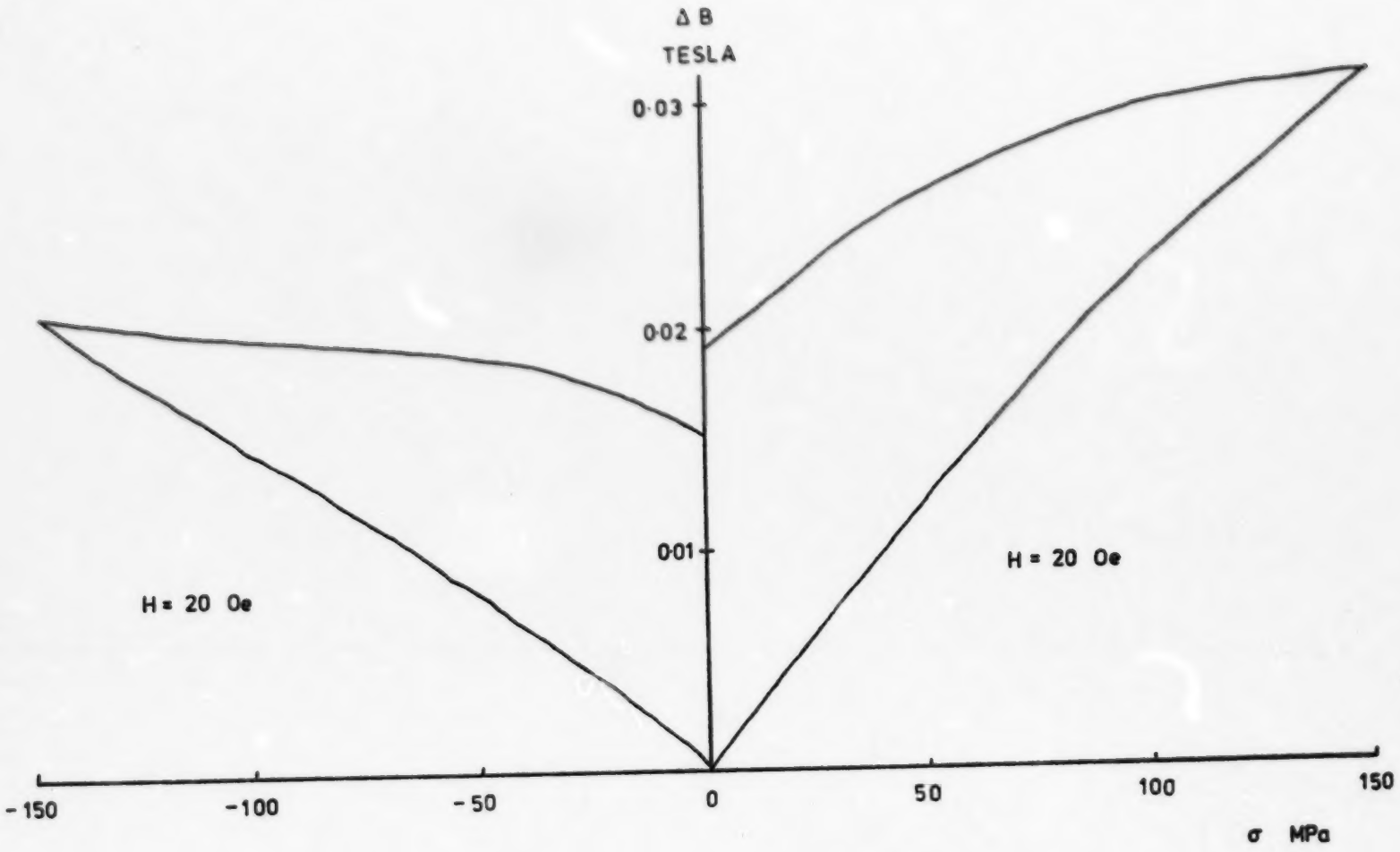
Δ B
TESLA
0·03
0·02
0·01
H = 20 Oe
H = 20 Oe
-150
-100
-50
0
50
100
150
σ MPa

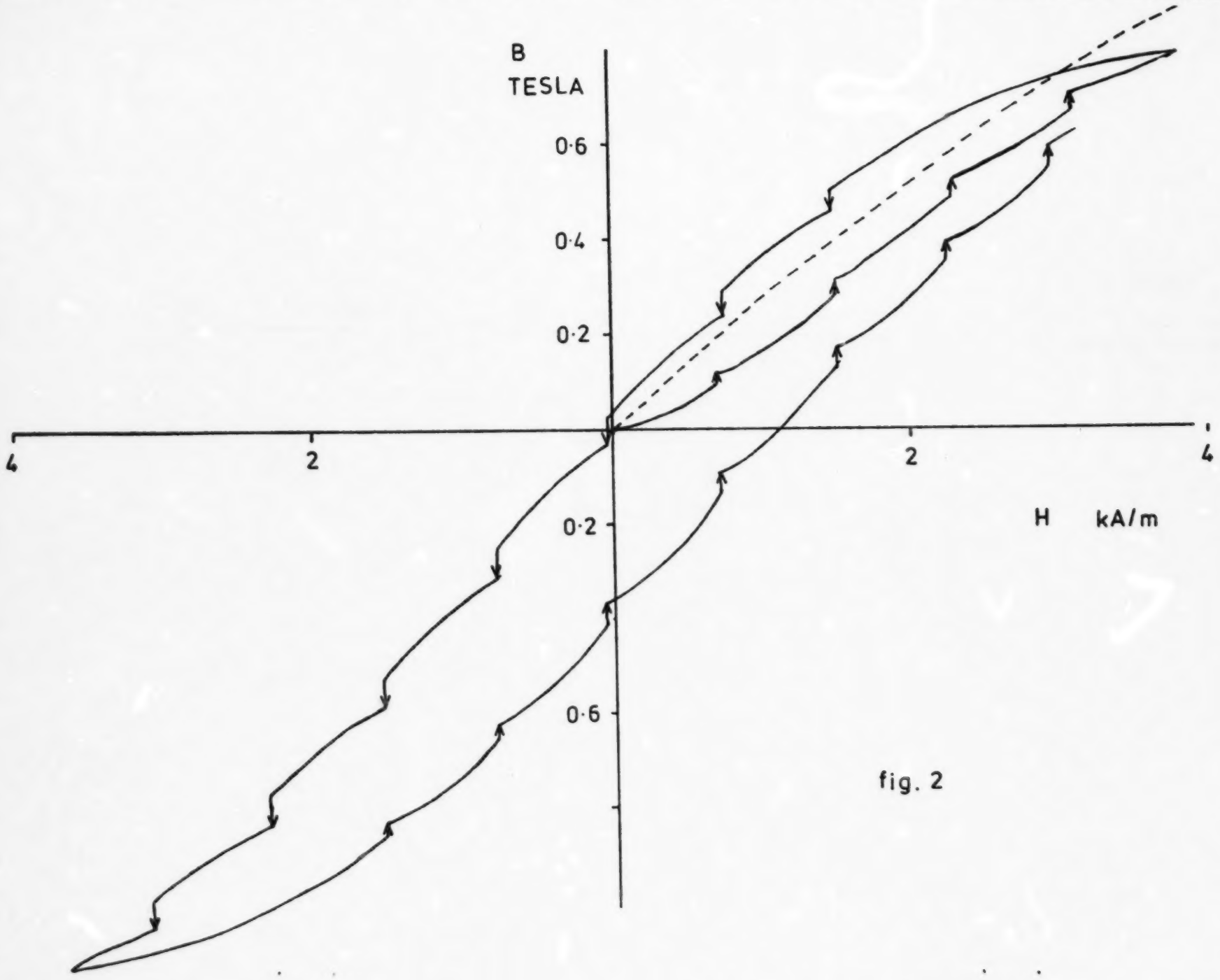

fig. 2

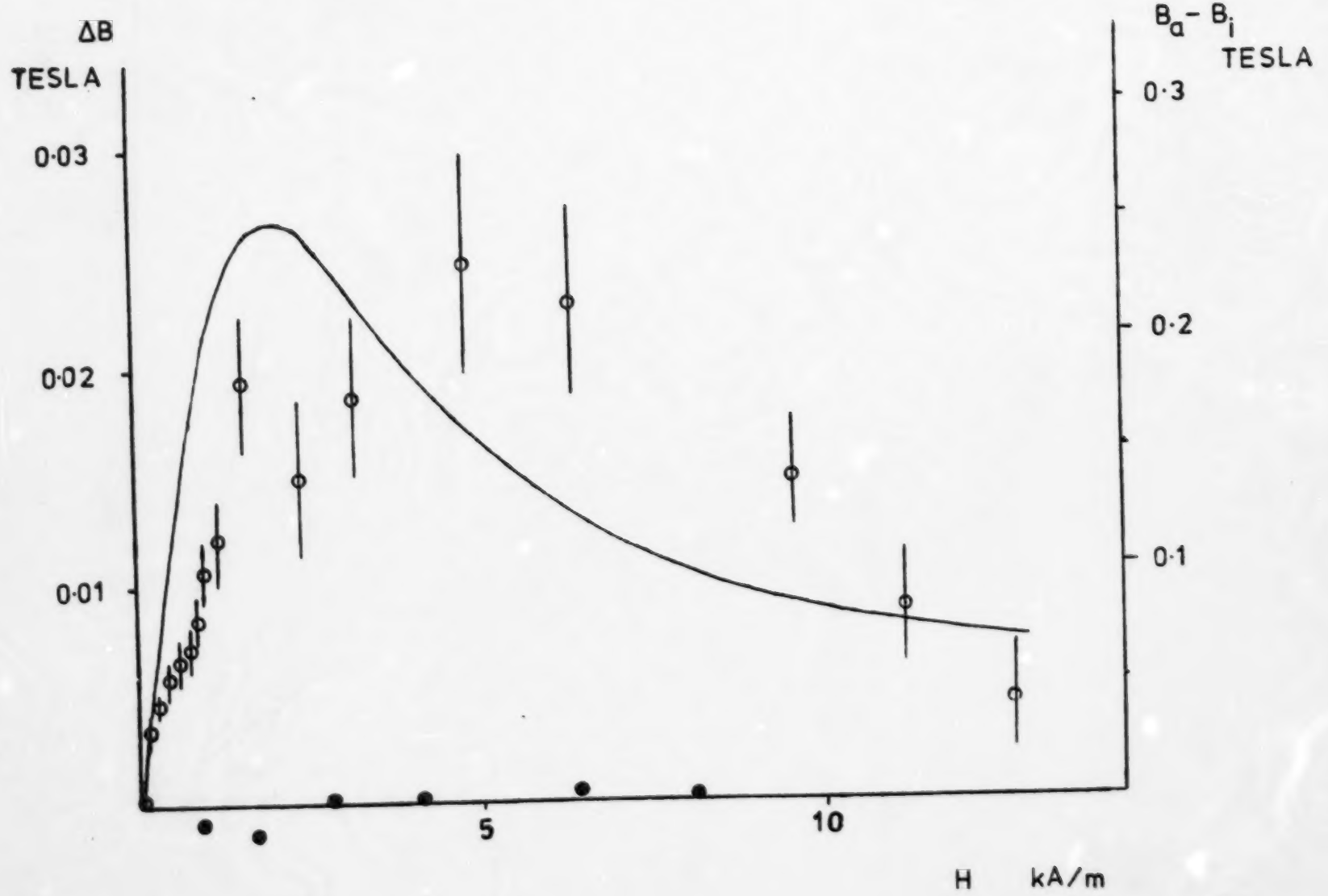

fig. 3

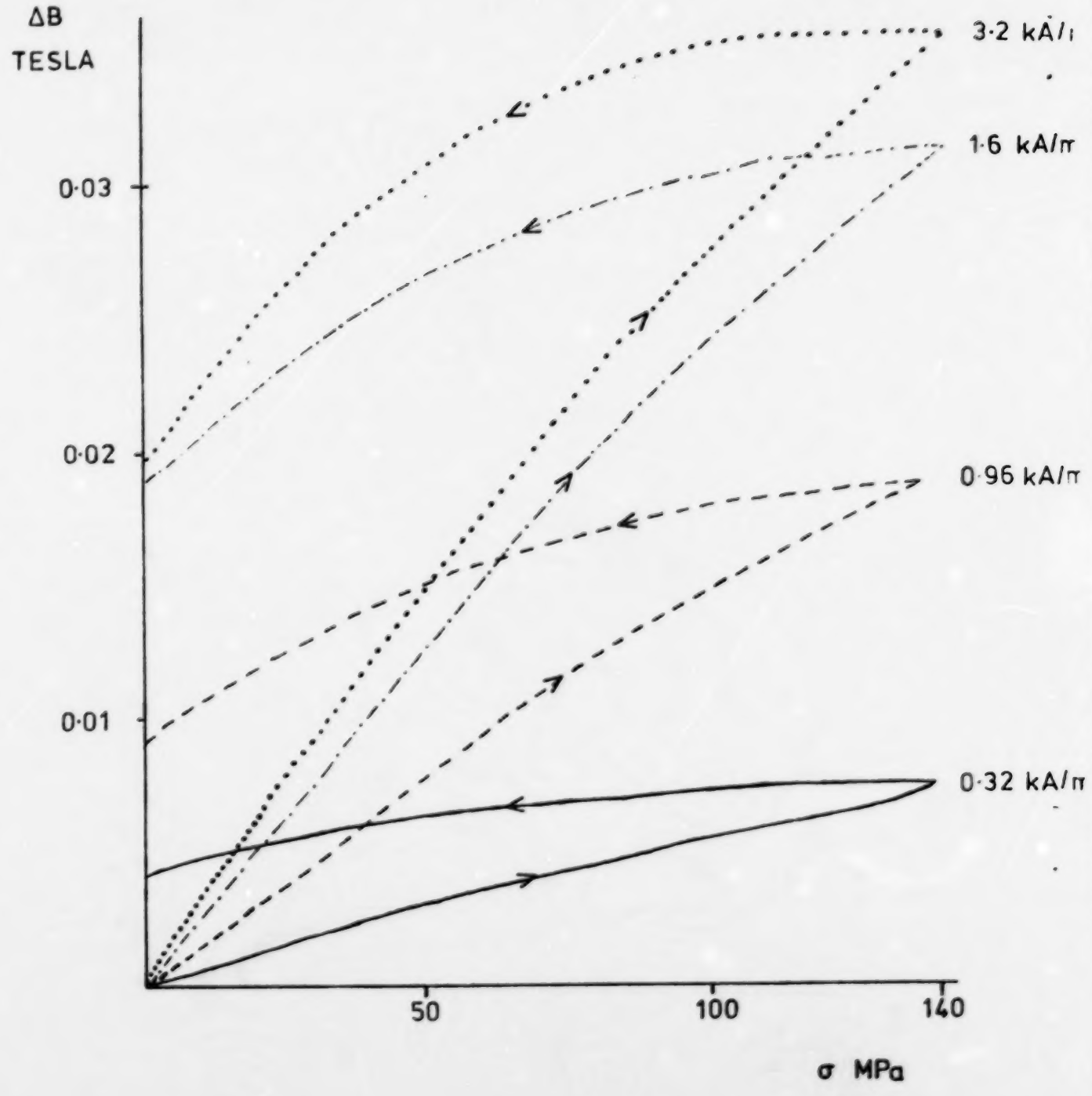
ΔB
TESLA
0·03
0·02
0·01
3·2 kA/m
1·6 kA/m
0·96 kA/m
0·32 kA/m
50
100
140
σ MPa

fig. 4

Invited paper presented at the "Conference on Magnetism and Magnetic Materials", Pittsburgh, November 1983 and Journal of Applied Physics, 1984.

THEORY OF FERROMAGNETIC HYSTERESIS: (INVITED)

D.C. Jiles and D.L. Atherton, Physics Dept., Queen's University, Kingston K7L 3N6, Canada.

The macroscopic magnetic properties of a ferromagnet, the initial and anhysteretic magnetisation curves and the major and minor loops may be described by a simple differential equation derived from a model based on considerations of domain wall motion and domain rotation.

The energy per unit volume of a typical domain with magnetic moment m per unit volume in an applied flux density $\underline{B}_a$ is $E = -\underline{m}\cdot\underline{B}_a = -\mu_o \underline{m}\cdot\underline{H}_a$ where H_a is the intensity of the applied field. If there is interdomain coupling then $E = -\mu_o\underline{m}(H_a+\alpha\underline{M}) = -\underline{m}\cdot\underline{B}_{eff}$ where α is a mean field parameter. Application of Maxwell-Boltzmann statistics leads to a modified Langevin equation for the magnetisation.

$$M = M_s \left\{ \coth\left(\frac{\mu_o m(H+\alpha M)}{kT}\right) - \frac{kT}{\mu_o m(H+\alpha M)} \right\} = f\left(\frac{H+\alpha M}{a}\right)$$

where $a = kT/\mu_o m$. This is the solution for the anhysteretic curve. Under normal D.C. field conditions the process of domain wall motion, whereby the magnetisation changes, is impeded by pinning. By considering a density of pinning sites n with average pinning energy E_p the above equation for magnetisation is modified to give

$$M = f\left(\frac{H+\alpha M}{a}\right) - K\delta\left(\frac{dM}{dB_{eff}}\right)$$

where $K = \frac{nE_p}{2m}$ and $\delta = \pm 1$ is a directional parameter.

The change in the macroscopic magnetisation dM consists of the change due to domain wall motion dM_w and that due to rotation of domains dM_r. The effective value of pinning K is therefore related to the total domain wall pinning K_o by

$$K = K_o\left(1 - \frac{dM_r}{dM}\right)$$

and consequently K decreases with M.

Category 20

Regular Session

D.C. Jiles

D.L. Atherton

D.C. Jiles
Physics Dept.,
Queen's University
Kingston, Ontario
Canada K7L 3N6

Paper submitted to the "Conference on Magnetism and Magnetic Materials", Pittsburgh, November 1983.

EFFECTS OF STRESS ON THE MAGNETISATION OF STEEL

D.C. Jiles and D.L. Atherton, Physics Dept., Queen's University, Kingston, K7L 3N6, Canada.

Stress ranks with field strength and temperature as one of the primary factors influencing magnetisation [1]. Some authors have even considered stress to be equivalent to an effective magnetic field [2]. According to others the effects of stress on magnetisation can be adequately explained by considering the magnetostriction coefficient λ and the sign of the stress.

The result of the present investigation shows that this interpretation is oversimplified. Changes in magnetisation with stress at low fields can be of the same sign whether under compression or tension given the same initial conditions of M and H. This type of behaviour has been predicted by others [3]. Furthermore the changes in magnetisation with a particular stress, eg. tension, can have different sign depending on the location of the initial conditions relative to the anhystcretic.

The application of stress to samples of ferromagnetic steel at low fields causes an irreversible change in the magnetisation towards the anhysteretic due to domain walls breaking away from their pinning sites. The direction of the change has been explained on the basis of the model of hysteresis derived in conjunction with this work [4]. The change in magnetisation caused by a single stress cycle of fixed amplitude σ_{max} has been found to be proportional to the displacement of the magnetisation from the anhysteretic. The change in magnetisation has also been found to be approximately proportional to stress.

1. R.M. Bozorth and H.J. Williams, Revs. Mod. Phys 17 72 (1945)
2. D.J. Craik and M.J. Wood, J. Phys. D., 3 1009 (1970).
3. W.F. Brown, Phys. Rev. 75 147 (1949).
4. D.C. Jiles and D.L. Atherton, Intermag Conference 1983 and IEEE Trans. Mag. MAG-19 Sept. 1983.

Category 5

Regular Session

D.C. Jiles

D.L. Atherton

D.C. Jiles
Physics Dept.,
Queen's University,
Kingston, Ontario
Canada K7L 3N6

APPENDIX VIII

Published in IEEE Transactions on Magnetics, July 1983

STRESS INDUCED MAGNETISATION CHANGES OF STEEL PIPES - LABORATORY TESTS

David L. Atherton, L.W. Coathup, D.C. Jiles,

L. Longo and C. Welbourn

Department of Physics, Queen's University,

Kingston, Ontario K7L 3N6 Canada

and

A. Teitsma

Pipeline Monitoring, TransCanada Pipelines, 1320 Ellesmere Road,

Unit 3, Scarborough, Ontario M1P 2X9 Canada

Research supported in part, by Natural Sciences and Engineering Research Council.

Stress Induced Magnetization Changes of Steel Pipes—Laboratory Tests

DAVID L. ATHERTON, MEMBER, IEEE, L. W. COATHUP, D. C. JILES, L. LONGO, C. WELBOURN, AND A. TEITSMA

Abstract—Magnetometer surveys above gas pipelines show stress induced magnetic anomalies at pipe bends. This suggests a potential technique for the noninvasive monitoring of stress in buried pipelines, etc. Laboratory measurements of the magnetic field changes due to the elastic bending of 110 mm diameter pipe are presented. The effects of orientation with respect to the earths field and of internal pressure are reported. Hysteretic effects are found to be important.

INTRODUCTION

PIPELINES constructed on unstable terrain (e.g., permafrost), submarine lines, etc. may shift producing bending stresses which can, in extreme cases, lead ultimately to failure. We have reported previously [1] that magnetometer surveys can be used to indicate bending stresses in buried pipelines and to monitor new construction. Magnetometer surveys show that perturbations of the earth's field are large and complex; typically fluctuations of several kilogamma are found 2 m above 1-m diameter buried line. The individual joints of the line behave rather like semi-randomly aligned bar magnets. The survey log signals record initial magnetizations, joints, construction history, etc. and include the results of stress induced magnetization changes. Cold bends made in the field to allow the pipeline to follow the natural terrain contours produce large signals. We have made magnetometer surveys before and after cold bending and have shown that the effects on the survey patterns can be summarized most simply by describing them as extra bar magnets added into the string used to represent the pipeline. It is hoped that the technique can be developed to monitor pipelines for changes in stress or for unusual stress concentrations since it is probable that this could be done noninvasively and without removing the line from service [2]. The magnetometer survey patterns are however complex, and experience is essential for their interpretation.

Magnetostriction (magnetization induced strain) is well-known. The behavior of iron is complex with the sign of the magnetostrictive coefficient being dependent on both field and stress. The inverse effect, namely stress induced change in magnetization has not been widely investigated. We have therefore undertaken a basic investigation of the effects of stress on the magnetization of pipeline steels in order to

Manuscript received November 15, 1982; revised January 24, 1983. This work was supported in part by the Natural Sciences and Engineering Research Council.

D. L. Atherton, L. W. Coathup, D. C. Jiles, L. Longo, and C. Welbourn are with the Department of Physics, Queen's University, Kingston, Ontario K7L 3N6 Canada.

A. Teitsma is with Pipeline Monitoring, TransCanada Pipelines, 1320 Ellesmere Road, Unit 3, Scarborough, Ontario M1P 2X9 Canada.

0018-9464/83/0700-1564$01.00 © 1983 IEEE

assist in interpreting our pipeline magnetometer surveys. Early experimental results [3] indicate that the behavior of pipeline steels, which are magnetically relatively hard, is quite different from previously reported results obtained with magnetically soft materials [4] (iron and silicon-iron) and that hysteretic effects are dominant. The effects are however explicable using a mean field model of the hysteresis mechanism [5].

The stress distribution in pipelines is very complex and the direct calculation of stress induced in the fringing fields, even with information on the effects of uniform stress on the magnetization of simple samples, does not appear feasible, although data and understanding of the basic effects will certainly help to interpret pipeline magnetometer surveys. Furthermore, magnetometer surveys conducted in the field are often performed under far from ideal conditions and often parameters, which it might be desirable to test, cannot be well-controlled, if at all. We have therefore undertaken some laboratory scale demonstrations and tests to further assist in interpreting our magnetometer survey results and to gain experience of the effects of various parameters. We report here on one of these demonstrations in which bending stresses within the elastic limit are applied to 3.38-m lengths of 110-mm diameter pipe. These demonstrations are being conducted concurrently with both our full-scale field magnetometer pipeline surveys and our basic investigations of the effects of mechanical stresses on small samples of pipeline steels. The results from each of these studies have helped to elucidate and confirm the others.

Objectives

The initial objectives of our pipe bending demonstrations were to investigate the effects of varying bending stresses within the elastic range (as opposed to "before" and "after" deformation as observed in our field surveys of cold bends), to determine the effects of orientation with respect to the earth's field and to investigate the effects of internal pressure (as would be produced by gas line pressure) all in a controlled laboratory scale demonstration.

It should be emphasized that, since this is a new area of study, it is not obvious at the outset exactly what needs to be controlled in order to ensure controlled conditions and that a major part of the experience gained is needed to help define these parameters.

Apparatus

The apparatus used in these tests is shown in Fig. 1. It consists of two parallel pipes held together by cable at one end and sprung together by a jack at the other while the centers are supported by a saddle. The pipes can be swung to any declination and tilted to any dip on the nonmagnetic support structure. The two pipes are spiral welded pressure tested steel with a listed yield strength of 250 MPa (A53B ASTM schedule 40). They are 110 mm in diameter, have a wall thickness of 6.0 mm, and are 3.38-m long; their geometry and that of the saddle support is shown in Fig. 2.

Peak bending stresses, at the outside mid plane, are measured using a strain gage bridge. These stresses have been verified both by calculation from the measured deflections and also from the jack forces determined from the compression of a stack of cupped disc spring washers. A fluxgate magnetometer (RFL model 101) has been used to survey the radial and axial components of the pipe fringing fields.

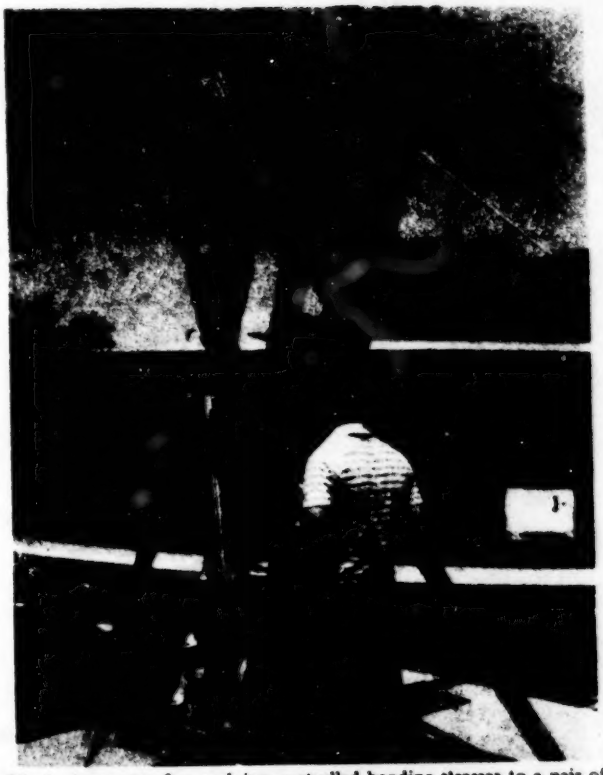

Fig. 1. Apparatus for applying controlled bending stresses to a pair of pipes which may be orientated in any direction with respect to the earth's magnetic field. Fluxgate magnetometer is being used to log stress induced changes in the pipe fringing fields.

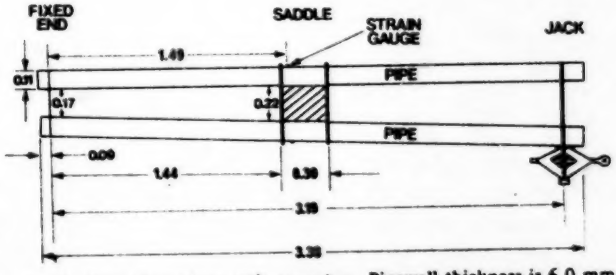

Fig. 2. Pipe dimensions and geometry. Pipewall thickness is 6.0 mm. All dimensions in meters.

Results

The stress induced changes in the fringing fields can be summarized by saying that there appears to be an additional bar magnet induced in the pipe producing axial and radial field component changes above the pipe as indicated in Fig. 3. Typically we find the radial field changes are somewhat more distinct. It should be noted though that while the bending stresses increase linearly from zero at the end clamps to a maximum at the saddle, giving a relatively short highly stressed length, the induced bar magnets in these isolated pipes appear to have lengths nearly equal to that of the pipes.

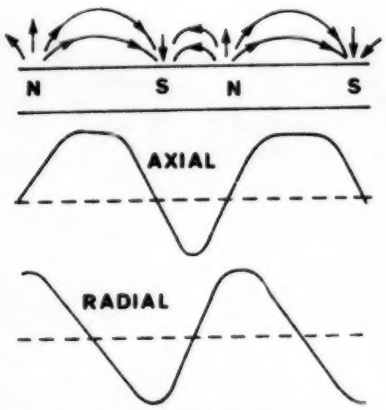

Fig. 3. Stress induced changes in pipe magnetization can be represented as an induced bar magnet additional to bar magnet field of pipe joint together producing axial and radial fields above the pipe as shown.

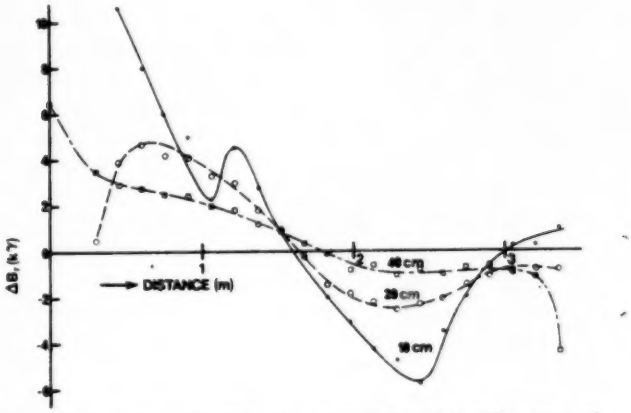

Fig. 5. Changes in radial fields due to central peak bending stress of 85 MPa measured for pipe #2 aligned horizontally N-S at distances of 10, 20, and 40 cm.

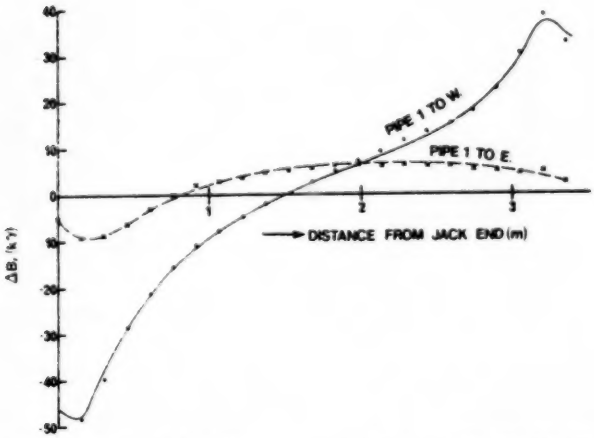

Fig. 4. Absolute radial field components. 10 cm outside pipe #1 measured with pipes aligned horizontally N-S shown with pipe #1 on the E side of pipe #2 and on the W side (errors ±2.5 kγ).

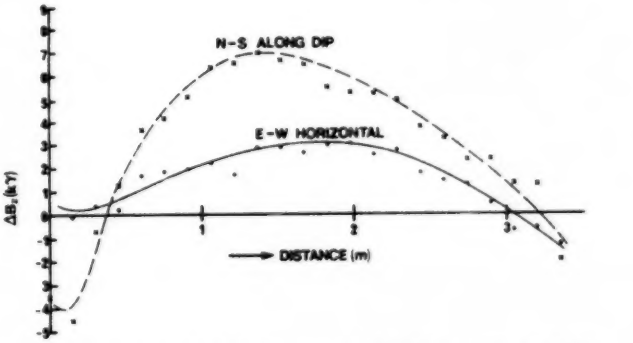

Fig. 6. Changes in axial field due to a peak bending stress of 140 MPa measured for pipe #1 aligned horizontally E-W and aligned N-S along the dip (errors 0.5 kγ).

We recorded the radial and axial field components along traverses of the pipes in a set position and orientation before and after swinging the pipes to and fro through various angles and found that there were no significant differences and therefore concluded that the pipe magnetization was not altered by rotation in the earth's field.

Traverses recorded with the pipes at different orientations were of course different due both to the differing components of the earth's background field and due to the different interaction between the pipes and the earth's local field. In general the behavior of both test pipes was similar but it was found that when the pipes were aligned horizontally N-S the W pipe, whichever was positioned there, had a much greater indicated induced magnetization, as shown in Fig. 4. There had been no change when the pipes were rotated back to the horizontal E-W reference position. We believe that this was due to a perturbation of the earth's field probably caused by structural steel in the building on whose roof the tests were performed. The perturbation was presumably comparatively large scale since we were unable to identify it by local magnetometer measurements over the pipe region before installing the pipes.

Because of the positional variations in the absolute field components we have found it generally most convenient to show the induced field component changes.

Fig. 5 shows the changes in radial field components on bending to a peak stress of 85 MPa for distances from the pipe of 10, 20, and 40 cm. Subsequent measurements were normally made at a distance of 10 cm, approximately one pipe diameter, so as to be scaled approximately to ground level measurements above a full-scale buried line and to show good detail, however Fig. 5 shows that the changes are readily detectable much further away.

Figs. 6 and 7 show changes in axial and radial fields after stressing to 140 MPa with the pipe oriented horizontally E-W and aligned N-S dipping with the field, i.e., with the pipe along and perpendicular to the earth's field. In both cases the changes are large and readily detectable. The differences between the two are probably attributable more to stress induced changes in hysteresis (see subsequently) rather than to the difference in alignments and we conclude that stress induced changes are detectable at any orientation to the earth's field.

Figs. 8 and 9 and also Figs. 10 and 11 show radial and axial field changes at progressively higher stresses of 35, 70, 105, and 140 MPa. The changes generally increase progressively with increasing stress but the results are somewhat irregular and not

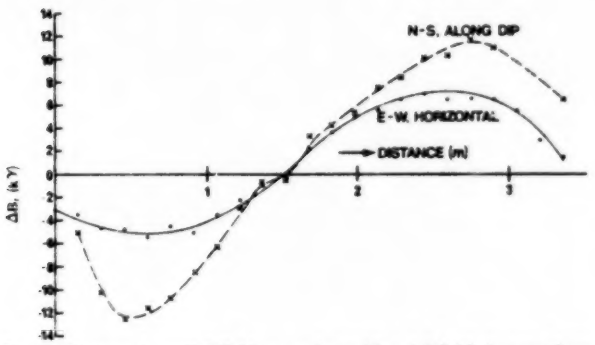

Fig. 7. Changes in radial field occurring with axial field changes shown in Fig. 6 (errors 2.5 kγ).

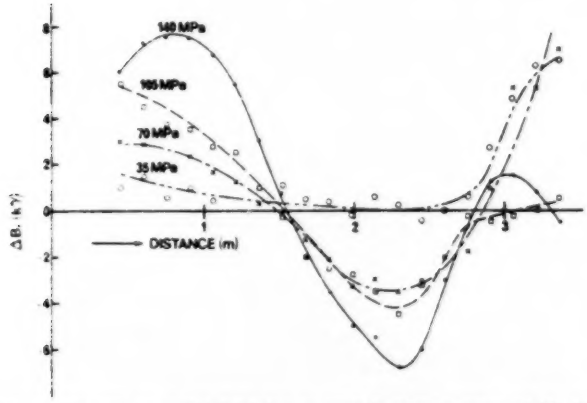

Fig. 8. Changes in radial field due to peak bending stresses of 35, 70, 105, and 140 MPa (stress reduced to zero between each stress increase) (errors ±2.5 kγ).

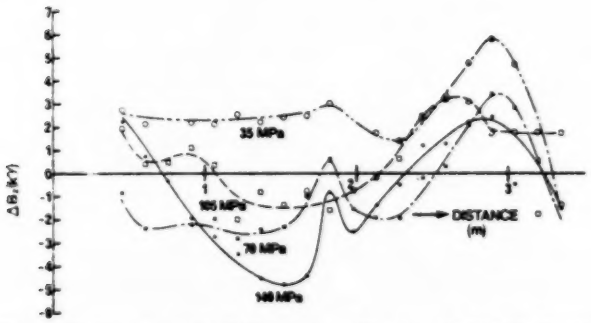

Fig. 9. Changes in axial field corresponding to radial field changes shown in Fig. 8 (errors ±0.5 kγ).

reproducible in detail. In fact many of our initial results were irregular and nonreproducible suggesting stress irregularities.

Figs. 8 and 9 were obtained relaxing the pipe to zero stress between each successively higher stress level and determining the changes from the successive relaxed values, whereas Figs. 10 and 11 were obtained by increasing the stresses directly and noting the changes from the initial relaxed values. In general the former procedure produced somewhat more irregular results.

Our concurrent basic investigations showed that stress cycling tends to diminish the magnetic hysteresis, i.e., the magnetization is shifted towards the anhysteretic curve (which is also

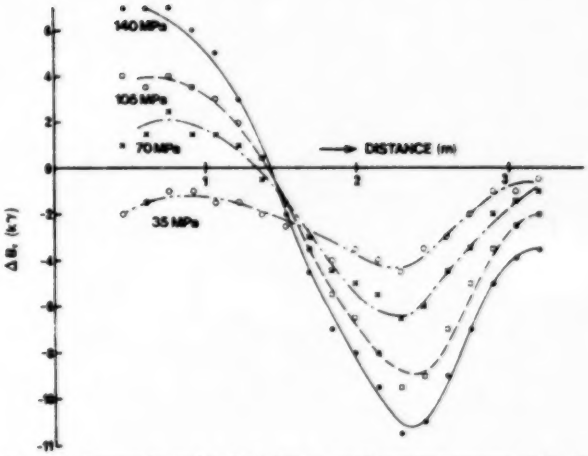

Fig. 10. Changes in radial field due to peak bending stresses of 35, 70, 105, and 140 MPa (stress increased monotonically) (errors ±2.5 kγ).

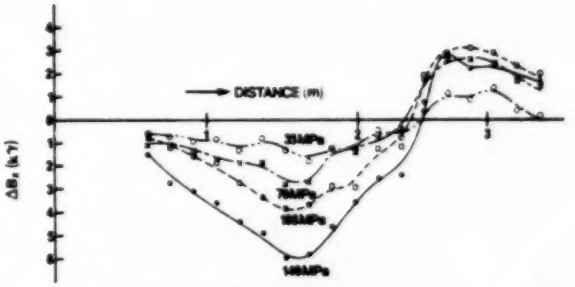

Fig. 11. Changes in axial field concurrent with radial field changes shown in Fig. 10 (errors ±0.5 kγ).

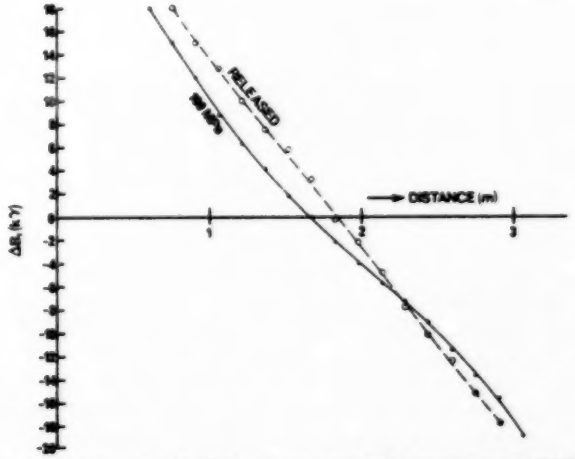

Fig. 12. Changes in radial field due to hydraulically stressing to 100 MPa and after releasing both measured from initial unstressed values (error ±2.5 kγ).

stress dependent). For relatively hard magnetic materials such as pipe steels the hysteretic effects are pronounced. This therefore implies that stress induced changes should increase more regularly when measured during a single cycle with monotonically increasing stress, as we found in the tests described above.

Fig. 12 shows changes in radial fields occurring on hydraulically pressurizing the pipes to a wall stress of 100 MPa and

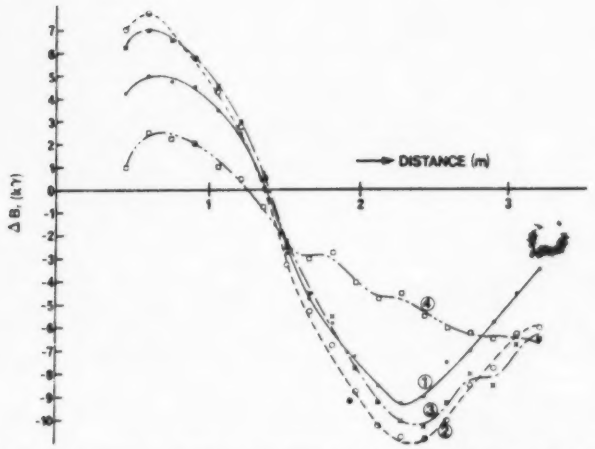

Fig. 13. Changes in radial fields from initial unstressed values due to 1) 140 MPa peak bending stress, 2) 140 MPa bending stress plus 100 MPa hydraulic pressure stress, 3) 140 MPa bending stress, hydraulic pressure released, 4) bending and hydraulic stresses released (errors ±2.5 kγ).

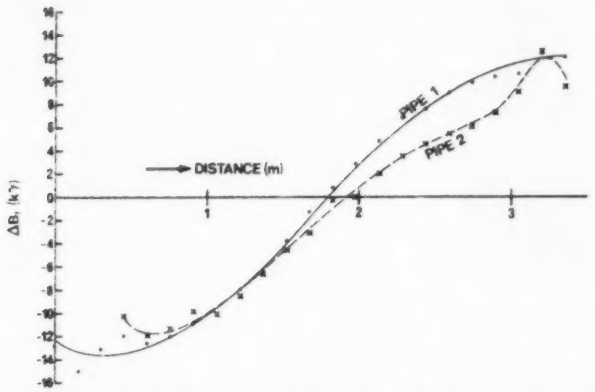

Fig. 14. Changes in radial fields for pipes #1 and #2 occurring between initially unstressed pipes and pipes finally unstressed after bending to peak stress of 140 MPa (errors ±2.5 kγ).

after releasing, both changes being measured from the initial unstressed values. The hydraulic stressing also acts so as to induce a superimposed bar magnet but most of the change remains after the stress is relaxed indicating again changed magnetic hysteresis.

Fig. 13 shows the changes in radial fields produced by successively applying 1) bending stress of 140 MPa, 2) bending stress of 140 MPa combined with a hydraulic pressure stress of 100 MPa, 3) after releasing the hydraulic pressure leaving the 140 MPa bending stress, and 4) after releasing both hydraulic and bending stress.

All the changes are measured with respect to the initial unstressed state. The changes appear to be dominated by those due to bending stress but there is substantial hysteresis.

Fig. 14 is another example of hysteretic effects; it shows changes in radial fields for both pipes which occurred after the pipes had been bent to 140 MPa and released. The changes are unusually large. Unfortunately not enough is known yet about the fundamental effects of stress on magnetized pipeline steel to be sure of the detailed causes of these changes.

Conclusion

These are, of course, early experiments in a new field and much more remains to be learned but we can already draw some useful and encouraging conclusions.

Throughout this work we have used only the natural pipe magnetization so that it would be representative of full-scale pipelines but partly because, even for pipes of this size, it is difficult to induce a controlled small magnetization particularly because of the difficulty of initially demagnetizing. We were therefore encouraged that pipe magnetization did not appear to be altered by swinging in the earth's field and established as a reference state a set position with zero applied stress from which to measure field changes. Our subsequent discovery of the significance of hysteresis in the stress induced changes in magnetization indicates that the stress history, which also governs the magnetization, should also be determined in order to give controlled conditions. An alternative may be to reset by demagnetizing and remagnetizing in a set orientation with zero stress.

Initially there had been some concern that orientation with respect to the earth's field might be an important parameter and that there might be possible null positions. Fortunately our tests show that pipe magnetization is not changed significantly by the earth's field so that orientation has little effect on stress induced field changes.

Because of the known reversal in sign of the magnetostrictive coefficient for iron we had also been concerned that the induced field changes might have a rather complex behavior with stress; however we find that, in general over our operating ranges, the stress induced field changes increase simply with increasing stress.

The field changes produced by (hydrostatically simulated) line pressure are much the same as those produced by bending stress and these changes can also be simply represented as being due to a superimposed induced bar magnet. The field changes are readily detectable even at a few pipe diameters away.

Our results support the expectation that magnetometer surveys can be used for noninvasive monitoring of buried pipelines and that changes in fields can be used to indicate changes in stress such as might be due to bending resulting from unstable support. A great deal of development is still needed before the technique can be used routinely in the field but our tests have helped the progress and are generally encouraging.

References

[1] D. L. Atherton and A. Teitsma, "Detection of anomalous stresses in gas pipelines by magnetometer survey," *J. Appl. Phys.*, vol. 53, no. 11, part II, pp. 8130–8135, Nov. 1982.

[2] A. Teitsma, H. A. French, D. L. Atherton, and D. C. Jiles, "The development of an above ground stress measurement method," presented at *Int. Conf. Pipeline Inspection*, Edmonton, June 13–16, 1983.

[3] D. L. Atherton and D. C. Jiles, "Effects of stress on the magnetization of steel," presented at 1983 INTERMAG Conf., *IEEE Trans. Magn.*, vol. MAG-19, no. 5, Sep. 1983, to be published.

[4] D. J. Craik and M. J. Wood, "Magnetization changes induced by stress in a constant applied field," *J. Phys. D: Appl. Phys.*, vol. 3, pp. 1009–1016, 1970.

[5] D. C. Jiles and D. L. Atherton, "Ferromagnetic hysteresis," presented at 1983 INTERMAG Conf., *IEEE Trans. Magn.*, vol. MAG-19, no. 5, Sep. 1983, to be published.

APPENDIX IX

Algorithm for Obtaining the Anhysteretic Curve

The magnetisation at any point on the ideal or anhysteretic (or hysteresis free) curve is determined solely by the prevailing D.C. field under given conditions of temperature. That is to say, the anhysteretic magnetisation is independent of the magnetic history of the sample. The anhysteretic curve is of great interest in magnetic recording where the general technique is known as A.C. bias recording.

The method of obtaining the anhysteretic magnetisation has been described by Mee(1). A large, symmetrical A.C. field is superimposed on the applied D.C. field. The amplitude of the A.C. field, which is initially sufficient to practically saturate the magnetisation, is gradually reduced to zero. This means that in order to reach the anhysteretic in theory an arbitrarily large number of A.C. cycles should be used with an infinitesimally small decrement in amplitude per cycle. This, of course, is not very practical and so experimentally some compromises have to be made.

From a practical point of view therefore, we need an algorithm in which the smallest possible A.C. field amplitude and the largest possible amplitude decrement per cycle are used, without causing significant deviation from the true anhysteretic magnetisation. In order to judge the magnitude of this deviation, it was decided to run the algorithm for D.C. field increasing and decreasing from a certain maximum field $(H_{D.C.})_{max}$. The precision with which the algorithm could produce the anhysteretic curve could then be measured from the deviation between the curve of increasing D.C. field, and the curve of decreasing D.C. field. If the algorithm were exact, these two curves should be identical. Of course with any practical method of obtaining the curve, there would be some deviation which could only be removed by using an infinitesimally small decrement

of the A.C. field per cycle together with an infinite amount of time to decrease the A.C. field to zero.

The method of reaching the anhysteretic curve which was used in the present work is outlined in the accompanying figure. Starting from the demagnetised state at $H_{D.C.} = 0$, the D.C. field component was incremented by 1.6 kA/m. An A.C. field of maximum amplitude 8 kA/m was then superimposed on the D.C. field. The A.C. field amplitude was decremented by 10% per cycle, first at the positive maximum, then at the negative maximum, in effect every 1½ cycles. When the amplitude of the A.C. field was reduced below 0.2 kA/m the decrement per cycle was set at the fixed rate of 0.02 kA/m to expedite the completion of the process.

The D.C. amplitude was then incremented by 1.6 kA/m and the whole A.C. cycling process repeated. This was continued in steps of 1.6 kA/m to an arbitrarily set maximum D.C. field which defined the range of field over which the anhysteretic was to be determined. In this particular case, the upper limit chosen was 16 kA/m. Once this upper limit has been reached, the D.C. field was decremented in steps of 1.6 kA/m with decaying A.C. fields applied at each step as described above. The process finished after the completion of A.C. field decay at zero D.C. field. The loci of points for increasing and decreasing D.C. fields could then be compared to give an indication of the accuracy with which the method produced the true anhysteretic.

Reference

1. C.D. Mee, "The Physics of Magnetic Recording", North Holland, Amsterdam, 1964.

Anhysteretic Routine

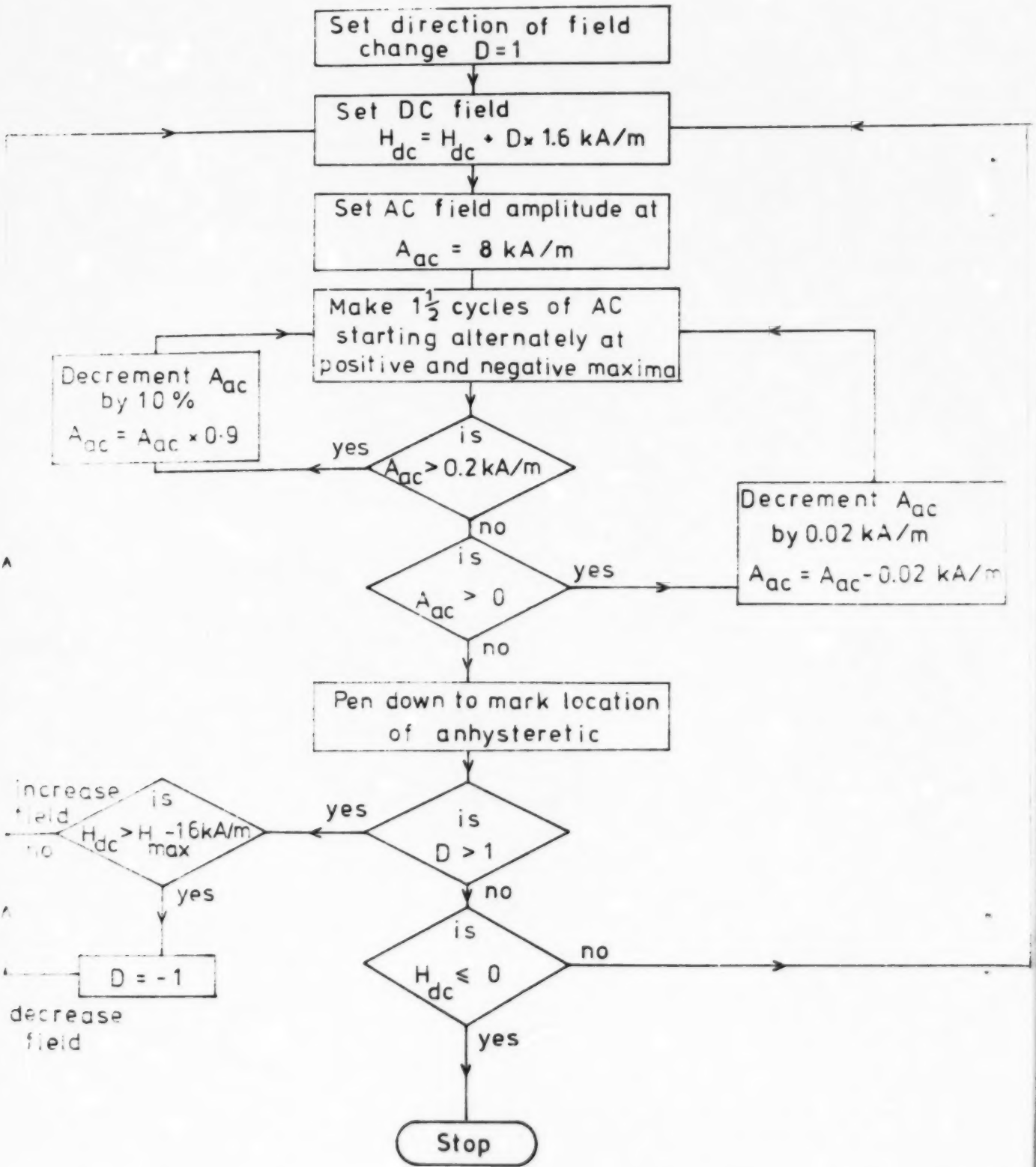
Set direction of field change D=1
Set DC field $H_{dc} = H_{dc} + D \times 1.6$ kA/m
Set AC field amplitude at $A_{ac} = 8$ kA/m
Make $1\frac{1}{2}$ cycles of AC starting alternately at positive and negative maxima
Decrement A_{ac} by 10 % $A_{ac} = A_{ac} \times 0.9$
is $A_{ac} > 0.2$ kA/m
yes
no
Decrement A_{ac} by 0.02 kA/m $A_{ac} = A_{ac} - 0.02$ kA/m
is $A_{ac} > 0$
yes
no
Pen down to mark location of anhysteretic
is $D > 1$
yes
no
increase field
is $H_{dc} > H_{max} - 16$kA/m
yes
no
D = -1
decrease field
is $H_{dc} \leq 0$
no
yes
Stop

POOR

QUALITY

ORIGINAL